A PATH TO THE FORMULATION OF NEW GENERATIONS OF SYNTHETIC JET FUEL DERIVED FROM NATURAL GAS

A Thesis

by

IBRAHIM AWNI OMAR HASSAN AL-NUAIMI

Submitted to the Office of Graduate Studies of
Texas A&M University
in partial fulfillment of the requirements for the degree of

MASTER OF SCIENCE

Chair of Committee,	Nimir Elbashir
Committee Members,	Mahmoud El-Halwagi
	Khalid Qaraqe
Head of Department,	Nazmul Karim

August 2013

Major Subject: Chemical Engineering

ABSTRACT

Characterization of jet fuels obtained from sources other than crude oil is a modern area of research that is developing continuously to replace available petroleum-based fuels with *'drop-in'* alternative fuels. Therefore, reliable composition-property relations are developed to correlate the hydrocarbon compositions of formulated synthetic fuels with their properties to be certified for aviation commercial use.

Intensive studies have been initiated at Texas A&M University Qatar in collaboration with industry and academia to study synthetic jet fuels derived from natural gas. These studies are being implemented at its Fuel Characterization Lab where the most advanced testing equipment is used and strict Quality Management and safety systems are followed.

This study is divided into two tracks. The first track is focused on conducting experimental investigations using in-house formulated synthetic jet fuels derived from natural gas via Gas-to-Liquid technology and Fischer-Tropsch chemistry. Throughout this research work, these fuels will be referred to as Synthetic Paraffinic Kerosene (SPK). These experimental investigations activities are composed of three phases: the first phase focuses on the influence of SPK building blocks (paraffinic hydrocarbons) on fuels' properties, the second phase concerns evaluating the role of aromatics and *cyclo*-paraffins on properties, and the third phase studies the influence of mixing SPK with conventional Jet A-1 derived from crude oil. All of the aforementioned experimental investigations are aimed at building an experimental data bank to assist the efforts of the

formulation of new generations of SPKs that meet aviation industry standards. On the other hand, the second track is directed towards the development of mathematical correlations for four properties of high importance to SPK certification. These correlations aim at optimizing fuel composition whereby major physical/chemical properties of ASTM D1655 are met at the lowest cost of composed fuel.

The primary findings of this study showed that GTL derived SPK paraffinic constituents can improve certain properties while affecting others negatively, and emphasizing the necessity of aromatics in improving specific properties. Further studies compensating the absence of aromatics and sulfur through blended Jet A-1 revealed a practical solution through jet fuels optimization based on cost and technical effective manners.

DEDICATION

To my parents and my relatives

ACKNOWLEDGMENTS

I would like to thank my committee chair, Prof. Elbashir, and my committee members, Prof. El-Halwagi, and Prof. Qaraqe, for their guidance and support throughout the course of the research, and enhancing the quality of the work.

I would like to thank also my friends, colleagues, and the Chemical Engineering program faculty for making my time at TAMUQ a great experience. I also, want to extend my gratitude to all research team members for giving time to my research and helping me in conducting both experimental investigations and statistical analysis necessary for the completion of the study. The research associates (Elfatih Elmalik, Jan Blank, and Rehan Hussain) for resolving the various issues faced and for aiding me in preparing the GC-FID analysis part. In addition, undergraduate and graduate students (Layal Bani Nasser, Samah Warrag, Shiakh Afzal, Jahanur Rahman, Haider Ramadan, Moiz Borha, and, Asma Sadia) for extended support and helping me in the experimental work

I would like to extend my acknowledgments to the industries specially Q-Jet and Shell for providing me the necessary samples for completing the desired experimental testing, and for providing another source of data to ensure the reliability and reproducibility of generated data.

Finally, I would like to extend my thanks to my parents for their endless efforts to provide me a suitable learning environment throughout the Masters study at Texas A&M University.

NOMENCLATURE

ASTM	American Standard Testing Methods
TAMUQ	Texas A&M University at Qatar
FCL	Fuel Characterization Laboratory
GTL	Gas-to-Liquid
SPK	Synthetic Paraffinic Kerosene
US	United States
n-	*normal*-paraffins
iso-	*iso*-paraffins
cyclo-	*cyclo*-paraffins
Tcf	Trillion cubic foot
Mta	Million tons per annum
LNG	Liquefied Natural Gas
QP	Qatar Petroleum
FT	Fischer-Tropsch
GHG's	Greenhouse Gases
GC	Gas Chromatography
^{13}CNMR	Carbon 13 Nuclear Magnetic Resonance
HPLC	High-Performance Liquid Chromatography
SMDS	Shell Middle Distillate Synthesis
DLR	German Aerospace Institution

$\bar{\rho}$	Average density of hydrocarbons mixture
ω_i	Mass fraction of each hydrocarbon type in the mixture
ρ_i	Density of each hydrocarbon type in the mixture
$\overline{\Delta H_{comb}}$	Average net heat of combustion of hydrocarbons mixture
$\Delta H_{comb,i}$	Net heat of combustion of each hydrocarbon type in the mixture
$\overline{FP}$	Flash point of hydrocarbons mixture
$n_{C,i}$	Individual carbon numbers of hydrocarbons in the mixture
ISP	Increasing structural parameter for pure hydrocarbon
DSP	Decreasing structural parameter for pure hydrocarbon
$\overline{Fr\ P}$	Freezing point of hydrocarbons mixture
CRM	Certified Reference Material
QMS	Quality Management System
DMS	Data Management System
CAS	Chemical Abstracts Service
PPE	Personal protective equipment
ANN	Artificial Neural Network
Cst	Centi-Stokes
ESEM	Environmental Scanning Electron Microscopy
DIA	Doha International Airport
GTL_SPK	GTL SPK contribution in jet fuel mixture
Jet_A1	Jet A-1 contribution in jet fuel mixture
VolP	Volume percentage of contribution in jet fuel mixture

Fractions	Total volumetric compositions in jet fuel type
Mix	Jet fuels mixture
V	Volumetric composition in jet fuel type.
NP	*normal*-paraffins
IP	*iso*-paraffins
CP	*cyclo*-paraffins
Mw	Average molecular weight
D	Average density
NP_IP	*normal*- and *iso*-paraffins mixture

TABLE OF CONTENTS

Page

ABSTRACT ii

DEDICATION iv

ACKNOWLEDGMENTS v

NOMENCLATURE vi

TABLE OF CONTENTS ix

LIST OF FIGURES xi

LIST OF TABLES xv

CHAPTER I INTRODUCTION AND LITERATURE REVIEW 1

- Introduction 1
- Background 5

CHAPTER II RESEARCH PROBLEM AND OBJECTIVES 10

- Motivation 10
- Objectives 12

CHAPTER III RESEARCH METHODOLOGY 14

CHAPTER IV EXPERIMENTAL INVESTIGATIONS 17

- Pipettes Cleaning 20
- Beakers Cleaning 21
- Bottles and Flasks Cleaning 21
- Blends Preparation 22
- Density Test 23
- Viscosity Test 24
- Flash Point Test 26
- Net Heat of Combustion Test 28
- Freezing Point Test 30
- Elastomers Compatibility Test 32

CHAPTER V MODELING AND OPTIMIZATION 35

Properties Correlative Models....35
LINGO Formulation Description....42

CHAPTER VI RESULTS AND DISCUSSIONS....47

First Experimental Testing Set....47
Elastomers compatibility testing based on paraffinic building blocks....54
Statistical analysis for paraffinic based hydrocarbons....57
Second Experimental Testing Set....58
Elastomers compatibility testing based on aromatics contribution....65
Third Experimental Testing Set....66
The influence of binary mixture combinations on jet fuel properties....69
Comparison of resulted data with Shell lab in Qatar....76
The influence of jet fuels building blocks on jet fuel properties....77
Statistical analysis for jet fuels mixtures....88
LINGO Formulation Outcomes....89

CHAPTER VII CONCLUSIONS....91

REFERENCES....94

APPENDIX A....101

APPENDIX B....106

APPENDIX C....112

APPENDIX D....113

APPENDIX E....116

APPENDIX F....118

APPENDIX G....120

APPENDIX H....122

LIST OF FIGURES

FIGURE		Page
1	The divisions of GTL jet fuel program among Qatar research consortium	8
2	Blends tested in first experimental set of the study	10
3	Blends tested in second experimental set of the study	11
4	Duties involved in Quality Management System	17
5	Duties involved in Data Management System	18
6	The Anton Paar DMA 4100 device	24
7	The experimental setup required for viscosity test	25
8	The experimental setup required for flash point test	27
9	The flash point test tools	27
10	The experimental setup required for net heat of combustion test	29
11	The net heat of combustion test tools	29
12	The Petrotest K2276 device	31
13	The freezing point assembly tools	31
14	The accuracy of developed model for density property	37
15	The accuracy of developed model for net heat of combustion property	38
16	The prediction of developed flash point model	40
17	The large scatter in freezing point correlative model	41
18	Coherence between experimental and theoretical densities	49
19	Density with respect to *cylco*-paraffins content in jet fuel mixture	50

FIGURE Page

20 Net heat of combustion with respect to *cylco*-paraffins content in jet fuel mixture 51

21 Flash point with respect to *normal*-paraffins content in jet fuel mixture.. 52

22 Freezing point with respect to *normal*-paraffins content in jet fuel mixture 53

23 Viscosity with respect to *normal*-paraffins content in jet fuel mixture..... 54

24 Weight change of elastomers with respect to paraffinic components 56

25 Average weight change of elastomers with respect to paraffinic components after completion of the test 56

26 Improvement of GTL SPK properties using specific addition of *cyclo*-paraffins 59

27 Density with respect to *mono*-aromatics content in jet fuel mixture..... 61

28 Density with respect to *cyclo*-paraffins content in GTL SPK mixture..... 61

29 Net heat of combustion with respect to *mono*-aromatics content in jet fuel mixture 62

30 Net heat of combustion with respect to *cyclo*-paraffins content in GTL SPK mixture 63

31 Flash point with respect to *mono*-aromatics content in jet fuel mixture ... 64

32 Freezing point with respect to *cyclo*-paraffins content in GTL SPK mixture 65

33 Average weight change with respect to aromatics based jet fuel mixtures 66

34 Jet fuel mixtures of third experimental set of the study 68

35 Density with respect to jet fuels binary mixture combinations 70

36 Viscosity with respect to jet fuels binary mixture combinations 71

37 Net heat of combustion with respect to jet fuels binary mixture combinations 72

FIGURE Page

38 Flash point with respect to jet fuels binary mixture combinations 74

39 Flash point with respect to jet fuels binary mixture combinations through extended scale view 74

40 Freezing point with respect to jet fuels binary mixture combinations 75

41 Freezing point with respect to jet fuels binary mixture combinations after repetition 77

42 Density with respect to normal and *iso*-paraffins content in jet fuels mixture 78

43 Density with respect to *cyclo*-paraffins content in jet fuels mixture..... 79

44 Density with respect to aromatics content in jet fuels mixture 79

45 Viscosity with respect to normal and *iso*-paraffins content in jet fuels mixture 80

46 Viscosity with respect to *cyclo*-paraffins content in jet fuels mixture 81

47 Viscosity with respect to aromatics content in jet fuels mixture..... 81

48 Net heat of combustion with respect to normal and *iso*-paraffins content in jet fuels mixture..... 82

49 Net heat of combustion with respect to *cyclo*-paraffins content in jet fuels mixture..... 83

50 Net heat of combustion with respect to aromatics content in jet fuels mixture 83

51 Flash point with respect to normal and *iso*-paraffins content in jet fuels mixture 84

52 Flash point with respect to *cyclo*-paraffins content in jet fuels mixture ... 85

53 Flash point with respect to aromatics content in jet fuels mixture..... 85

54 Freezing point with respect to normal and *iso*-paraffins content in jet fuels mixture..... 86

55 Freezing point with respect to *cyclo*-paraffins content in the mixture..... 87

FIGURE Page

56 Freezing point with respect to aromatics content in jet fuels mixture..... 87

LIST OF TABLES

TABLE		Page
1	Conventional jet fuel chemical components	2
2	Selected properties from ASTM D1655 limits	4
3	Timeline of contributions published in open literature in jet fuel characterization	5
4	Tests ASTM's and their relative testing devices used in experimental work	14
5	Materials needed for the experimental investigations	18
6	Chemicals required for the experimental investigations	19
7	The random non-linear models tested on freezing point data	41
8	Summary of correlative models developed for the properties of interest	42
9	LINGO formulation statements description	43
10	Tested blends of the first experimental set	48
11	Comparison between research team and Professor Wilson's analysis	57
12	Tested blends of the second experimental set	59
13	Jet fuels mixtures of the third experimental set	67

CHAPTER I

INTRODUCTION AND LITERATURE REVIEW

INTRODUCTION

Petroleum-based jet fuels, or simply named conventional jet fuels, were the main sources of fuel supply to run gas-turbine engines in aircrafts in the past. Conventional jet fuels are categorized into three main divisions following standardized international specifications to withstand the severe conditions during flights: Jet A, Jet A-1, and Jet B [1]. Jet A is a special jet fuel cut produced by US oil refineries and has been used in the United States since the 1950's [1]. Whereas, Jet A-1 is another jet fuel type with quite similar specifications to Jet A being used in the rest of the world [1]. Jet B is a special cut from naphtha-kerosene region that is rarely used. It can withstand extreme cold-weather conditions (used mostly in Russia) [1]. Including other jet fuels customized with unique specifications intended for military use, such as: JP-4, JP-5, and JP-8 [2]. In which JP stands for "Jet Propellant".

Conventional jet fuel is a complex blend which consists of hundreds of hydrocarbons that fit into four principal hydrocarbon groups: *normal*-paraffins, *iso*-paraffins, *cyclo*-paraffins (*naphthenes*), and aromatics [3]. Including traces of other chemical compounds, such as oxygenates, olefins, antioxidants, metal deactivators and antifreeze (please refer to Appendix E). Table 1 provides general chemical structures of these hydrocarbons together with illustrative examples.

Table 1. Conventional jet fuel chemical components.

Hydrocarbon Group	Chemical Structure	Structure Shape	Illustrative Example
***n*-Paraffins**	C_nH_{2n+2}	Straight Chains	$H_3C\ CH_2\ CH\ CH_2\ CH\ CH_2\ CH_3$
***iso*-Paraffins**	C_nH_{2n+2}	Branched Chains	$H_3C\ CH_2\ \underset{\displaystyle CH_3}{CH}\ CH_2\ \underset{\displaystyle CH_3}{CH}\ CH_2\ CH_3$
***cyclo*-Paraffins**	C_nH_{2n}	Cyclic Chains	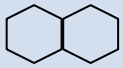
Aromatics	C_nH_{2n-6}	Benzene Ring	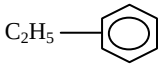

Due to supply security fears, frequent increase in oil prices and rapidly increasing transportation demand worldwide, new resources of jet fuels have been sought recently [4,5,6]. The target is to investigate new energy resources that have sufficient energy content, are thermally stable in combustion chambers, and can generate reduced environmental impact to the surroundings [5, 7]. This was the starting point for modern fuels synthesized from sources other than crude oil, such as coal, natural gas, or biomass; jet fuels obtained from these resources are known as *"Synthetic Jet Fuels"*.

Gas-To-Liquid (GTL) synthesized fuels have become promising resources for alternative fuels. They offer several advantages, such as being cleaner sources of energy with an abundant supply that can replace dwindling oil resources and can meet the increasing worldwide demand of energy as in the case of the past two decades. Qatar is known to have the third largest natural gas reserve in the world with a total capacity approaching 900 tcf [8]. This has motivated Qatar to have a long-term vision of investing huge expenditures on establishing world-class commercial scale natural gas

processing facilities, and to produce fine quality added-value liquid hydrocarbons. LNG production capacity in Qatar reached a net of 77 Mta at the end of 2010 through premium producers RasGas and QatarGas, putting Qatar on the top of the list in LNG production worldwide [9]. Moreover, Qatar has considered raising its natural gas processing activities through constructing commercial scale GTL plants. These plants are represented by Oryx GTL plant of Sasol's technology which was started in 2006. Following this step Qatar currently is hosting the largest GTL plant in the world (the Pearl GTL plant) owned by Shell and QP which has been commissioned last year [10,11]. These unique large scale GTL industrial plants give Qatar its name as the *"World Capital of GTL"* [11]. The Pearl GTL plant of Shell is envisioned to become the world's largest producer of SPK fuels that could reach 1 million tons annually. The main consumer of these synthetic jet fuels will be Qatar Airways [12].

The civil aviation industry is growing rapidly to meet the worldwide continuous transportation demand, and to provide the most attainable levels of comfort for passengers. The rapid increase in civil aviation demand has been accompanied with extended consumptions in petroleum-based jet fuels namely Jet A or Jet A-1, and has led to larger carbon footprint through higher greenhouse gases emissions. Thus, studies have been intensified in the field of GTL synthetic jet fuel characterization, which is commercially named as SPK, to formulate the new generations of synthetic jet fuels via better understanding of the composition-property relationship [13]. The formulated SPKs are supposed to have properties similar to regular crude oil derived jet fuels (e.g. Jet A-1) as specified by the aviation industry and stated in the ASTM D1655, or in the

more recent ASTM standards for semi-synthetic jet fuels (ASTM D7566) [14,15]. These physical and chemical characteristics strongly correlate with the fuel's combustion behavior and performance as well as post combustion emissions. GTL SPK covers a wide spectrum of carbon numbers ranging between C_7 - C_{16}, and is composed of three main hydrocarbon building blocks: *normal*-paraffins, *iso*-paraffins, and *cyclo*-paraffins [13,16]. Research attempts are aiming to develop what are called *"drop-in"* alternative fuels, in which it can be supplied to current fuel systems without any technical drawbacks, or mixed perfectly with remaining fuel in the tank to avoid substantial fuel waste during sequential flights [5]. Aviation fuels driven from synthetic crudes are certified for commercial use if their physical characteristics meet ASTM D1655 [14]. Table 2 displays part of the ASTM D1655 limits for synthetic jet fuel to be certified as Jet A-1 or Jet A.

Table 2. Selected properties from ASTM D1655 limits [13].

Analyzed Property	ASTM Method	Unit	Minimum Limit	Maximum Limit	Repeatability Limits
Density	D4052	g/cm^3	0.775	0.840	0.0006
Viscosity	D7042	cSt	-	8.000	-**
Flash Point	D56	^oC	38.0	-	1.2 or 1.6***
Freezing Point	D2386	^oC	-	-40.0* - 47.0	1.5

Table 2. Continued.

Analyzed Property	ASTM Method	Unit	Minimum Limit	Maximum Limit	Repeatability Limits
Net Heat of Combustion	D240	MJ/kg	42.8	-	0.1300

* Freezing point for Jet A is a little different from Jet A-1 [14].

** No repeatability limits could be located for viscosity in ASTM D7042 [17].

*** Depending on the flash point of the blend around the 60 ^{o}C [18].

BACKGROUND

Jet fuel characterization serves to develop the well-known composition-property relationship is an area of research that was started by the Cookson study in the 1980's. Table 3 provides chronological order of major studies published in open literature in the field of jet fuel characterization and in the field of relationship fuel's composition versus property.

Table 3. Timeline of contributions published in open literature in jet fuel characterization.

Year of Publication	Source	Title of Publication	Authors	Study Focus
1987	Energy & Fuels Journal	Investigation of the Chemical Basis of Kerosene (Jet Fuel) Specification Properties [16].	Cookson, et al.	Correlation of specific fuel's properties with their compositions utilizing GC, C^{13}NMR, and HPLC in fuel characterization.

Table 3. Continued.

Year of Publication	Source	Title of Publication	Authors	Study Focus
1990	Energy & Fuels Journal	Calculation of Jet and Diesel Fuel Properties Using 13C NMR Spectroscopy [19].	Cookson et al.	Developing simple linear relationships correlating specific properties with fuel's compositions using 13C NMR spectroscopy
1995	Fuel Journal	Composition-property relations for jet and diesel fuels of variable boiling range [20].	Cookson et al.	Developing simple linear models correlating other properties with fuel's compositions.
2007	Fuel Journal	Artificial neural network approaches on composition–property relationships of jet fuels based on GC–MS [21].	Guozhu et al.	Utilizing different Artificial Neural Networks in developing composition-property relationship.
2008	Science in China Series B: Chemistry	Theoretical design and preparation of high thermal-stable jet fuel [5].	Guozhu et al.	Developing theoretical design method using composition-property relationship.
2011	12th International Conference on Stability, Handling, and Use of Liquid Fuels	Use of Surrogate Blends to Explore Combustion-Composition Links for Synthetic Paraffinic Kerosines [13].	Bauldreay et al.	Highlighting the composition-property relationship as part of Qatar research consortium activities.

Considering the aforementioned literature survey, none of the studies addressed detailed assessment of composition versus property relationship for jet fuel mixtures

composed of GTL SPK and conventional Jet A-1 at different ratios. The only located research attempts in this field were blending SPK's from two different natural sources; coal and natural gas with conventional jet fuel to maximum volume percentage of 50 vol% [22]. Furthermore, the report states explicitly that there was need to study the role of aromatics on semi-synthetic jet fuel properties, and identify the minimum content of aromatics needed [22]. Including another study for full range mixing based on synthetic SMDS kerosene from GTL plant with another conventional jet fuel cut [23]. These previous studies were conducted on Jet A-1 cuts obtained from different oil refineries. Whereas current study conducted the experimental testing on Jet A-1 obtained from domestic provider at Doha International Airport that is Q-jet. Nevertheless, still two practical applications were published earlier considering Qatar Airways flight from Gatwick Airport in London to the Doha Airport (Qatar), for Airbus A340-600 aircraft with flight duration of around 6 hours that was fueled with blend of 50:50 ratio in respect to GTL synthetic jet fuel and conventional Jet A-1 fuel [24], including another recent flight based on unknown blending ratio of jet fuels of GTL SPK from Pearl plant with conventional Jet A-1. Moreover, it was found that these flights were preceded with another non-commercial flight for a prototype aircraft of Airbus A380 which ran by GTL/conventional Jet A-1 blend between Filton in United Kingdom and Toulouse in France in 2008. However, no additional technical details were provided specially related to the blending ratio [25].

A research consortium concerned about studying synthetic jet fuels driven from Fischer-Tropsch process was constructed in Qatar in 2009, after the publication of

ASTM D7566 [13]. This consortium involves world leaders in GTL and jet fuel researchers and covers three main areas of interest to synthetic jet fuel: Properties, Combustion, and Performance [13]. The GTL jet fuel consortium was sponsored by Qatar Science and Technology Park together with Qatar Airways and involved in its Properties team TAMUQ, Shell Global Solution, University of Sheffield, and Qatar Shell Research and Technology Center. Rolls Royce and DLR involved in Combustion team. And Airbus involved in Performance team. Figure 1 shows the main divisions of the GTL jet fuel program and the research consortium that completed its activities very recently.

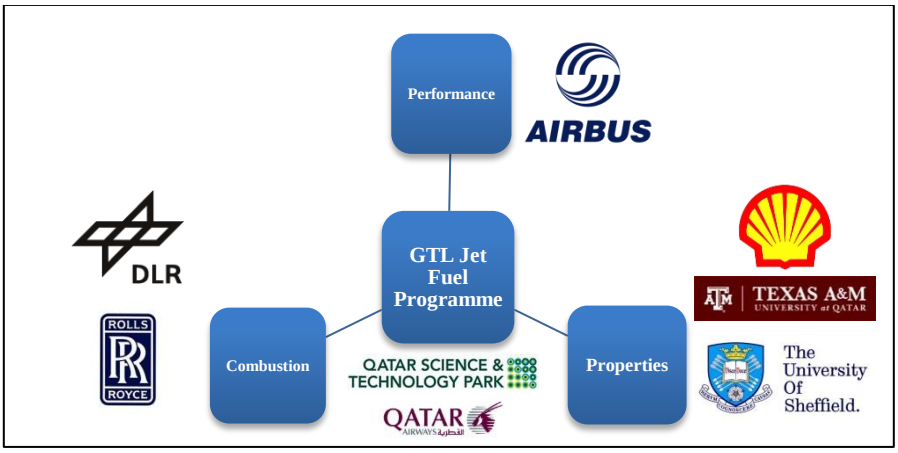

Figure 1. The divisions of GTL jet fuel program among Qatar research consortium.

The research team at Texas A&M University at Qatar took the lead on the Properties Division of the consortium as part of a unique collaboration research project between academia and industry as described above. TAMUQ built a world-class Fuel

Characterization Lab that is equipped with more than 20 advanced analytical devices to support this project as well as hosting research activities in synthetic fuels from GTL.

CHAPTER II

RESEARCH PROBLEM AND OBJECTIVES

MOTIVATION

Previous studies aiming to design future generations of synthetic jet fuels from GTL have developed several models for the composition-property relationship as summarized in previous chapter. The research team at TAMUQ conducted a series of studies on number of blends made from GTL building blocks. The selection of these blends of different composition of SPK building blocks as well as the experimental investigations were based on a well-established experimental plan covering most of the critical regions around the ternary diagram, as shown in Figure 2 [26].

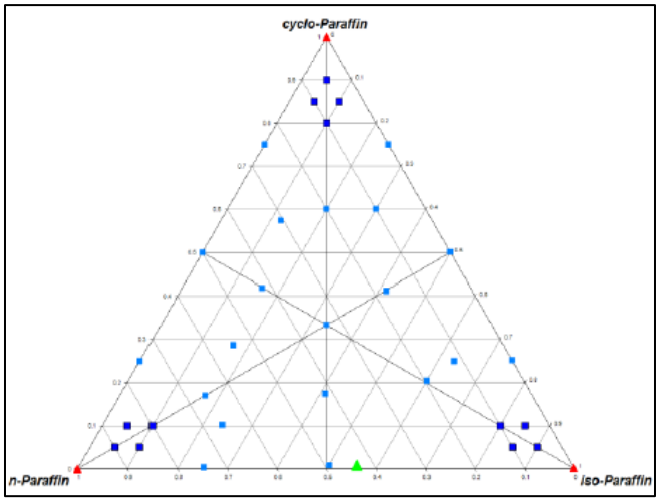

Figure 2. Blends tested in first experimental set of the study.

GTL paraffinic constituents were observed to impact specific properties positively while impacting other properties negatively. Studies in understanding the influence of GTL jet fuel composition on their properties were expanded to include the role of aromatics on these properties that were hardly met by the paraffinic composition. The reason behind initiating this investigation path is to improve the density of the mixture and the elastomers swelling through the rubber joints in the fuel system. Figure 3 shows the blends that have been tested in the second set of experiments.

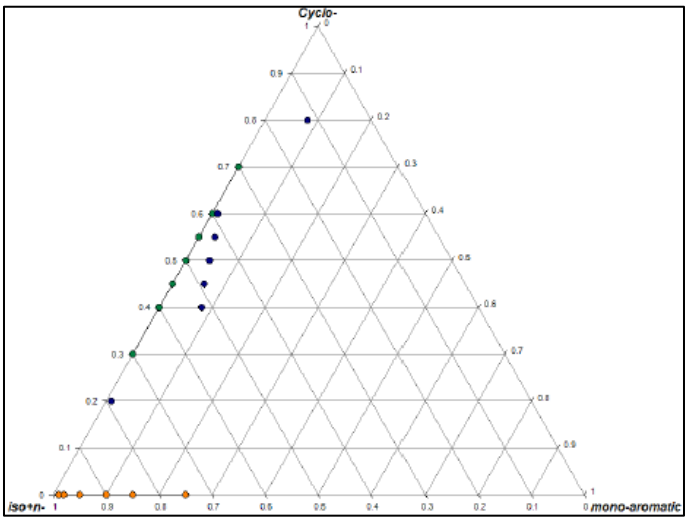

Figure 3. Blends tested in second experimental set of the study.

Promising outcomes were gathered from the latest studies emphasizing the advantages of adding aromatics to GTL jet fuel [27]. The density was increased slightly to be within ASTM limits and the required absorption of the rubber joints among the fuel tanks system was achieved. The resulted data from previous sets of experiments were

linked to comprehensive statistical analysis, in order to predict the overall behavior of properties along the various hydrocarbons compositions. Further details about previous studies outcomes conducted by the research team are provided in Chapter VI further in the context. Current studies are being directed towards the compensation of necessary limited content of aromatics in GTL jet fuel because of the infeasibility in traditional addition procedures. One way to accomplish this intent is by mixing jet fuels, in which cleaner synthetic jet fuel is mixed with a specific amount of conventional jet fuel. Thus, anticipated synthetic fuel with properties of interest at acceptable ranges will be produced, providing safer and smoother flights to air crafts.

In summary, the current challenges facing the jet fuel characterization field can be summarized in the following two points:

1. Despite extensive research work there is still a need to explore other feasible options for improving synthetic jet fuel properties to be within aviation market demand. Also, the fuel needs to be certified for civil use and verified through other research consortium divisions towards practical applications.

2. Update design of future generations of SPK's mainly depend on availability and composition of Fischer-Tropsch fuels. There is a need to identify new design techniques such as the property integration method.

OBJECTIVES

The major objectives of this study is to utilize experimental techniques while coupled with property integration methods to optimize the design of new generations of GTL

synthetic jet fuels through the optimization of jet fuels blend between Jet A-1 and GTL SPK. To be more specific, the objectives can be summarized as follows:

1. Establish data bank on SPK jet fuel blends versus their properties following standard ASTM certified tests for major physical properties. The experimental campaign will be based on three sets of experiments as follows:
    a. First experimental set to Study the overall effect of paraffinic blending on GTL synthetic jet fuel properties, namely the paraffinic constituents of GTL jet fuel.
    b. Second experimental set to study the influence of aromatics as required component for GTL SPK certification and the combined or individual role of *cyclo*-paraffiinic constituent on GTL SPK properties. The main focus on this section is to improve SPK jet fuels' density and elastomer compatibility to meet ASTM 1655.
    c. Third experimental set to study the practical applications of blending GTL synthetic jet fuel with conventional Jet A-1 fuel together to account for both advantages of cleaner source of fuel to environment and better performance fuel due to limited and necessary aromatics and sulfur presence.
2. Develop mathematical correlations for the five properties of interest: density, viscosity, net heat of combustion, flash point, and freezing point as a function of GTL SPK paraffinic hydrocarbon building blocks, capturing the overall trend of resulted data in the first experimental investigation of the study.
3. Optimize the jet fuels blending ratios between GTL SPK and Jet A-1 through optimization software supported with developed mathematical correlations for properties of interest.

CHAPTER III

RESEARCH METHODOLOGY

The following context summarizes the proposed plan for tackling this study:

1. The experimental testing campaign has been carried out at TAMUQ FCL, whereby measurements of properties of interest have been conducted utilizing advanced analytical devices following standard testing methods as described in Table 4.

Table 4. Tests ASTM's and their relative testing devices used in experimental work.

Analyzed Property	ASTM Method	ASTM Title	Testing Device
Density	D4052	Density, Relative Density, and API Gravity of Liquids by Digital Meter.	Anton Paar DMA 4100
Viscosity	D7042	Standard Test Method for Kinematic Viscosity of Transparent and Opaque Liquids (and Calculation of Dynamic Viscosity)	Anton Paar SVM 3000
Flash Point	D56	Flash Point by Tag Closed Cup Tester.	Petrotest Tag 4TM
Freezing Point	D2386	Freezing Point of Aviation Fuels.	Petrotest K2276
Net Heat of Combustion	D240	Standard Test Method for Heat of Combustion of Liquid Hydrocarbon Fuels by Bomb Calorimeter.	Parr 6200EF

2. Properties integration and the correlations between composition and properties were conducted by utilizing mathematical models. An Excel spread sheet was used for the

calculation of the density and net heat of combustion for mixtures of synthetic jet fuel from its paraffinic hydrocarbon building blocks, using linear models as described below:

a. Density [28]: $\bar{\rho} = 1/\sum_{i=1}^{n=3} \frac{\omega_i}{\rho_i}$ (1)

b. Net heat of combustion [29]: $\overline{\Delta H_{comb}} = \sum_{i=1}^{n=3} x_i \Delta H_{comb,i}$ (2)

3. Mathematical correlation for the measured flash point of synthetic jet fuel blends with their paraffinic hydrocarbon building blocks has been developed utilizing latest linear model for pure hydrocarbons proposed by Keshavarz [30]:

$$FP(K) = A + 16.15\, n_c + 16.68\, ISP - 24.71\, DSP \quad (3)$$

4. Mathematical correlation trending freezing point of synthetic jet fuel blends with their paraffinic hydrocarbon building blocks has been developed using non-linear modeling, which is going to be discussed later in Chapter V.

5. The optimum blending ratios of mixed jet fuels as a function of synthetic jet fuel paraffinic compositions that meet the aviation industry standard for semi-synthetic jet fuels (ASTM D7566), was determined using well-known optimization software 'LINGO'. The objective function took into consideration the blending ratios together

with recent market values of conventional Jet A-1 and GTL SPK. The outcome of this process identified the optimum blend composed from paraffinic hydrocarbon building blocks as well as the best blending ratio between GTL synthetic jet fuels and conventional Jet A-1. The details of this activity will be discussed further in Chapter V.

CHAPTER IV

EXPERIMENTAL INVESTIGATIONS

The experimental investigations of this study were conducted at a well-established Fuel Characterization Laboratory within Texas A&M University campus at Qatar. An efficient Quality Management System and Data Management System were established to maintain both the quality of outcomes and the reputation of testing facility among domestic and international well-known testing centers. In addition, this laboratory follows strict safety protocols putting safety on the top of the list of the priorities. Figures 4 and 5 illustrate the main tasks which Quality Management System and Data Management System rely on.

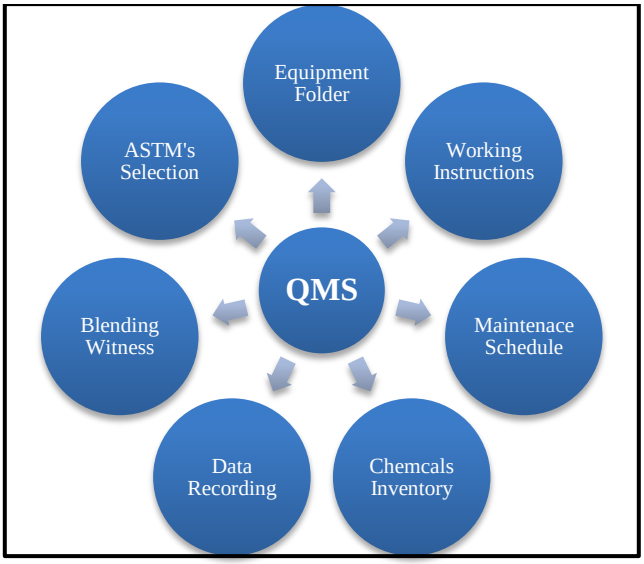

Figure 4. Duties involved in Quality Management System.

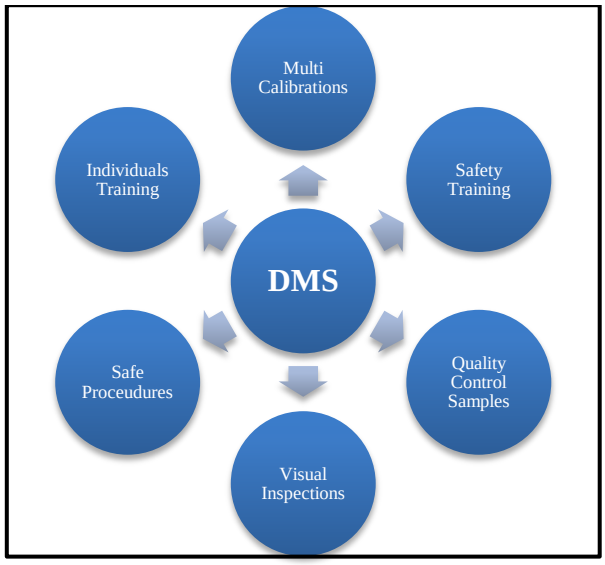

Figure 5. Duties involved in Data Management System.

Five principal testing devices listed earlier in Table 4 were required to complete this study beside other necessary chemicals, materials, and peripherals. Tables 5 and 6 provide complete listing of needed materials and chemicals to accomplish the experimental investigations of this study, respectively.

Table 5. Materials needed for the experimental investigations.

Material	Number of Units
Graduated glass pipette of 25 ml	6
Glass pipette of 25 ml	6
Glass pipette of 50 ml	6
Glass pipette of 100 ml	6
Glass Erlenmeyer flask of 2,000 ml	6
Tissue paper role	2
Pack of rubber bands	1

Table 5. Continued.

Material	Number of Units
Dishes soap	1
Glassware brush	1
Plastic droppers of 500 ml	2
Fumehood	2
Pack of glass beakers of 100 ml	1
Sensitive balance with 4 decimal digits	1
Pack of plastic pipettes of 2 ml	1
Pack of plastic syringe of 6 ml	1
Two stage pressure regulator	1
Gas connection line and fittings set	1
Hot air gun	1
Glass vacuumed tube	2
Low temperature thermometer of -80 ^{o}C	2
Metal stirrer	2
Rubber cork with two holes	2
Small glass tube	2
Fuel pump	4
Acrylonitrile elastomers (O-rings)	20
Oil bath	1
Pack of filtration paper	1
High elastic string roll	1
Metal hooks	20
Digital caliber	1

Table 6. Chemicals required for the experimental investigations.

Chemical	CAS Number
Ethanol of assay ≥ 99.99%, (2,000 ml)	64-17-5
Acetone of assay ≥ 99.99%, (2,000 ml)	67-64-1
Decane of assay ≥ 99.99%, (10,000 ml)	124-18-5
Decahydronephthalne (cis + trans) of assay ≥ 99.99%, (20,000 ml)	91-17-8

Table 6. Continued.

Chemical	CAS Number
Shell Sol-T blend, (5,000 ml)	-
GTL KERO Shell blend, (5,000 ml)	-
Toluene of assay 100%, (1,000 ml)	108-88-3
Jet A-1, (5,000 ml)	-
Distilled water, (20,000 ml)	-
Isopropyl of assay ≥ 99.99%, (2,000 ml)	67-63-0
Oil, (2,000 ml)	-

Another significant point to highlight here is the personal safety measure represented by necessary PPE to conduct further experimental investigations, which are: fuel non-absorvitive lab coat type, powder-free nitrile gloves, safety glasses, and mask occasionally while dealing with strong odor chemicals.

The Following context is a complete description about the cleaning procedures for the glassware used in the study, including some important highlights about the five tests of the study and the supplementary elastomer compatibility test.

PIPETTES CLEANING

All the pipettes were cleaned vigorously before they have been used according to the following strict cleaning procedure.

1. The pipette is rinsed with ethanol plastic dropper until droplets are dropping at the tip end of the pipette. The pipette has to be rotated slowly while rinsing to assure complete coverage to pipette surfaces.

2. The pipette is dried out through air supply source at the fumehood while continuous rotation movement is maintained. The tip end of the pipette is covered firmly with tissue paper to receive the residues of ethanol that were initially present in the pipette.
3. Previous procedure is repeated again however this time with the acetone plastic dropper to remove any remaining traces of ethanol on the surfaces.

BEAKERS CLEANING

All the beakers were cleaned very well before they have been used according to the following strict cleaning procedure.

1. The top edge of the beaker is rinsed with ethanol plastic dropper all around while the beaker is rotated slowly, in order to ensure complete coverage to all side surfaces. Then, the beaker is shacked vigorously to ensure sufficient coverage to bottom surface. After that, the beaker is dried with air supply source at the fumehood while slow continuous rotation is maintained.
2. The same procedure is repeated again however this time with the acetone plastic dropper to remove any remaining traces of ethanol on the surfaces.

BOTTLES AND FLASKS CLEANING

All the bottles were passed through perfectly proposed cleaning procedure to provide high quality results at highest accuracy possible. The cleaning procedure was running through the following detailed steps:

1. The bottle is rinsed very well with brush wetted with dishes soup all around to remove all dust particles inside. In addition, the lid is rinsed from the inside with the same wetted brush.
2. The bottle and the lid are left to dry up on the rack for 20 minutes. Next, the bottle is dried further with tissue paper followed by air supply source at the fumehood. The bottle is rotated gently while drying to ensure complete dryness to all side and bottom surfaces.
3. The bottle is rinsed with ethanol plastic dropper all around while the bottle is rotated slowly, in order to ensure complete coverage to all side surfaces. Then, the bottle is shacked vigorously to ensure sufficient coverage to bottom surface. After that, the bottle is dried with air supply source at the fumehood while slow continuous rotation is maintained.
4. Previous procedure is repeated again however this time with the acetone plastic dropper to remove any remaining traces of ethanol on the surfaces.
5. The bottle is dried further with hot air gun at moderate temperature of 50 ^{o}C to ensure complete absence to acetone residues inside the bottle.

BLENDS PREPARATION

The blends were prepared based on simple manual addition procedure after all the required glassware's were cleaned properly according to previously stated procedures. The general procedure can be described as follows:

1. The desired composition of the blend is translated into respective volumes by simply multiplying the volume percentage by total volume of the blend.
2. The resulted volumes for the blend aid in choosing the appropriate number and size of pipettes, which are taken for cleaning thereafter.
3. Desired chemicals for blending are sucked from stock tanks into cleaned Erlenmeyer flasks using individual fuel pumps.
4. The bottle is labeled with a fully descriptive label indicating the name of the blend and the date of preparation.
5. The bottle is filled with respective volumes of the solvents starting by the heaviest solvent going to the lightest at the end of the blending, in order to ensure perfect mixing at the end. As the last droplet is poured inside the tank, the bottle is closed very well with respective lid and shacked vigorously in horizontal movement to ensure well mixing to the blend.

DENSITY TEST

Density is the most significant property in certifying the jet fuel. It is one of the properties that describe the fluidity of the fluid. Moreover, it is used as blend confirmation test since the density property is observed to follow almost perfect linear behavior as going to be emphasized further in the context. Accordingly, the theoretical density computed from the respective compositions of the mixture components into corresponding pure values compares very well with the experimental values obtained

from density test. The density test is carried out in Anton Paar DMA 4100 device which is illustrated though Figure 6.

The principle of density test can be described as follows. The tested sample is injected into the testing tube which is formed as U-shape passage. The U-shaped tube oscillates at specific frequency while an electronic excitation system excites the electrons. A digital analyzer receives the signal carried by excited electrons and translates it into density [31].

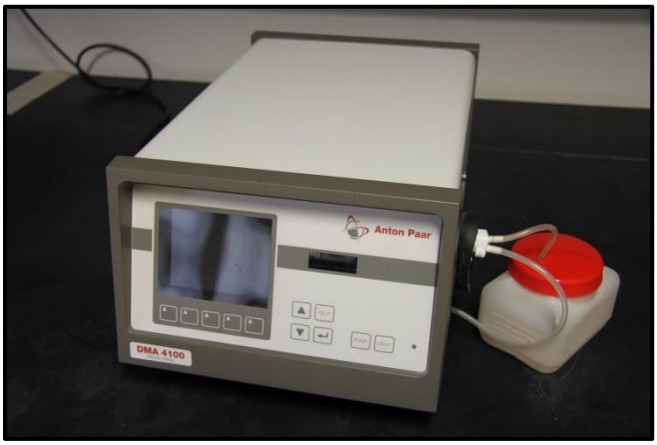

Figure 6. The Anton Paar DMA 4100 device.

VISCOSITY TEST

The viscosity test is another crucial test in certifying the jet fuel, as it continues with the density property the description of the fuel fluidity within the fuel system. Moreover, it helps in evaluating the combustion performance of the fuel combustors through the fuel

system. Viscosity of liquids is inversely proportional with temperature; as the temperature of the system increases, the viscosity of the fluid decreases and vice versa.

The viscosity test is carried out through a well-integrated experimental setup connecting the main device with chiller and supplementary air pump system. The setup is composed of the following objects beside the principal Anton Paar SVM 3000 device: chiller filled with ethylene glycol to lower the temperature of the system to desired cryogenic condition of -20 ^{o}C, external air pump system, and small printer for data recording. Figure 7 illustrates the experimental setup for viscosity test.

Figure 7. The experimental setup required for viscosity test: a) chiller, b) printer, and c) air-pump system.

The principle of the viscosity device can be described elsewhere [17]. A rotational coaxial cylinder is used in the measuring system, which is composed of two main parts; outer tube rotates at constant and uniform rotational speed, and low-density

inner tube held at axis of rotation by centrifugal forces of higher density fluid together with magnet and soft iron rings. A permanent magnet is introduced in the inner tube to generate eddy currents among surrounding copper casing. Finally, the rotational speed of the inner tube is determined by the balance between driving torque and eddy currents torque. In which a special electronic system is used to detect the frequency of rotating magnetic field.

FLASH POINT TEST

The flash point test is another significant test in certifying jet fuel, it is considered as one of the safety measures for the fuel. Flash point is defined as the temperature at which the fuel mixture gives sufficient vapor to become ignitable upon the presence of oxygen in the air [32]. The fuel become more favorable as the flash point becomes higher, since the mixture will have reduced tendency to ignite upon the presence of ignition source.

The flash point test is carried out in Petrotest Tag 4TM device connected to computer to record the obtained data. The device has a big opening where the container holding the tested sample is placed at with a large object to fit on where the igniter is controlled above the container. In addition, this device is equipped with golden metal container comes with special lid that can be opened to allow the igniter dip in partially and sense the vapors. Figures 8 and 9 show the Petrotest Tag 4TM device and the equipped tools.

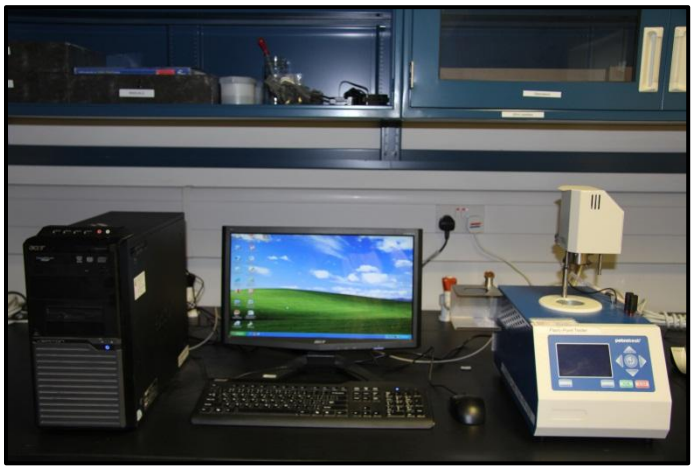

Figure 8. The experimental setup required for flash point test.

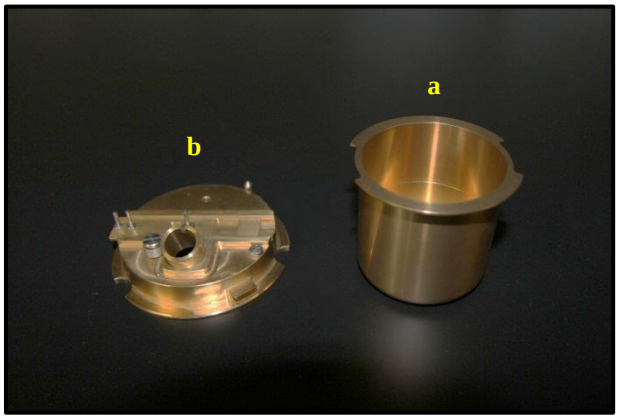

Figure 9. The flash point test tools: a) golden cup, and b) lid.

The principle of the flash point test can be explained elsewhere [18]. The tested sample is heated up to a certain temperature below the expected temperature by 5 ^{o}C. At which the igniter starts to dip in partially in the container every 0.5 ^{o}C by opening the upper door for couple of seconds. Once the igniter senses sufficient vapors from heated sample, the test will be terminated and the flash point will be determined.

NET HEAT OF COMBUSTION

The net heat of combustion test serves to identify the amount of energy released from fuels when burned at aircrafts engine, by estimating the gross heat of combustion 'Q_g' associated with tested fuel sample. Gross heat of combustion is defined as the amount of energy released by unit mass of the hydrocarbon when burned at constant volume system. The net heat of combustion 'Q_n' can be calculated from gross heat of combustion using the following mathematical expression mentioned in ASTM D240 [33]:

$$Q_n = 0.7195\, Q_g + 10.025 \quad (4)$$

The net heat of combustion test is carried out through a well-integrated experimental setup connecting the main device with gas supply source. The setup is composed of the following objects beside the principal bomb calorimeter (Parr 6200EF device): oxygen gas cylinder, distilled water bath and circulator, water tank with multifunctioning valve, and a small data recoding printer. The device is also equipped with side tools to contain the tested sample through safely, which are: metal crucible, special clamp, heavy metal container, top lid with gas release valve, and container screw. Figure 10 illustrates the experimental setup for net of heat combustion test. Figure 11 shows the different tools needed for completing this test.

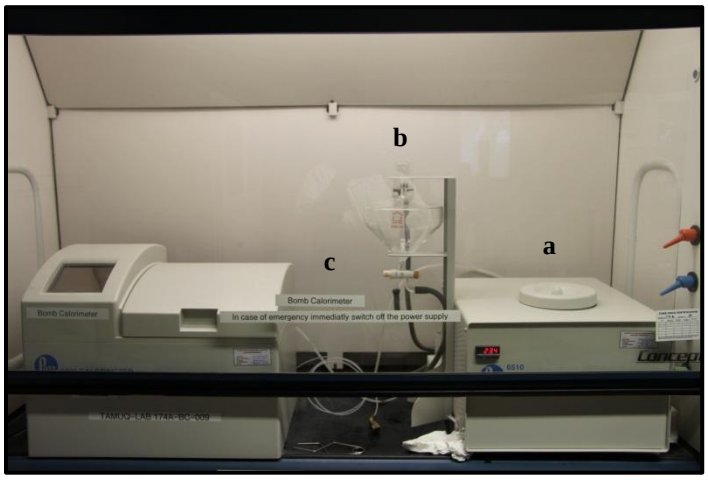

Figure 10. The experimental setup required for net heat of combustion test: a) distilled water tank and circulator, b) water tank with multi functioning valve, and c) Oxygen cylinder line.

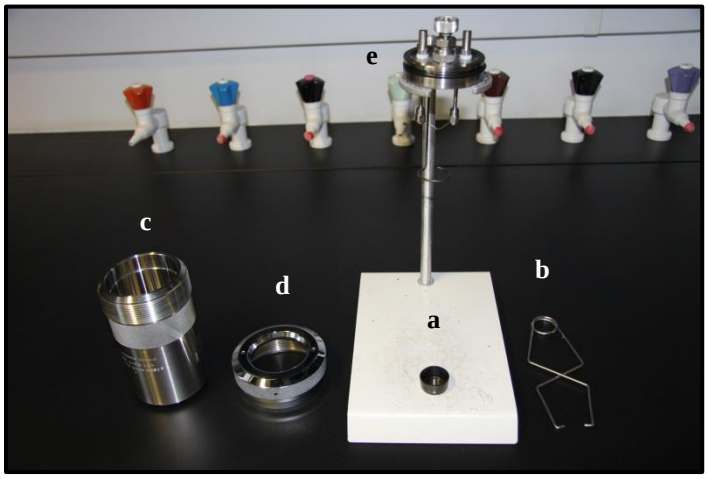

Figure 11. The net heat of combustion test tools: a) crucible, b) clamp, c) heavy container, d) container screw, and e) container top lid.

The principle of the net heat of combustion test can be simply described elsewhere [34]. Oxygen enriched environment is provided for the tested sample, while it is burned inside the bomb that acts as constant volume system. Furthermore, the system

is kept at relatively constant temperature using the cooling jacket that surrounds the bucket.

Net Heat of Combustion test is preceded with GTL SPK testing on daily basis to act as an internal standard for the test and to give the indication for carrying on the testing for desired fuel blends. In addition, the device is calibrated with Benzoic acid at higher weight just exceeding 1.00 g as external standard on monthly basis.

FREEZING POINT TEST

Freezing point is one of the important properties to be monitored in jet fuel. The fuel should be able to sustain its lubricity and fluidity under the severe thermal conditions that it could face during flight. Temperatures during Qatar's summer may reach 50 °C on the ground, and in contrast, the temperature at high altitudes approaches -65 ^{o}C. The fuel has to be maintained in a liquefied state during the whole range of operational temperatures; freezing fuel in the aircraft may lead to mechanical and operational problems. Freezing point is defined as the temperature at which equilibrium is established between the solid and liquid states of the mixture [35]. This point is impossible to notice while the blend inside the device. Thus, the freezing point of the blend is considered as the melting point of last crystal of the blend at the bottom of the tube, which is a reasonable assumption stated in ASTM D2386 [34].

The freezing point test is carried out in Petrotest K2276 freezing point apparatus combined with digital camera to document the data. The bath is filled with isopropyl to volume of 2 L to fully cover the cooling coil inside, in order to act as efficient refrigerant

for the immersed blends. In addition, this experimental setup is equipped with freezing assembly composed of: glass vacuumed tube, small top tube, rubber cork, metal stirrer, and low-temperature thermometer. Figures 12 and 13 show the Petrotest K2276 device and freezing assembly tools, respectively.

Figure 12. The Petrotest K2276 device.

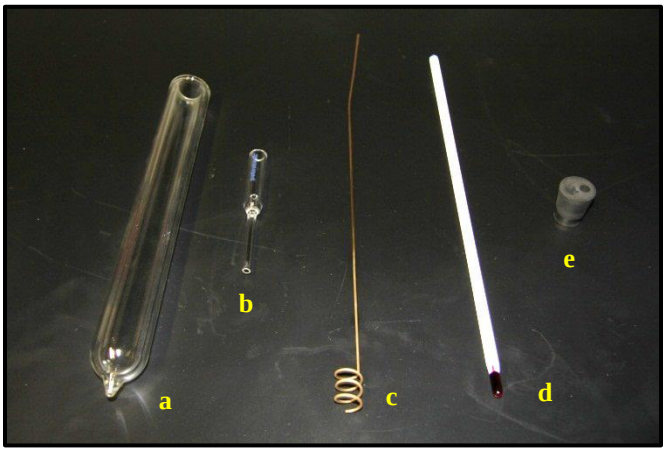

Figure 13. The freezing point assembly tools: b) vaccumed tube, b) top tube, c) stirrer, d) thermometer, and e) rubber cork.

Despite the well-established measurement procedure for the freezing point it still comes with its challenges since the test is operator dependent. First of all, the various crystal shapes and phases observed, made the task of monitoring the disappearance of last crystal quite difficult. These challenges could also be attributed to the fact that the blends were experiencing different melting behaviors and in some the crystals were hardly seen even with focused views on the position where the melting process is taking place. Such conditions made slight discrepancies in recorded data and extended the required time for completing the test for number of blends. In addition, laboratory lights had to be dimmed to certain extent in order to get high quality images with flash. Moreover, the lens sensitivity to vibrations made it extremely difficult to stay stable on the tripod after pressing the shutter. On the other hand, the tubes removed from the device normally cold and therefore they form foggy surface on the walls as soon as they face the ambient condition. Thus, the walls have to be wiped up vigorously and this simply causes negligible vibration that is enough to distort the image quality.

ELASTOMERS COMPATIBILITY TEST

Elastomer compatibility test is another significant test in jet fuel characterization. Fuel systems contain a lot of joint rubbers that seal the connection between the different parts in the system. These rubber joints have to be kept in safer operation condition all the time throughout the flight, to avoid any fuel leakages or major technical failures [5]. This test serves to analyze the time averaged impact of swelling the rubber joints or

usually called “O-rings” caused by the jet fuel stored among the fuel system. There are two types of elastomer compatibility testing: statistic and dynamic. The research team was focused on the static testing for the pure hydrocarbons utilized in first experimental set including GTL SPK. Furthermore, the data generated from this study have been correlated with dynamic testing results conducted by Professor Chris Wilson team at the University of Sheffield. A good agreement was observed between the two sets of testing at different conditions as going to be emphasized further in Chapter VI [36].

The elastomer compatibility test implemented among both experimental sets 1 and 2 was carried out according to ASTM D471 which can be summarized as follows:

1. The oil bath is filled with oil till the half of the metal container and the device is switched on. Then, the temperature of the system is set to temperature of 40 ^{o}C.
2. The cleaned long glass tubes are filled with 100 ml of tested samples. Next, the tested elastomers are hanged out on metal hooks and poured inside the tested samples while the strings are tightly hold by the tubes cap. The tubes have to be tightly closed to avoid any evaporation to tested samples as the test takes place.
3. The elastomers are removed out thereafter from the bath for mass and volume measurements according to following schedule stated in ASTM D471: first day, third day, ninth day, and day 43 [37].
4. The elastomer is dried very well with special filtration paper. Then, the elastomer is dipped quickly into beaker filled with acetone and dried with filtration paper again, to remove any tested sample residue before measurement. Next, the weight of the elastomer is measured using balance zeroed after it is equipped with beaker filled with

water. After that, the elastomer is dipped quickly into beaker filled with ethanol to remove any water residues on the body. Then, the thickness of the elastomer is measured to high accuracy using digital caliber. Finally, the elastomer is returned back to the hook again and placed inside the tube for further measurements at subsequent mentioned schedule.

CHAPTER V

MODELING AND OPTIMIZATION

This chapter discusses the attempts been done on the data of first experimental set studying the influence of composition on GTL synthetic fuel properties, to generate models for the five properties under study, and optimize the blending strategy between Shell GTL SPK and local Jet A-1 through specialized LINGO optimization software. The following subsections summarize the approach been followed to come up with correlative models for the properties of interest. In addition, provide step-by-step description of developed LINGO formulation.

PROPERTIES CORRELATIVE MODELS

Four different correlative models were developed for the five properties under study using Excel 'Solver' feature; these models describe the behavior of density, net heat of combustion, flash point, and freezing point with respect to GTL SPK mixture compositions. The fifth model describing the viscosity property was realized to be unnecessary for the optimization path, since all the tested blends which covered most of the critical areas among the ternary diagram were observed to rely within the ASTM D1655 limit. Thus, further analysis was suspended and optimization attempts carried on with current developed correlative models. Following context explains briefly the approach been followed to develop these models.

Density model was the easiest one to develop. Since density experiences a perfect linear profile as going to be emphasized in the coming chapter. The linear profile makes it relatively simpler to deal with. A famous mathematical relation considering the reciprocal of weighted sum of mass compositions was located in the literature [28]:

$$\bar{\rho} = 1/\sum_{i=1}^{i=3} \frac{\omega_i}{\rho_i} \quad (1)$$

However, all the models are required to be in mole fractions in order to facilitate the optimization search. Therefore, the mass fractions in the model are converted into mole fractions using the following equation while assuming a basis of 1.00 g [28]:

$$\omega_i = \frac{(x_i \; x \; 1.00) \; x \; Mw_i}{\sum_{i=1}^{3}(x_i \; x \; 1.00) \; x \; Mw_i} \quad (5)$$

The data were estimated based on the first mathematical model and compared with experimental values obtained from density meter. The relative errors were very small and in turn the average error of the whole data was less than 1%. However, still few 'Solver' attempts were done on highest relative errors to minimize the average error. The maximum and average errors were reduced to 0.94% and 0.11%, respectively. Figure 14 shows the perfect match between predicted and experimental density data.

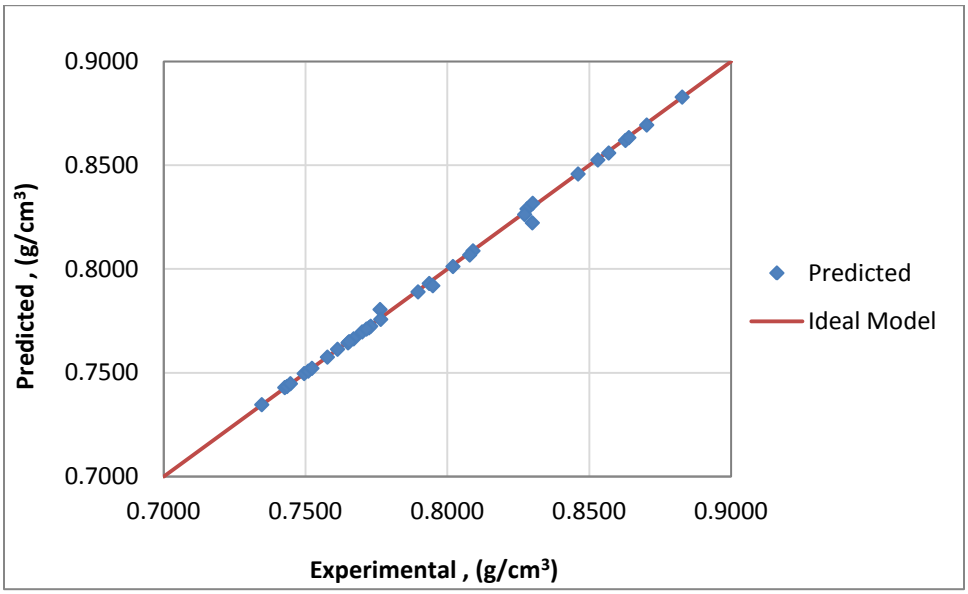

Figure 14. The accuracy of developed model for density property.

Net heat of combustion model was another easy one to develop. Literature presents the mathematical model for any change in heat as the weighted sum of the molar compositions multiplied into pure components values as follows [29]:

$$\overline{\Delta H_{comb}} = \sum_{i=1}^{n=3} x_i \Delta H_{comb,i} \quad (2)$$

The data were estimated based on this mathematical model and compared with experimental values obtained from bomb calorimeter. The relative errors and average error of the whole data were a little higher than the density case. Thus, several 'Solver' attempts were done on highest relative errors to minimize the average error. The maximum and average errors were reduced to 0.64% and 0.55%, respectively. Figure 15

shows the excellent match between predicted and experimental net heat of combustion data.

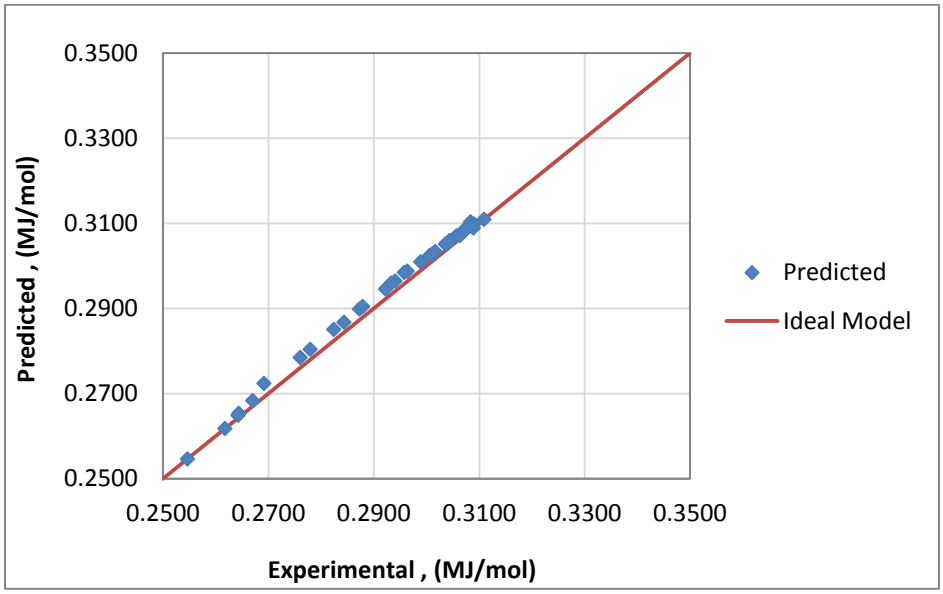

Figure 15. The accuracy of developed model for net heat of combustion property.

The difficulty started by generating correlative model for flash point property. Extensive research has been implemented earlier in this field, since flash point is a crucial property that serves as a significant safety measure for the mixture. The major challenge faced at this stage is the selection of suitable model to describe the behavior of current hydrocarbons mixtures, and the proper manipulation to adapt the case under study. Keshavarz model describing the behavior of hydrocarbon mixtures was found to be the best to describe the jet fuel mixtures. Keshavarz mathematical model is expressed as follows [30]:

$$FP(K) = A + 16.15\, n_c + 16.68\, ISP - 24.71\, DSP \quad (3)$$

Keshavarz model is for predicting flash points of single components. Furthermore, several model specialized parameters need to be estimated. Thus, these were the issues been raised where the model had to be fitted to ternary hydrocarbon mixtures. This issue was resolved by considering the weighted sum of molar compositions multiplied into respective 'A' parameters, carbon numbers, increasing structural parameters, and decreasing structural parameters (M. Castier, oral communication, September 2012). Both ISP and DSP parameters recommended in the paper were realized not applicable to current mixtures under study and therefore they were assigned with zero values. However, the 'A' parameters had to be manipulated using Excel 'Solver' since the listed ones do not suit the application under consideration directly. Finally, the carbon numbers of *n*-decane and decalin are known explicitly as 10. On the other hand, the average carbon number of Shell Sol-T was obtained as 12 from confidential document provided by the supplier. The resulted model was associated with maximum and average errors of 2.14% and 0.75%, respectively. Figure 16 illustrates the small deviation in predicted flash points with respect to ideal model.

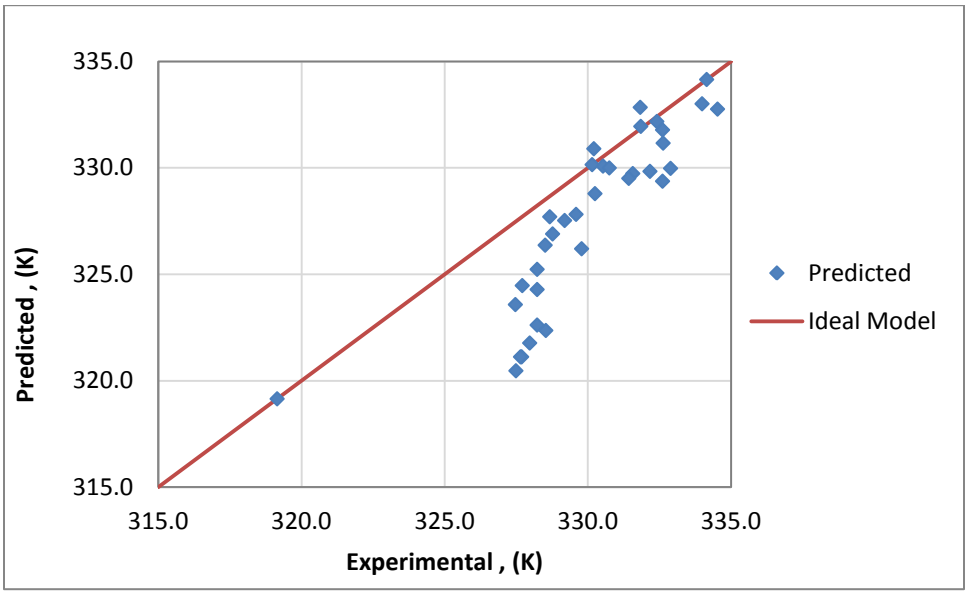

Figure 16. The prediction of developed flash point model.

Freezing point model was the last model to develop for this study. Freezing point model was another difficult task to tackle, since there was no related models could be located in literature. Accordingly, random non-linear models were tested to comply with the observation been obtained as going to be highlighted in the following chapter. Table 7 lists down the various non-linear models tested on freezing point data together with associated maximum and average errors. Figure 17 emphasizes the larger discrepancy in predicted freezing point data due to the several sources of error explained in previous chapter.

Table 7. The random non-linear models tested on freezing point data.

Freezing Point Tested Models	Maximum Error	Average Error
$243.15\ x_{n-p}{}^{1.011} + 196.15\ x_{iso-p}{}^{0.845} + 230.15\ x_{cyclo-p}$	6.79 %	2.03 %
$243.15\ x_{n-p}{}^{0.932} + 196.15\ x_{iso-p}{}^{0.825} + 230.15\ x_{cyclo-p}{}^{1.112}$	7.23 %	1.98 %
$243.15\ x_{n-p}{}^{1.020} + 196.15\ x_{iso-p} + 230.15\ x_{cyclo-p}{}^{0.886}$	8.30 %	2.15 %
$243.15\ x_{n-p} + 196.15\ x_{iso-p}{}^{0.808} + 230.15\ x_{cyclo-p}{}^{1.051}$	7.05 %	2.00 %
$243.15\ x_{n-p}{}^{0.913} + 196.15\ x_{iso-p}{}^{0.905} + 230.15^{0.454}\ x_{cyclo-p}{}^{1.096}$	5.77 %	2.25 %

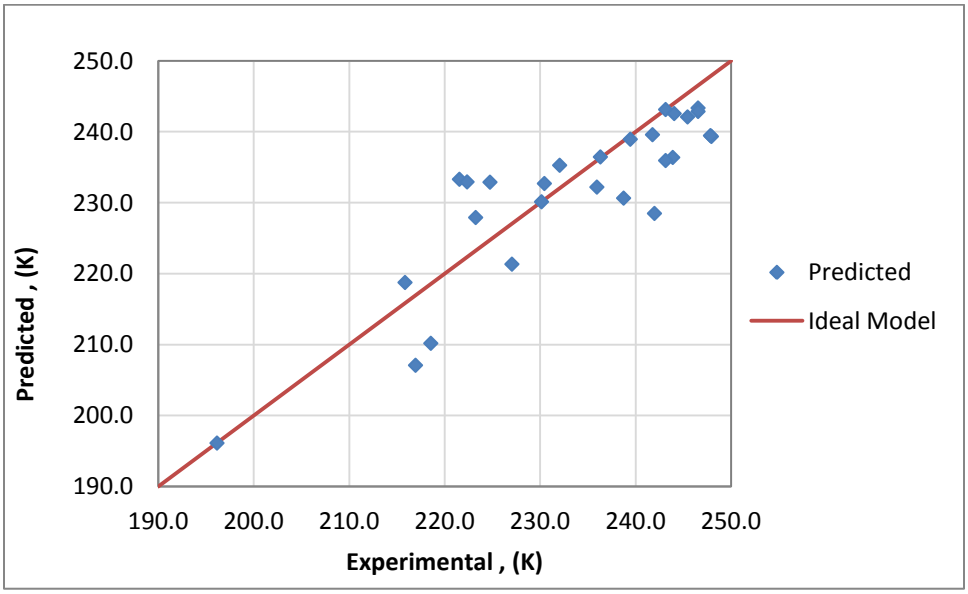

Figure 17. The large scatter in freezing point correlative model.

Table 8 summarizes the correlative models of the four properties under study been approved for further investigation into optimization attempt.

Table 8. Summary of correlative models developed for the properties of interest.

Analyzed Property	Developed Model	Maximum Error	Average Error
Density	$1/(\omega_{n-p}/0.73460 + \omega_{iso-p}/0.7613 + \omega_{cyclo-p}/0.88280)$	0.94 %	0.11 %
Net Heat of Combustion	$0.31094\ x_{n-p} + 0.25465\ x_{iso-p} + 0.30892\ x_{cyclo-p}$	1.20 %	0.55 %
Flash Point	$(157.6\ x_{n-p} + 168.6\ x_{iso-p} + 140.3\ x_{cyclo-p}) + (10\ x_{n-p} + 12\ x_{iso-p} + 10\ x_{cyclo-p}) + (0.000\ x_{n-p} + 0.000\ x_{iso-p} + 0.000\ x_{cyclo-p}) + (0.000\ x_{n-p} + 0.000\ x_{iso-p} + 0.000\ x_{cyclo-p})$	2.14 %	0.75 %
Freezing Point	$243.15\ x_{n-p} + 196.15\ x_{iso-p}{}^{0.902} + 230.15\ x_{cyclo-p}$	5.57 %	2.21 %

LINGO FORMULATION DESCRIPTION

LINGO is a powerful optimization software that has the ability to minimize or maximize a specified objective function, while it is supported with number of directive constraints. It is important to note here that minimizing the number of constraints input to the program, facilitates the overall optimization attempt of the software by providing more flexibilities to locate the local or global minimum/maximum of the objective function. That's why the viscosity correlative model was unnecessary to complete the description of GTL SPK mixing correlations. Two different cases were established for this jet fuels optimization problem. The first case locates the minimum price of jet fuels blending, while it is kept free for the software to determine the appropriate GTL SPK fractions for satisfying the condition. This case looks quite difficult to apply in reality since here the conditions and in turn the catalyst environment have to be manipulated properly, in order to have the required GTL SPK fractions needed for the blending as suggested by the

program. In addition, it is important to note here that the resulted combination of GTL SPK fractions in this case is one of several possibilities that satisfy current conditions. Therefore, another case was initiated to express a closer application to reality, where the price of jet fuels blending is again minimized. However, this time the specific combination of GTL SPK fractions exists among the available stock is added to the formulation.

Table 9 explains in depth every set of statements in the LINGO formulation that was developed to optimize the blending strategy between GTL SPK and Jet A-1 and is located in Appendix B. It is important to note here that each executive statement should be terminated with semicolon. In addition, notes can be placed in the formulation without been executed in the code by preceding the statement with explanation mark.

Table 9. LINGO formulation statements description.

Set of Statements	Description
`Min = (GTL_SPK_VolP*GTL_SPK_Cost) + (Jet_A1_VolP*Jet_A1_Cost);`	• Objective function of the formulation. • Minimizing the objective function by considering: jet fuels production costs and jet fuels blending ratios.
`Jet_A1_VolP = 1.00 - GTL_SPK_VolP;`	• The final mix composed of two different jet fuels: GTL SPK and Jet A-1.

Table 9. Continued.

Set of Statements	Description

`GTL_Subsidy = 25;`
 	
`Jet_A1_Cost = 128.6;`
`GTL_SPK_Cost = 150.0 - GTL_Subsidy;`
	• Reduction in GTL SPK price as matter of governmental subsidy to produce a more greener fuel.
	• Gathered Jet A-1 cost from IATA website [38].
	• Estimated GTL SPK production cost (N. O. Elbashir, oral communication, August 2012).

`Case (1):`
`GTL_SPK_V_NP + GTL_SPK_V_IP + GTL_SPK_V_CP = 1.0000;`
 	
`Case (2):`
`GTL_SPK_V_NP = 0.4340;`
`GTL_SPK_V_IP = 0.5570;`
`GTL_SPK_V_CP = 0.0090;`
	• The only difference in cases formulations:
	• Stating explicitly that GTL SPK is composed of three main components: *n*-, *iso*-, and *cyclo*-paraffins.
	• The sum of fractions should be equated to unity.
	• Feeding in known combination of GTL SPK fractions in available stock.

`Jet_A1_V_NP_IP = 0.5878;`
`Jet_A1_V_CP = 0.2131;`
`Jet_A1_V_Aromatics = 0.1991;`
	• Providing respective compositions of a model Jet A-1 sample found in the literature.

`Density_GTL_SPK = 1/((GTL_SPK_V_NP/87.59838) + (GTL_SPK_V_IP/90.78226) + (GTL_SPK_V_CP/105.27069));`	• First correlative model for estimating density of GTL SPK mixture in the jet fuels mixture. • The pure densities were converted into volume basis, where current values are in kg/bbl.
`Net_Heat_of_Combustion_GTL_SPK = (3875.352*GTL_SPK_V_NP) + (3976.262*GTL_SPK_V_IP) + (4495.623*GTL_SPK_V_CP);`	• Second correlative model for estimating net heat of combustion of GTL SPK mixture in the jet fuels mixture. • The pure values were converted into volume basis, where current values are in MJ/bbl.

Table 9. Continued.

Set of Statements	Description

`Flash_Point_GTL_SPK = A_Bar + Cn_Bar;`
`A_Bar = (157.6*GTL_SPK_V_NP) + (168.6*GTL_SPK_V_IP) + (140.3*GTL_SPK_V_CP);`
`Cn_Bar = 16.15*((10*GTL_SPK_V_NP) + (12*GTL_SPK_V_IP) + (10*GTL_SPK_V_CP));`
	• Third correlative model for estimating flash point of GTL SPK mixture in the jet fuels mixture.

`Freezing_Point_GTL_SPK = (243.15*GTL_SPK_V_NP) + (196.15*(GTL_SPK_V_IP^(0.902)) ) + (230.15*GTL_SPK_V_CP);`	• Fourth correlative model for estimating freezing point of GTL SPK mixture in the jet fuels mixture.

`Jet_A1_Density = 94.02576;`
`Jet_A1_Net_Heat_of_Combustion = 4082.627;`
`Jet_A1_Flash_Point = 314.05;`
`Jet_A1_Freezing_Point = 218.85;`
	• The relative properties of Jet A-1 measured in the Fuel Characterization Laboratory, expressed in terms of volume basis.

`Mix_Density = (Jet_A1_Density*Jet_A1_VolP) + (Density_GTL_SPK*GTL_SPK_VolP) ;`	• Estimating the average density of final mix between GTL SPK and Jet A-1.
`Mix_Net_Heat_of_Combustion = (Jet_A1_Net_Heat_of_Combustion *Jet_A1_VolP) + (Net_Heat_of_Combustion_GTL_SPK*GTL_SPK_VolP);`	• Estimating the average neat heat of combustion of final mix between GTL SPK and Jet A-1.
`Mix_Freezing_Point = (Jet_A1_Freezing_Point*Jet_A1_VolP) + (Freezing_Point_GTL_SPK*GTL_SPK_VolP);`	• Estimating the average freezing point of final mix between GTL SPK and Jet A-1.
`Mix_Flash_Point = (Jet_A1_Flash_Point*Jet_A1_VolP) + (Flash_Point_GTL_SPK*GTL_SPK_VolP);`	• Estimating the average flash point of final mix between GTL SPK and Jet A-1.

Table 9. Continued.

Set of Statements	Description
`Mix_Density >= 92.41593;` `Mix_Density <= 100.16694;`	• First main constraint for density. The density has to be bounded by ASTM D1655 limits (0.775 – 0.8400 g/cm^3) [14].
`Net_Heat_of_Combustion_GTL_SPK >= (42.80000*Density_GTL_SPK);`	• Second main constraint for net heat of combustion. The net het of combustion has to be upper than the single limit of ASTM D1655 (42.8 MJ/kg) [14].
`Flash_Point_GTL_SPK >= 311.15;`	• Third main constraint for flash point. The flash point has to be upper than the single limit of ASTM D1655 (38.0 ^{o}C) [14].
`Freezing_Point_GTL_SPK <= 226.15;`	• Fourth main constraint for freezing point. The freezing point has to be lower than the single limit of ASTM D1655 (-47.0 ^{o}C) [14].

CHAPTER V

RESULTS AND DISCUSSIONS

This chapter presents the outcomes been gathered in the three experimental campaigns conducted through this study. The first and second sections highlight the main results revealed in the first and second experimental sets, which were implemented through previous studies by the research team, respectively. While, the third section underlines the results of third experimental set that is considered as the principal contribution to the study, showing the effect of jet fuel binary mixture on the overall property of the mixture. In addition, the impact of combined *normal*- and *iso*-paraffins including *cyclo*-paraffins on the average property of the mixture. The analyses exclude the aromatics due to the similarity of the trends of the properties with respect to *cyclo*-paraffins and aromatics as emphasized through Appendix F. Furthermore, statistical analysis done by a research team member will be presented further.

FIRST EXPERIMENTAL TESTING SET

This experimental campaign studied the impact of GTL SPK building blocks on the properties of the jet fuel mixture. The study was based on a total of 32 binary and ternary mixtures prepared from GTL SPK base components: *n*-paraffins represented by *n*-decane ($C_{10}H_{22}$), *iso*-paraffins represented by special solvent obtained from Shell (Shell Sol T), and *cyclo*-paraffins represented by decalin ($C_{10}H_{20}$). In order to provide sufficient data points for describing the behavior of property through trained artificial neural

networks as going to highlighted further in the context. Table 10 shows the compositions of GTL SPK mixtures which were tested in the first experimental set.

Table 10. Tested blends of the first experimental set.

Tested Blend	*n*-Decane [*n*-Paraffins] (vol%)	Shell Sol-T [*iso*-Paraffins] (vol%)	Decalin [*cyclo*-Paraffins] (vol%)
IB1	0.00	24.94	75.07
IB2	0.00	49.87	50.13
IB3	33.33	33.25	33.42
IB4	20.00	19.95	60.05
IB5	10.00	29.92	60.08
IB6	0.00	74.81	25.20
IB7	20.00	59.84	20.16
IB8	42.00	41.89	16.11
IB9	60.00	29.92	10.08
IB10	66.00	16.96	17.04
IB11	75.00	0.00	25.00
IB12	60.00	14.96	25.04
IB13	42.00	15.96	42.04
IB14	50.00	0.00	50.00
IB15	30.00	9.97	60.03
IB16	25.00	0.00	75.00
IB17	17.00	41.89	41.11
IB18	11.00	63.83	25.17
IB19	49.00	49.87	1.13
IB20	74.00	24.94	1.07
IB21	5.00	89.77	5.23
IB22	5.00	84.78	10.22
IB23	10.00	84.78	5.22
IB24	10.00	79.79	10.21
IB25	5.00	4.99	90.01
IB26	10.00	4.99	85.01
IB27	5.00	9.97	85.03
IB28	10.00	9.97	80.03
IB29	90.00	4.99	5.01

Table 10. Continued.

Tested Blend	*n*-Decane [*n*-Paraffins] (vol%)	Shell Sol-T [*iso*-Paraffins] (vol%)	Decalin c*yclo*-Paraffins] (vol%)
IB30	85.00	4.99	10.01
IB31	85.00	9.97	5.03
IB32	80.00	9.97	10.03

Initial attempts by the research team in the jet fuel characterization field showed that the density test is an effective tool for blends confirmation, as there was clear coherence between experimental and predicted values using weighted sum of pure densities with respect to compositions as illustrated by Figure 18.

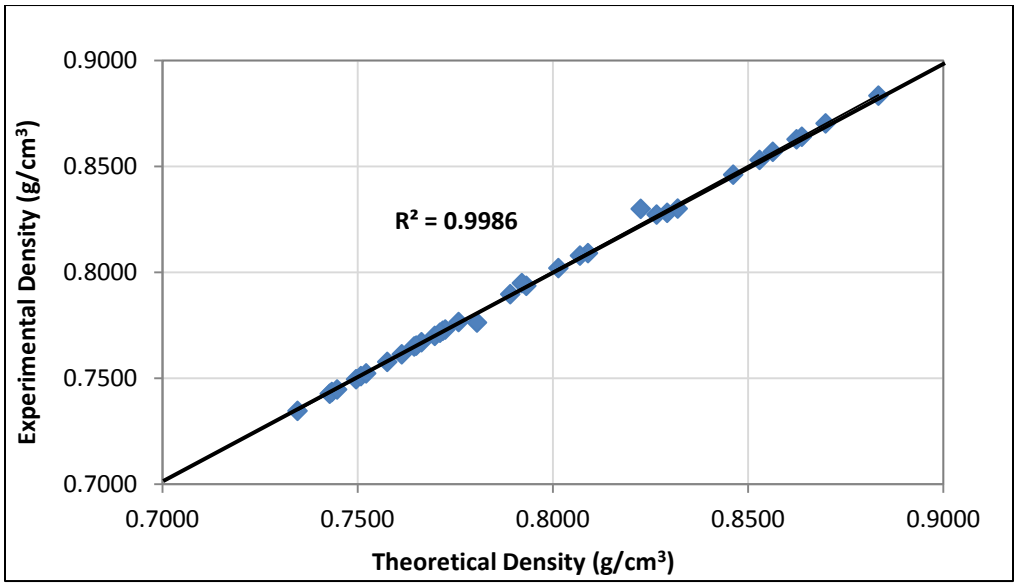

Figure 18. Coherence between experimental and theoretical densities.

The density of the majority of prepared blends was found to be outside the acceptable limits approved by ASTM D1655 that range between 0.7750 and 0.8400 g/cm^3. The recorded readings were bounded by lower boundary of 0.7346 and upper boundary of 0.8828 g/cm^3 [26]. Both of *n*-Decane and Shell Sol T were observed to have lower densities than the lower limit of 0.7346 and 0.7613 g/cm^3, respectively. On the other hand, decalin was found to have a higher density than the upper limit of 0.8828 g/cm^3. Meanwhile, the density was noticed to increase nearly linearly with increase in *cyclo*-paraffins content as shown in Figure 19. The slight deviation of least squares error R^2 from perfect linear behavior (1.0000) is due to the experimental error accounted for large population of data points. The perfect linear relationship will be highlighted through smaller number of data points as the case in third experimental set.

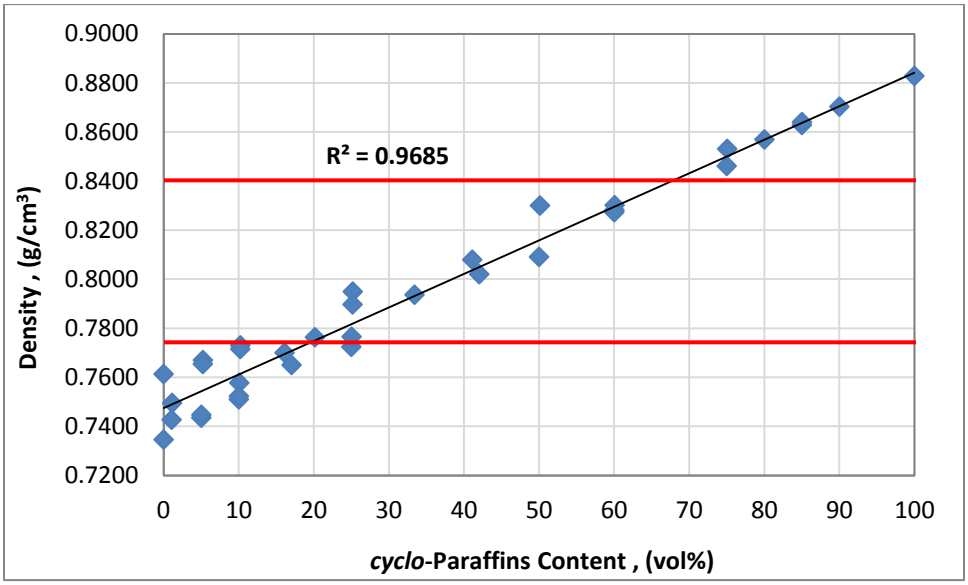

Figure 19. Density with respect to *cyclo*-paraffins content in jet fuel mixture. (Red lines represent the lower and upper boundaries of ASTM D1655).

The net heat of combustion for most of the blends was found to meet the limit of ASTM D1655 that is bounded by lower boundary of minimum of 42.8 MJ/kg. Three remaining samples with high *cyclo*-paraffins content were associated with lower values approaching minimum of 42.68 MJ/kg. Meanwhile, the mixture property was noticed to decrease nearly linearly with increase in *cyclo*-paraffins content as illustrated through Figure 20. Another important point to highlight here is that the values of both decane and Shell Sol-T were above the limit while decalin was slightly lower than the limit.

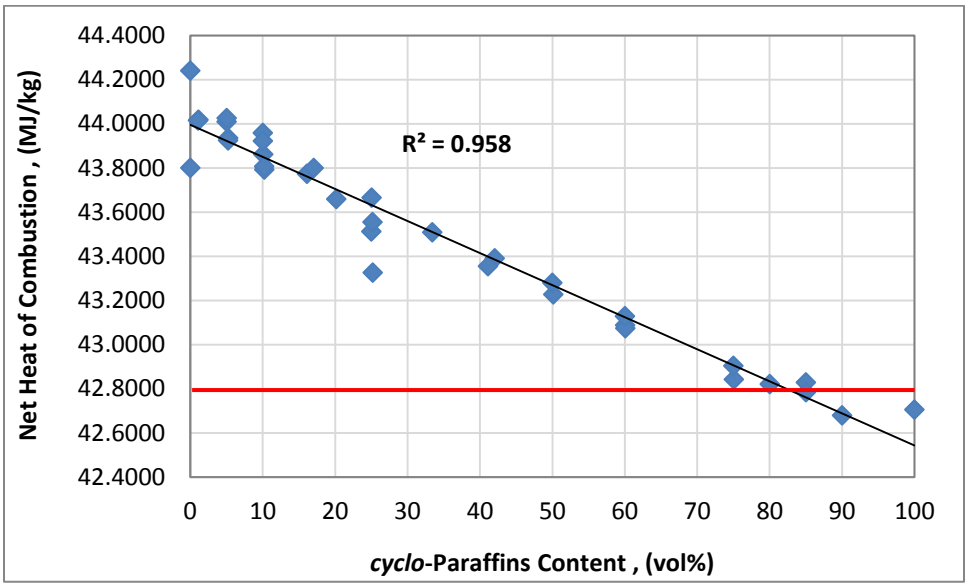

Figure 20. Net heat of combustion with respect to *cylco*-paraffins content in jet fuel mixture. (Red line represents the single boundary of ASTM D1655).

Flash points of the entire tested blends were observed to rely within the acceptable limit of ASTM D1655 that is bounded by single boundary of minimum of 38.0 ^{o}C. Flash point experienced a quite non-linear or strictly speaking a scattered trend

along the *cyclo*-paraffins content, at the time where noticeable decreasing behavior was obtained with respect to *normal*-paraffins content as illustrated through Figure 21. The data points were bounded by a minimum value of 46.0 ^{o}C attributed to pure *n*-decane and a maximum value of 61.4 ^{o}C.

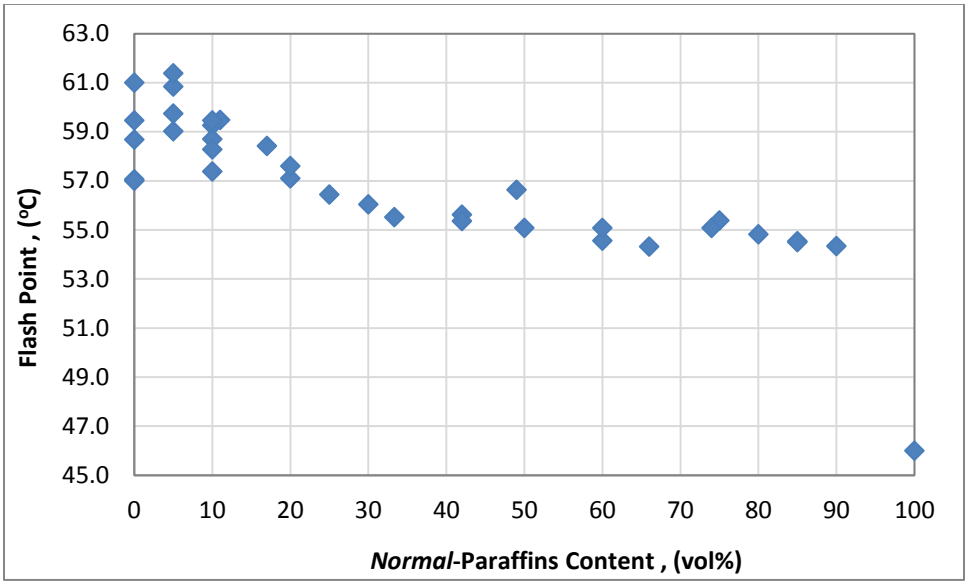

Figure 21. Flash point with respect to *normal*-paraffins content in jet fuel mixture.

Freezing points of few of the tested blends were realized to exist among the acceptable limit of ASTM D1655 that is bounded by single boundary of minimum of -47.0 ^{o}C. With another 8 blends experienced a freezing point lower than -75.0 ^{o}C, which sets the limitation of the freezing point device. Freezing point is ether like the flash point property experienced a quite non-linear or strictly speaking a scattered trend along the

cyclo-paraffins content, at the time where noticeable increasing behavior was observed with respect to *normal*-paraffins content as illustrated through Figure 22.

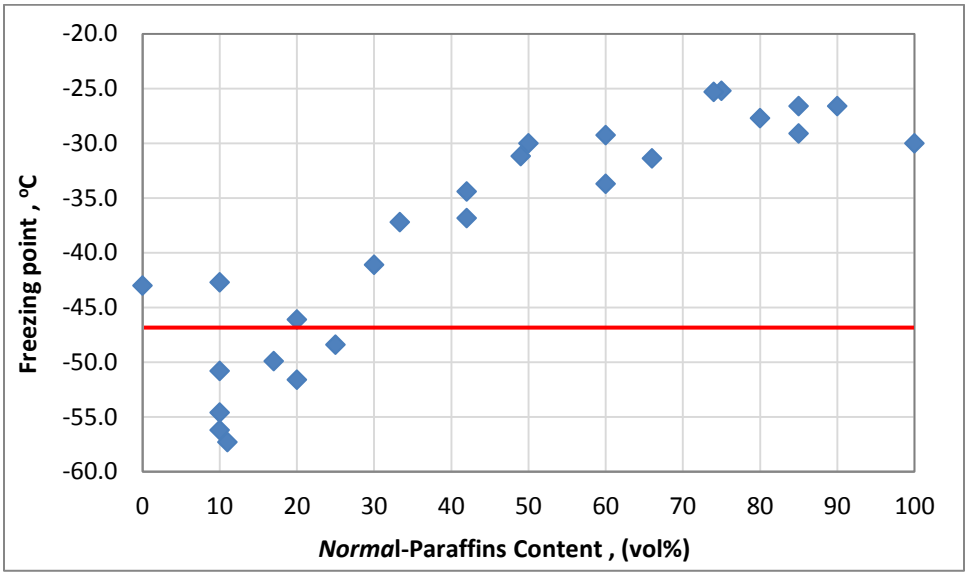

Figure 22. Freezing point with respect to *normal*-paraffins content in jet fuel mixture. (Red line represents the single boundary of ASTM D1655).

Viscosity of this set of experiment is another significant contribution to this study, as the data were required to be generated to refine further the characterization of the jet fuel, and generate correlative model needed for previous chapter. The viscosity of the entire tested blends was revealed to rely within the acceptable limit of ASTM D1655 that is bounded by a single boundary of maximum of 8.0000 mm^2/s (cst). An overall decreasing trend was observed for the viscosity in regard to *normal*-paraffins content as shown through Figure 23. The data points were bounded by a minimum value of 2.5708

mm^2/s attributed to pure *n*-decane and a maximum value of 7.5215 mm^2/s attributed to decalin.

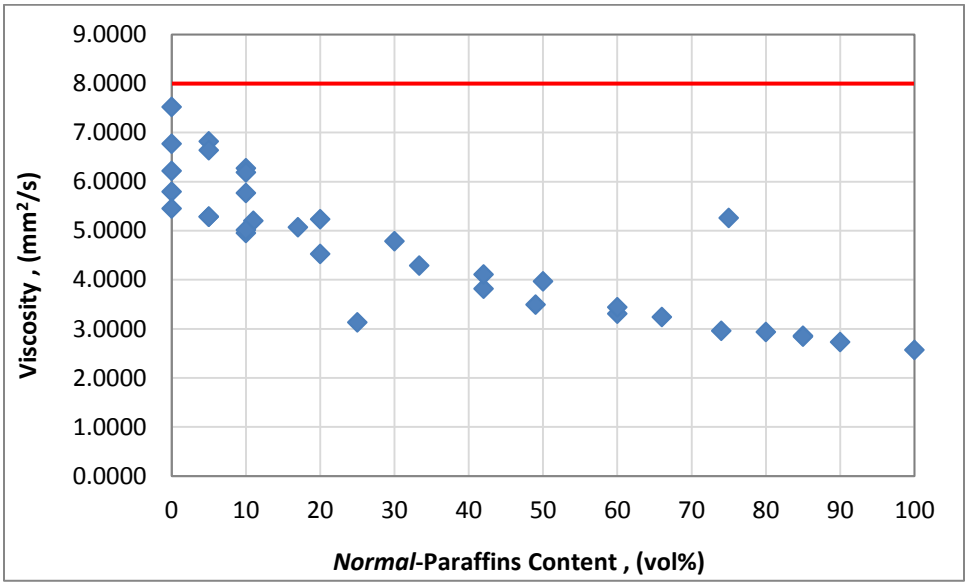

Figure 23. Viscosity with respect to *normal*-paraffins content in jet fuel mixture. (Red line represents the single boundary of ASTM D1655).

The following subsection provides a brief overview about the outcomes obtained in elastomers compatibility testing in regard to paraffins building blocks.

Elastomers Compatibility Testing based on Paraffinic Building Blocks

Four different paraffinic based components were considered for this set of experiment: *n*-decane, decalin, Shell Sol-T, and GTL SPK. It can be clearly seen that initial attempts were attributed to pure components or perfectly mixed industrial mixtures without any attention given to prepared blends. In order to build a solid ground for further studies

and verify the reliability of results in comparison to preceding studies in the field. The test was carried out according to ASTM D471 procedure explained in Chapter IV. Further context underlines the main outcomes gathered with respect to mass change, and overlook the volume change related outcomes, due to technical challenges faced by the research team and other researchers done the work previously.

It was revealed that all the tested components experienced noticeable increase in O-rings weight during the first 24 hours, highlighting the sharp increase of decalin to nearly 15% as illustrated through Figure 24. This observation should be regarded as positive impact to the fuel system, since the elastomers will swell and accordingly stay tight in their positions. However, gradual decrease in all the trends was observed after first day indicating undesirable impact where the elastomers will shrink and may allow the fuel to leak from the fuel system. This phenomenon was attributed to the chemical ability of hydrocarbons to remove filling materials and plasticizers from the O-rings, detected using ESEM analysis, which is beyond the scope of this study [39]. Figure 25 emphasizes the average of mass change of all tested components after the completion of the test. The obtained results were in good agreement with Professor Wilson work which was based on dynamic testing. Table 11 shows the difference between research team data and Professor Wilson's team data on dynamic testing.

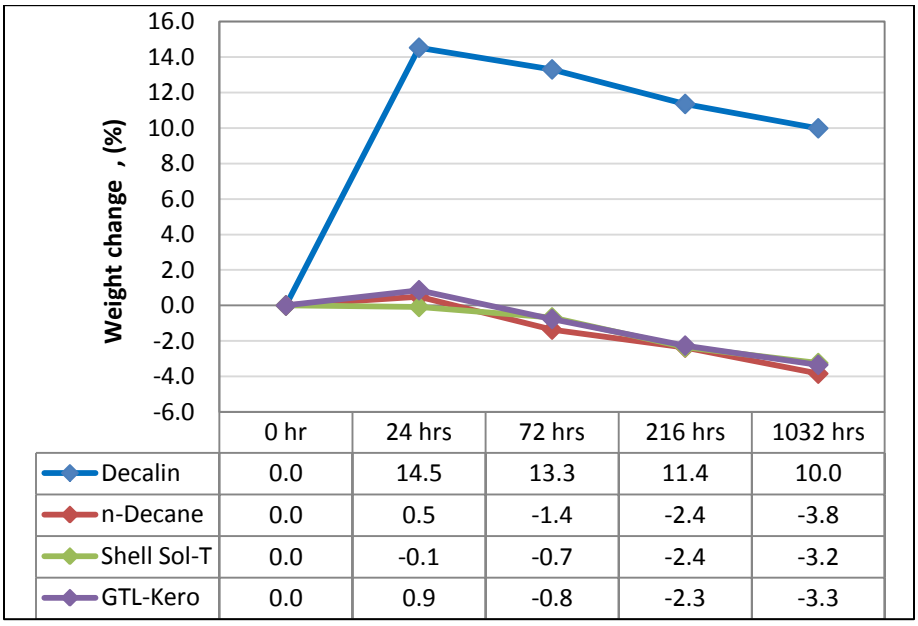

	0 hr	24 hrs	72 hrs	216 hrs	1032 hrs
Decalin	0.0	14.5	13.3	11.4	10.0
n-Decane	0.0	0.5	-1.4	-2.4	-3.8
Shell Sol-T	0.0	-0.1	-0.7	-2.4	-3.2
GTL-Kero	0.0	0.9	-0.8	-2.3	-3.3

Figure 24. Weight change of elastomers with respect to paraffinic components [39]. (GTL Kero is the product name of GTL SPK by Shell).

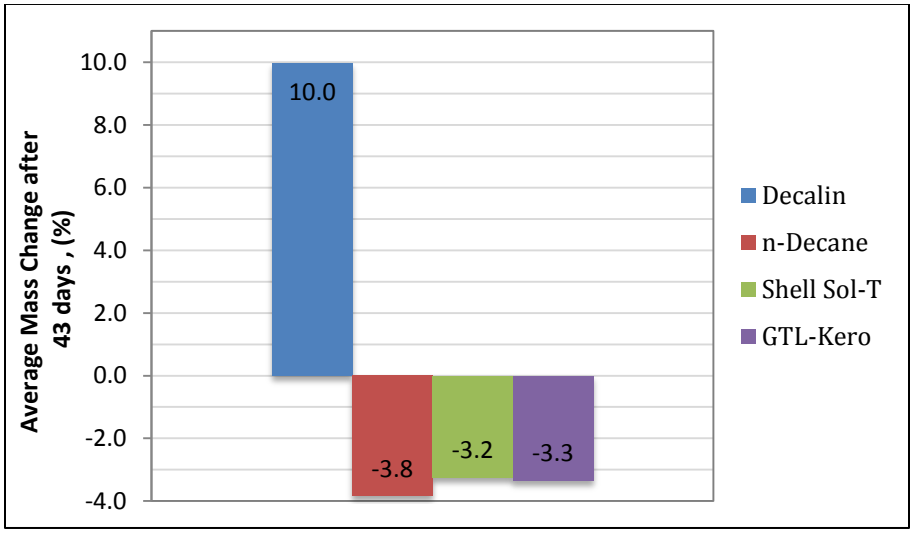

Figure 25. Average weight change of elastomers with respect to paraffinic components after completion of the test [39].

Table 11. Comparison between research team and Professor Wilson analysis [39].

Research Work	Decalin	*n*-Decane	Shell Sol-T	GTL Kero
Professor Wilson	10.0%	-2.0%	-2.7%	-1.7%
Research Team	10.0%	-3.8%	-3.2%	-3.3%

Statistical Analysis for Paraffinic Based Hydrocarbons

The resulted data for first experimental set were trained on Matlab based on specially developed programming code developed by one of the members in research team. The reason behind this statistical analysis is to continue the description of properties with respect to compositions by predicting the properties at untested points and generate reliable profiles for the whole ternary diagram.

Density had a very smooth profile along the *cyclo*-paraffins content which proved the linearity of the property. Then, net heat of combustion had nearly same reversed profile of density with respect to *cyclo*-paraffins content. Next, flash and freezing points were having unstable profiles where dramatic changes take place as going from the right to the left of the ternary diagram. After that, viscosity had a close profile to net heat of combustion with respect to *normal*-paraffins. Finally, an optimized plot was developed to show the region on the ternary diagram where all the properties meet the ASTM D1655 limits, with highest accuracy at the two dark red regions close to *cyclo*-paraffins and *iso*-paraffins apexes [27]. Nevertheless, the area of interest will be located at the bottom dark red spot where least *cyclo*-paraffins exist to maintain the net heat of combustion of the mixture. Artificial neural networks for the properties of interest together with the optimized plot are placed in Appendix G.

SECOND EXPERIMENTAL TESTING SET

This experimental campaign was initiated to refine the properties based on the outcomes from previous experimental set. Toluene as *mono*-aromatic was utilized in this study in order to introduce the aromatics to GTL SPK mixtures, and *cyclo*-paraffins were further investigated. The reason behind tackling these research paths is to improve the properties of jet fuel mixture, as it was noted earlier that *cyclo*-paraffins increases the density to rely within the ASTM D1655 limits, and follow up with recent studies in regard to elastomer compatibility and swelling behavior testing. Moreover, cyclo-paraffins were considered for further investigation since it was realized from resulted optimized region that the GTL SPK can be brought in, by adding specific percentages estimated between (30-70) vol% as illustrated through Figure 26. The study was based on a total of 20 binary and ternary mixtures divided into two main plans: Plan A studies the individual impact of *mono*-aromatics on the properties of GTL SPK, and plan B studies the effect of *cylco*-paraffins and *mono*-aromatics individually or combined together on the properties of GTL SPK. Table 12 lists the compositions of jet fuel mixtures which were tested in the two testing plans of this experimental set. It is important to point here that the properties analyses of GTL SPK mixtures with respect to *mono*-aromatics were bounded by 25 vol% to follow the ASTM D1655 requirements [14]. Thus, further graphs for these analyses are limited to small scale of 30 vol%.

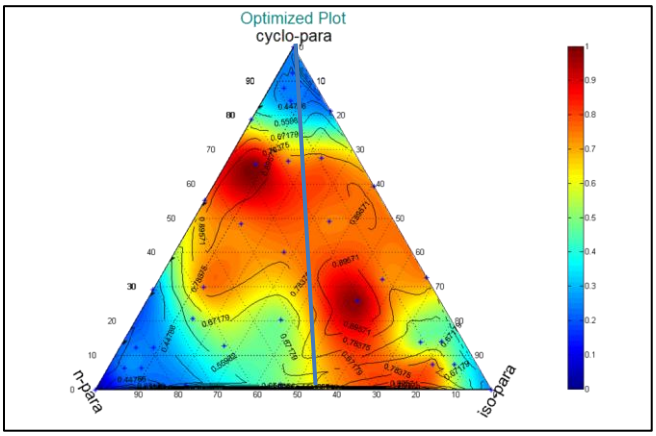

Figure 26. Improvement of GTL SPK properties using specific addition of *cyclo*-paraffins. (Blue line represents the region where GTL SPK could be brought in.

Table 12. Tested blends of the second experimental set.

Testing Plan	Tested Blend	Toluene [*Mono*-Aromatic] (vol%)	GTL SPK (vol%)	Decalin [*cyclo*-Paraffins] (vol%)	Total
Plan A	**IB 33**	1.00	99.00	0.00	100
	IB 34	2.00	98.00	0.00	100
	IB 35	5.00	95.00	0.00	100
	IB 36	8.00	92.00	0.00	100
	IB 37	10.00	90.00	0.00	100
	IB 38	15.00	85.00	0.00	100
	IB 39	25.00	85.00	0.00	100
Plan B	**IB 40**	0.00	30.00	70.00	100
	IB 41	0.00	40.00	60.00	100
	IB 42	0.00	45.00	55.00	100
	IB 43	0.00	50.00	50.00	100
	IB 44	0.00	55.00	45.00	100
	IB 45	0.00	60.00	40.00	100
	IB 46	0.00	70.00	30.00	100
	IB 47	1.00	39.00	60.00	100
	IB 48	3.00	27.00	70.00	100
	IB 49	3.00	47.00	50.00	100
	IB 50	3.00	67.00	30.00	100

Table 12. Continued.

Testing Plan	Tested Blend	Toluene [*Mono*-Aromatic] (vol%)	GTL SPK (vol%)	Decalin [*cyclo*-Paraffins] (vol%)	Total
Plan B	**IB 51**	5.00	35.00	60.00	100
	IB 52	5.00	55.00	40.00	100

Density test showed the expected linear increase in the density of jet fuel blends as the *mono*-aromatics are added. However, the increase in density did not qualify the blends to be within the acceptable limits of ASTM D1655, even with relatively large additions of 25 vol% as shown in Figure 27. Conversely, the density increased further as *cyclo*-paraffins are added separately to GTL SPK exceeding the upper boundary of ASTM D1655 limits slightly as illustrated through Figure 28. The densities for plan A were ranging between lowest end of 0.7396 and highest end of 0.7698 g/cm^3. On the other hand, the densities for plan B were relying within a region bounded by lower bound of 0.7778 and upper bound of 0.8658 g/cm^3.

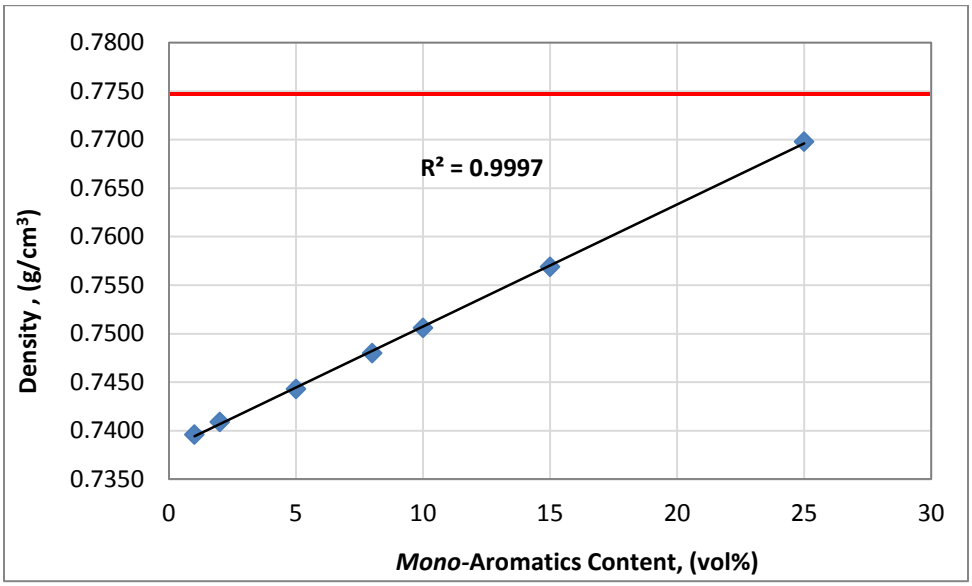

Figure 27. Density with respect to *mono*-aromatics content in jet fuel mixture. (Red line represents the lower boundary of ASTM D1655).

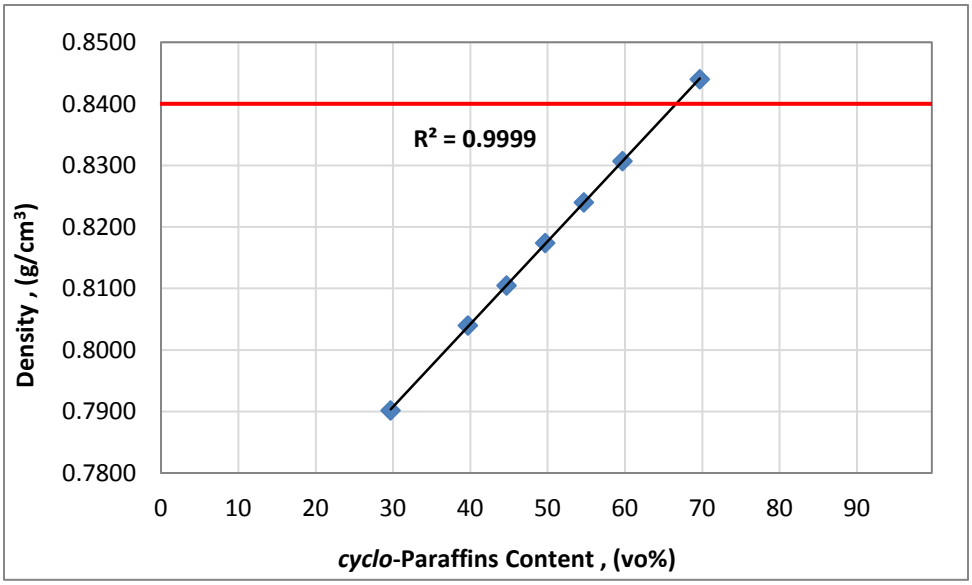

Figure 28. Density with respect to *cyclo*-paraffins content in GTL SPK mixture. (Red line represents the upper boundary of ASTM D1655).

The net heat of combustion for both tested plans was observed to decrease with nearly linear behavior, while it remains within the ASTM D1655 limit even after large additions of aromatics and *cyclo*-paraffins as illustrated through Figures 29 and 30, respectively. The values for plan A were found to rely among the region between 42.97 and 44.32 MJ/kg. Meanwhile, the values for plan B were realized to exist within the range between 43.31 and 43.85 MJ/kg.

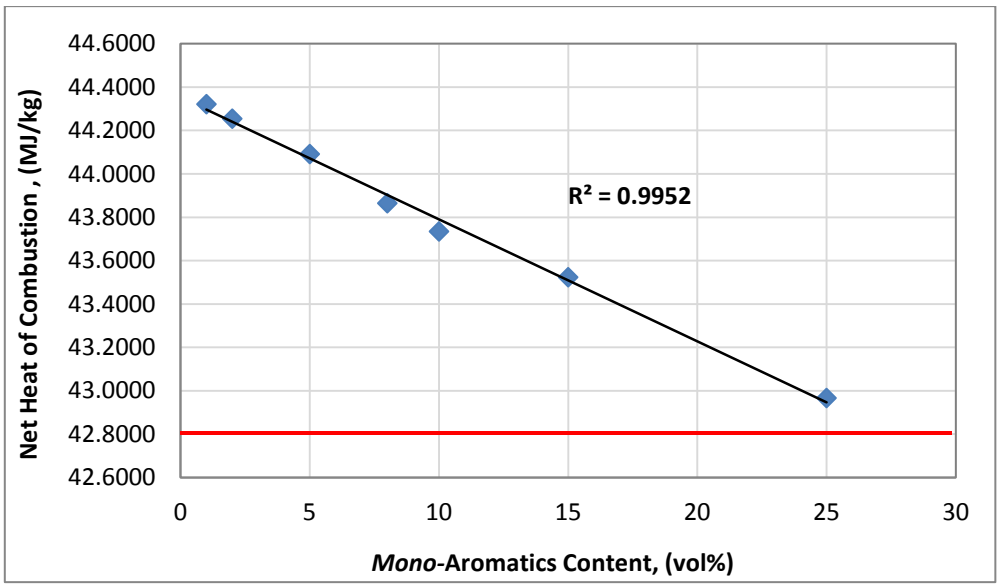

Figure 29. Net heat of combustion with respect to *mono*-aromatics content in jet fuel mixture. (Red line represents the single boundary of ASTM D1655).

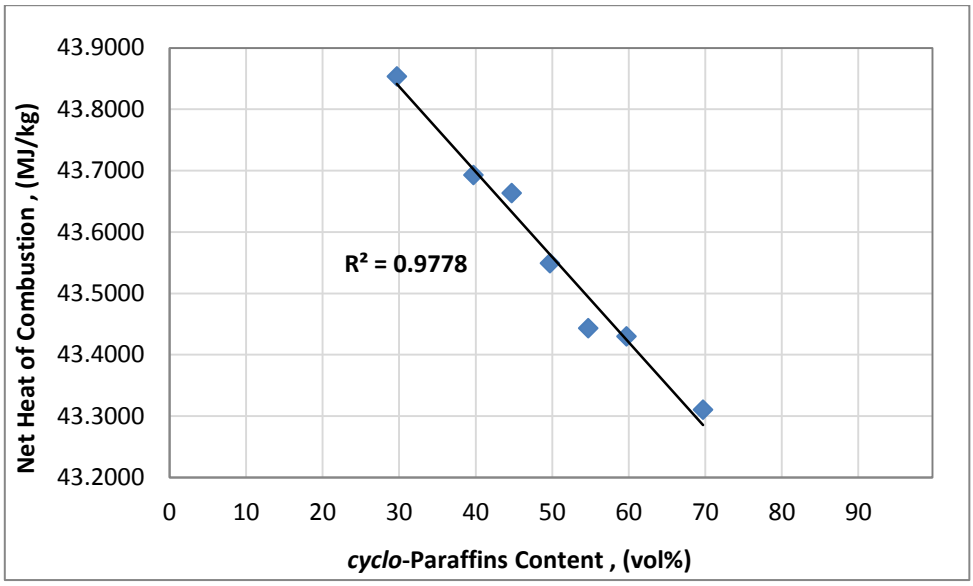

Figure 30. Net heat of combustion with respect to *cyclo*-paraffins content in GTL SPK mixture.

The flash point of tested blends was impacted negatively as the *mono*-aromatics content is increased in the jet fuel mixture. Only 2 out of 7 blends from plan A were found to meet the ASTM D1655 limit, while the rest were associated with lower flash points ranging between 20.8 and 34.4 ^{o}C as emphasized through Figure 31. On the other hand, no clear trend was able to extract from the generated data of testing plan B.

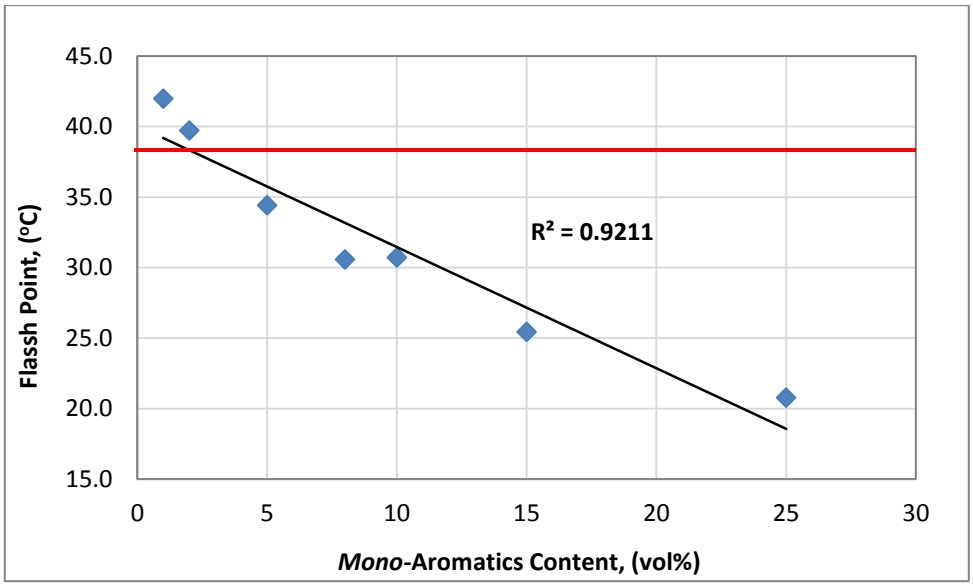

Figure 31. Flash point with respect to *mono*-aromatics content in jet fuel mixture. (Red line represents the single boundary of ASTM D1655).

Freezing point of tested blends was ether impacted negatively with increasing content in *mono*-aromatics. The freezing point was going to low temperatures approaching -59.0 ^{o}C in plan A and -49.0 ^{o}C in plan B. There was no clear trend to be observed in both plans A and B data. However, alternating trend was able to observe as shown in Figure 32.

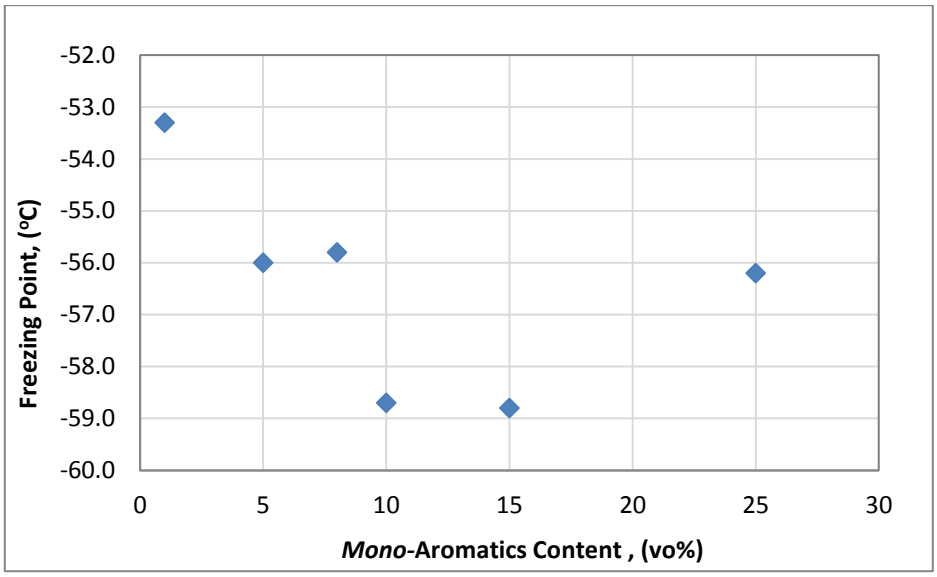

Figure 32. Freezing point with respect to *mono*-aromatics content in GTL SPK mixture.

Elastomer Compatibility Testing based on Aromatics Contribution

Six different blends containing percentages of aromatics 1, 2, 5, 8, 10, and 15% were considered for this set of experiment. This time some of the prepared blends were selected for the study, to mimic the upgraded GTL based jet fuel mixtures that contain appropriate extent of aromatics. In addition, a decent ground of work following ASTM D471 was established through first set of static testing.

The observations agreed with the expectations that jet fuel mixtures buffered with aromatics will swell more than aromatics-free mixtures. Furthermore, it was revealed that the extent of swelling increases with increasing aromatics content in the jet fuel mixture [39]. Nevertheless, previous studies implemented by Link showed that aromatics are not sufficient to provide the desirable swelling of O-rings in the fuel system; other additives are needed to support the stability of elastomers structure from

chemical point of view, such as phenols, naphthols, and benzyl alcohol [39]. Also, another interesting observation was gathered from this static testing, is that the O-rings gained weight as the aromatic content increased in the mixture after first and third day. Meanwhile, the weight loss increased substantially as the aromatics content is increased gradually. Figure 33 illustrates these two observations in this set of experiment.

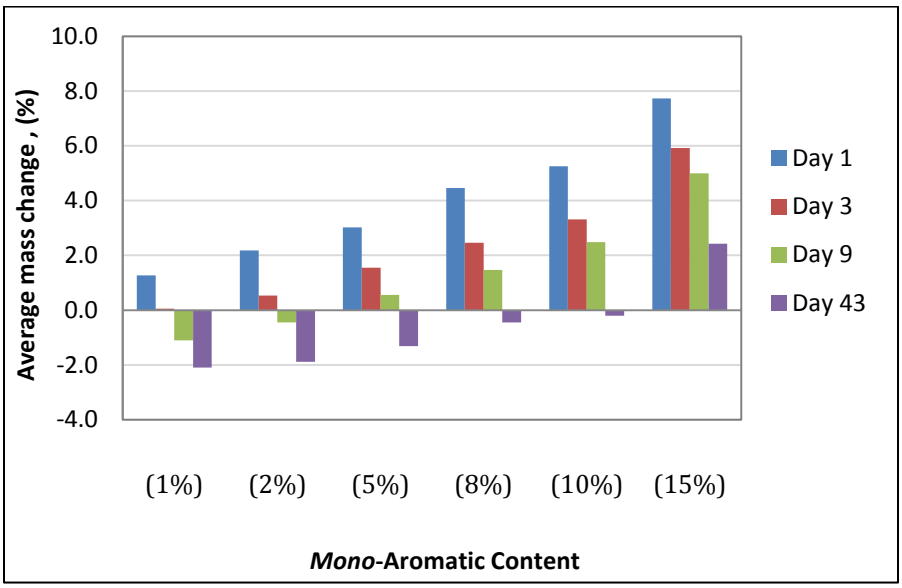

Figure 33. Average weight change with respect to aromatics based jet fuel mixtures [39].

THIRD EXPERIMENTAL TESTING SET

This experimental campaign studied the impact of jet fuels blending on the properties of the jet fuel mixture. The study was based on a total of 9 binary mixtures prepared from GTL SPK and Jet A-1 at an increment of 10 vol% of Jet A-1 from pure GTL SPK to pure Jet A-1, to provide sufficient data points for describing the behavior of property

with respect to jet fuels composition. Table 13 shows the compositions of jet fuel mixtures which were tested in the jet fuels blending study. Figure 34 illustrates the ternary diagram for the third experimental set.

Table 13. Jet fuels mixtures of the third experimental set.

Blend Name	Jet A-1 (%)	GTL SPK (%)	Total (%)
Shell GTL SPK	0	100	100
IA.IB1	10	90	100
IA.IB2	20	80	100
IA.IB3	30	70	100
IA.IB4	40	60	100
IA.IB5	50	50	100
IA.IB6	60	40	100
IA.IB7	70	30	100
IA.IB8	80	20	100
IA.IB9	90	10	100
Jet A-1 Q-Jet	100	0	100

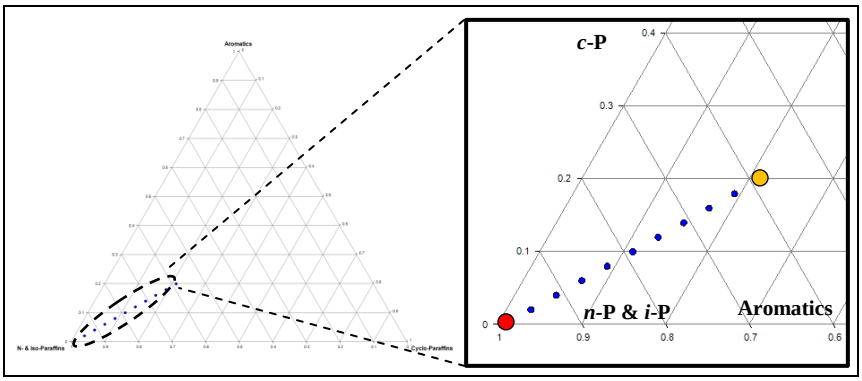

Figure 35. Jet fuel mixtures of third experimental set of the study. (Red and orange dots represent the pure GTL SPK and pure Jet A-1, respectively).

Figure 35 shows that a limited region around the combined *n*- and *iso*-paraffins apex was analyzed in this experimental set. Nevertheless, these data points represent the 10 vol% gradual increase in Jet A-1 content as going from pure GTL SPK to pure Jet A-1, based on the located compositions of Jet A-1 in literature [41]. This issue sets the limitation of this study and interprets the poor prediction of artificial neural network as going to be highlighted further in the context.

The experimental work of this part started after gathering Jet A-1 sample from Q-Jet, which acts as domestic supplier of jet fuels to air crafts at Doha International Airport. The sample had to be tested first to comply with the specifications provided in the certificate that is placed in Appendix E. All the required tests were implemented on pure Jet A-1 sample according to respective ASTM procedures, and the testing was terminated by having five consecutive readings within the ASTM repeatability limits. The results were in excellent match with the certificate specially those tests which were conducted based on the same testing procedure as emphasized through Appendix G.

To ensure the reliability of generated results, two extra confirmation tests beside the main density test were implemented. The first test was to allow two other certified operators in the lab to repeat two of the prepared blends, and measure their density according to respective ASTM D4052. In order to verify the reproducibility of generated data. Fortunately, the produced data were close enough to obtained ones earlier and were readily within the acceptable reproducibility limits in ASTM D4052 as highlighted through Appendix G. Furthermore, GC-MS and GC-FID were utilized to confirm the compositions of prepared jet fuel mixtures and ensure that they comply with the desired relative ratios at which they were prepared at. Appendix H illustrates the peak profiles of each of the tested blends in this experimental set together with relevant analysis to confirm the preparation of desired blending ratios.

The analysis of this study can be divided into two principal parts:

1. Binary mixture combinations influence on jet fuel properties.
2. Mixture building blocks impact on jet fuel properties.

The following subsections discusses the results been gathered through the study with regard to the influence of binary mixture combinations and mixture building blocks impact, respectively.

The Influence of Binary Mixture Combinations on Jet Fuel Properties

Density was the first property to be analyzed in this study, in order to confirm the blending strategy of the mixtures at the early stages of the campaign. Densities of all the tested blends were observed in perfect agreement with theoretical densities, which were

estimated through respective compositions and were associated with maximum deviation of 0.0002 g/cm^3 as shown in Appendix D. Moreover, the densities of all the blends were following a perfect linear trend with least squares error R^2 value exactly equal to 1 as illustrated through Figure 35.

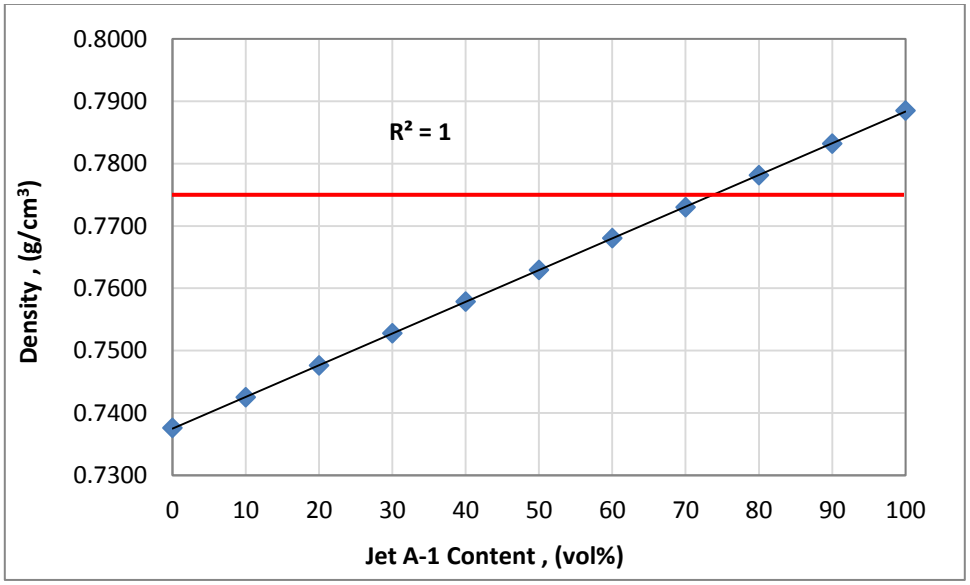

Figure 35. Density with respect to jet fuels binary mixture combinations. (Red line represents the lower bound of ASTM D1655).

It was observed that only two blends out of the nine tested blends were within the ASTM D1655 limits that range between 0.7750 to 0.8400 g/cm^3. Blend IA.IB5 which represents the 50:50 blend which was tested by Qatar Airways earlier, surprisingly was realized to be slightly lower than the lower border of ASTM D1655 with average value of 0.7629 g/cm^3. The probable reasons behind this observation are either special additives were added to the blend which caused desired increase in the mixture density,

or another heavier cut of conventional fuel was blended with synthetic jet fuel cut. This observation is in agreement with previous study highlighted earlier in chapter I, where nearly same conventional and synthetic jet fuels blended together up to 50 vol% [22].

Viscosity was the second property to be tested in this experimental set. All the tested blends were realized to exist within the ASTM D1655 limit of viscosity below than 8.0000 mm^2/s (cst) .Viscosities of all the tested blends were again found to follow almost linear behavior with least squares error R^2 of 0.9953. The property trend was revealed to increase with increasing Jet A-1 content, from pure GTL SPK at 2.5202 mm^2/s to pure Jet A-1 at 3.3850 mm^2/s as shown through Figure 36. In other words, the pure components were setting the limiting boundaries for all the tested blends.

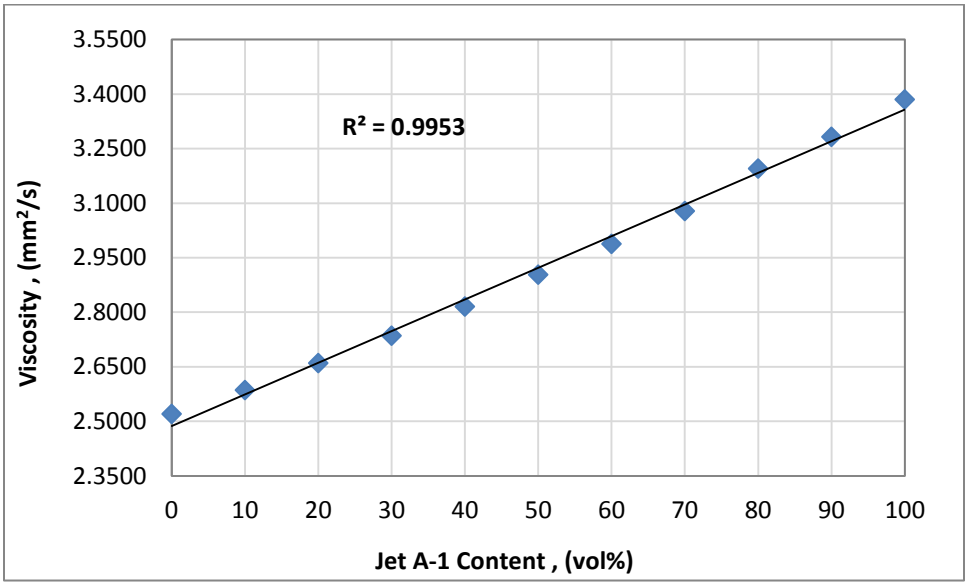

Figure 36. Viscosity with respect to jet fuels binary mixture combinations.

Net heat of combustion was the third property to be analyzed in this study. A slightly different observation in this property was observed compared to similar test in second experimental set. Although the aromatics content was increasing in the blends with increasing Jet A-1 content, still all the tested blends were qualified to exist within the ASTM D1655 limit of net heat of combustion more than 42.8 MJ/kg. Furthermore, an overall decreasing trend was observed throughout the data points, where the net heat of combustion for the jet fuels binary mixture varies between 43.42 and 44.07 MJ/kg as illustrated through Figure 37. The slight deviation from linearity as highlighted earlier in chapter V can be attributed to the precession error of the bomb calorimeter. The pure components were ether realized to set the limiting boundaries for all the tested blends.

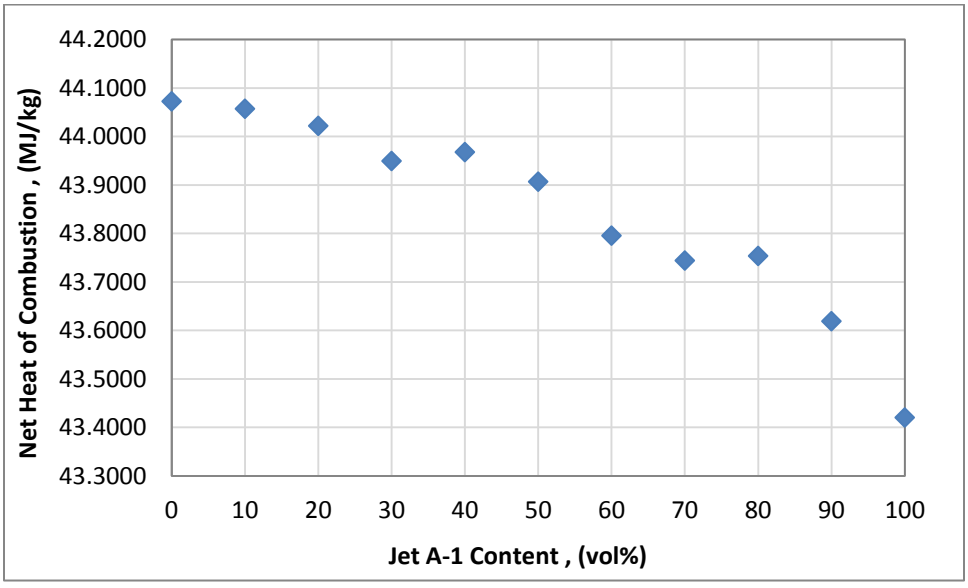

Figure 37. Net heat of combustion with respect to jet fuels binary mixture combinations.

Flash point property was the fourth property to be analyzed in this study. Once a again, all the tested blends were found to exist within the acceptable limit of ASTM D1655 that has only lower boundary of minimum value of 38.0 ^{o}C, where the values were ranging between lower boundary of 40.6 ^{o}C and upper boundary of 43.9 ^{o}C. A noticeable decreasing trend was observed with increasing Jet A-1 content in the binary mixture, with slight deviations in few data due to flash point device precision error. In addition, six of the tested blends were found to rely within the pure components region. While, the other three blends: IA.IB1, IA.IB5, and IA.IB9 were realized to exist beyond this region as emphasized through Figure 38. The apparent scatter in the data can be interpreted by representing the data among a limited small scale view, since the difference between highest and lowest value of the data is 3.3 ^{o}C. Figure 39 highlights this point by plotting the same data points for the flash point among extended scale view, to show the relative scatter of specific data with respect to the default trend.

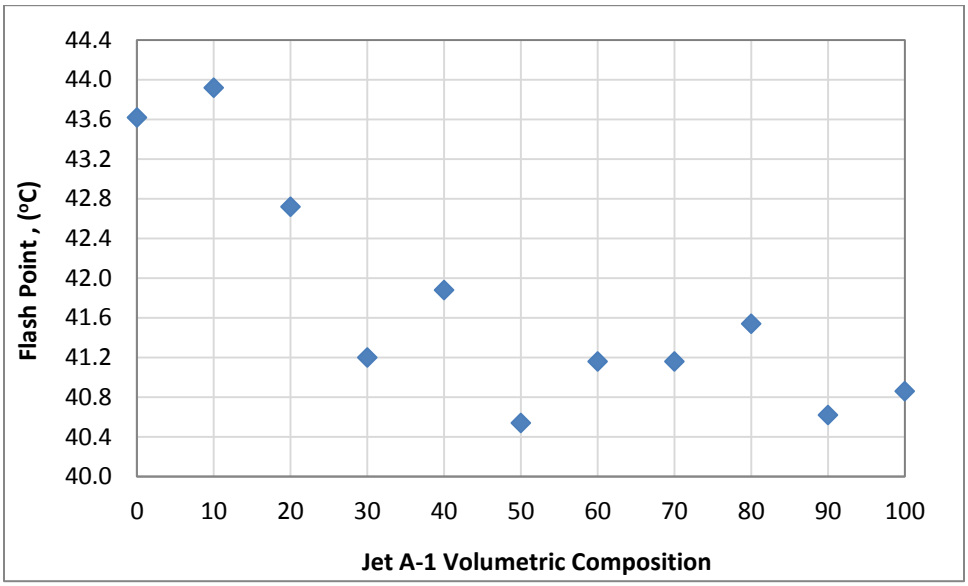

Figure 38. Flash point with respect to jet fuels binary mixture combinations.

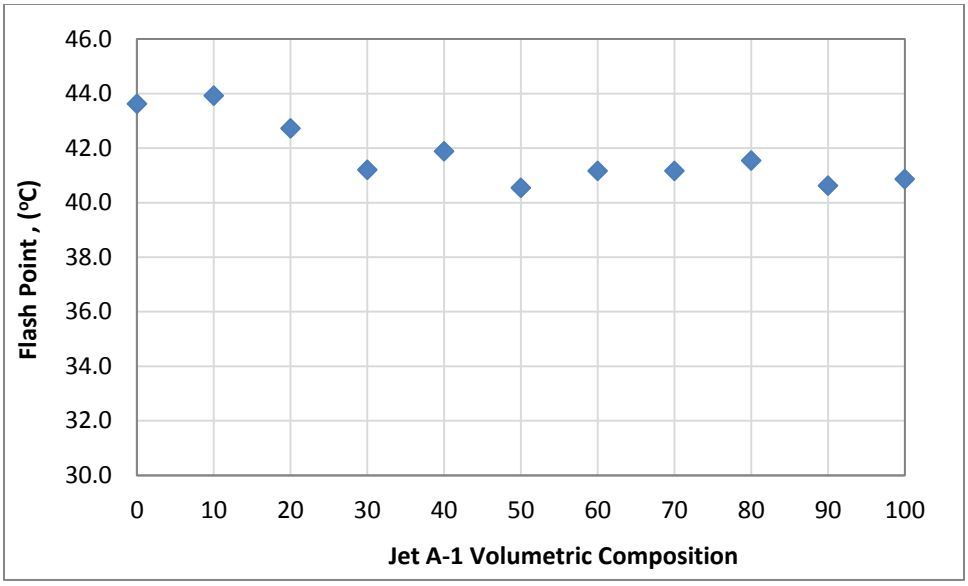

Figure 39. Flash point with respect to jet fuels binary mixture combinations through extended scale view.

Freezing point was the last property to be studied in this experimental set. All the tested blends were found to exist within the acceptable limit of ASTM D1655 that has only lower boundary of minimum value of -47.0 ^{o}C, in which the respective values were ranging between lower end of -54.3 and upper end of -65.4 ^{o}C. It was clearly seen from the resulted trend of data that there is depression in the freezing point of the mixture to minimum of -65.4 ^{o}C at Jet A-1 compositions ranging between (40-60)%, with the exception to 50-50 blend where the value is a little higher at -64.7 ^{o}C. Followed by, increase in the freezing point of the binary mixture towards pure Jet A-1 as shown through Figure 40. The slight deviation in the data with regard to blend IA.IB1 and IA.IB4 can be related to the many sources of error in the test as explained in Chapter IV.

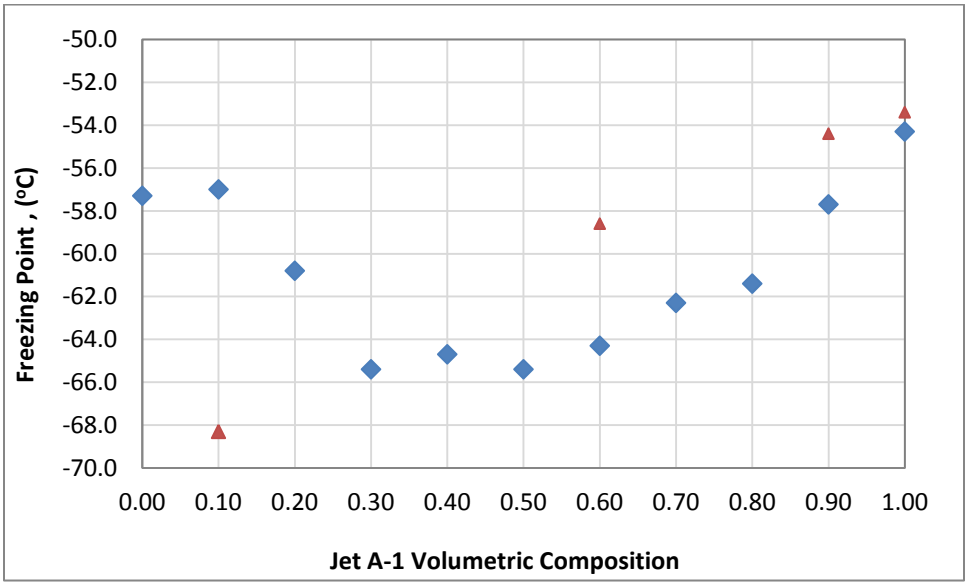

Figure 40. Freezing point with respect to jet fuels binary mixture combinations. (The red triangles represent the resulted data by Shell labs).

Comparison of Resulted Data with Shell Labs in Qatar

Three randomly selected samples from the tested samples were sent to Shell labs at Pearl plant in Ras Laffan city (Qatar), to check the reproducibility of the data and verify the reliability of the outcomes. The data were returned after a while for all the analyzed properties except for the net heat of combustion. The data for density and viscosity were in excellent agreement to generated data at fuel characterization lab even though a different testing method was used in viscosity test. The flash points were quite deviated from obtained data, and it they could not be compared with resulted data because a completely different testing method was used outside the ASTM range. Finally, the freezing point data were somehow deviated from gathered data since a more sophisticated testing method within the ASTM pool was used at which infrared beam is used to detect the disappearance of the extremely small solid crystals in the fuel sample. Appendix E displays the certificate of the results provided by Shell labs.

The freezing point for the sent samples including few other samples were repeated according to same testing method ASTM D2386 again, in order to get closer readings to Shell results and have better trend of the alternating behavior noticed earlier. The data points in general were found to be slightly higher than before at which they became more conservative conditions towards the single ASTM limit at -47 ^{o}C. Nevertheless, still it is important to note here that Shell results could not be approached perfectly due to the many sources of error inherited with current testing method, highlighting the confusion between reflection of the light on the glass tube and the inability of the naked eye and camera screen to notice the tiny crystal structures in the

fuel sample. Appendix G provides a comparison between generated data at FCL and Shell labs. Figure 41 illustrates the more pronounced alternating trend of freezing point property after repetition.

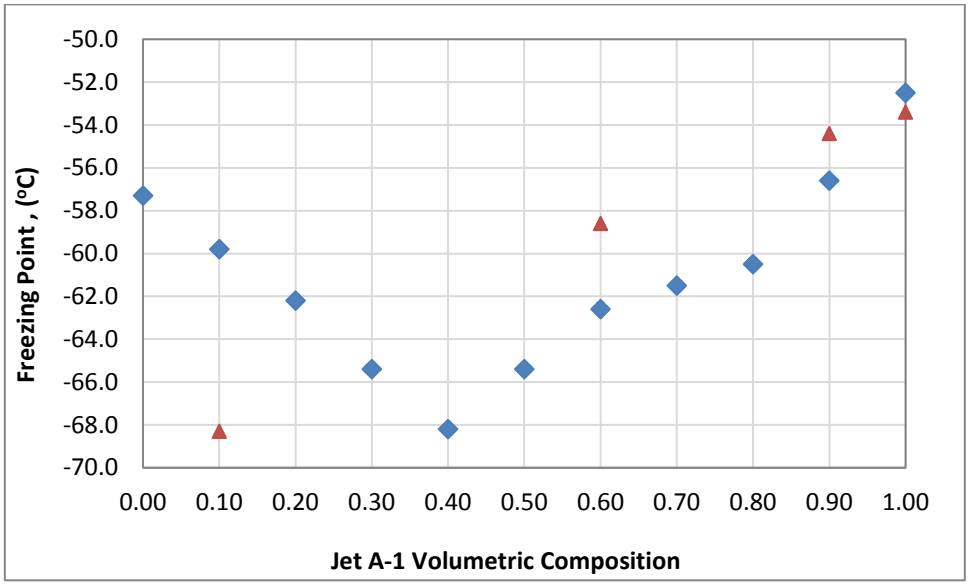

Figure 41. Freezing point with respect to jet fuels binary mixture combinations after repetition. (The red triangles represent the resulted data by Shell labs).

The Influence of Jet Fuels Building Blocks on Jet Fuel Properties

The perfect linear trend of density observed before with respect to jet fuels binary mixture combinations, was also observed against the combined *normal*-/*iso*-paraffins and *cyclo*-paraffins contents. The density of the blends was found to decrease linearly with increase in normal and *iso*-paraffins content. At the same time, the density was realized to increase linearly with increase in *cyclo*-paraffins or aromatics content as shown through Figures 42, 43, and 44. These two observations served as confirmation to

previous outcomes, as they were noted earlier in the first experimental test where the GTL SPK building blocks were tested.

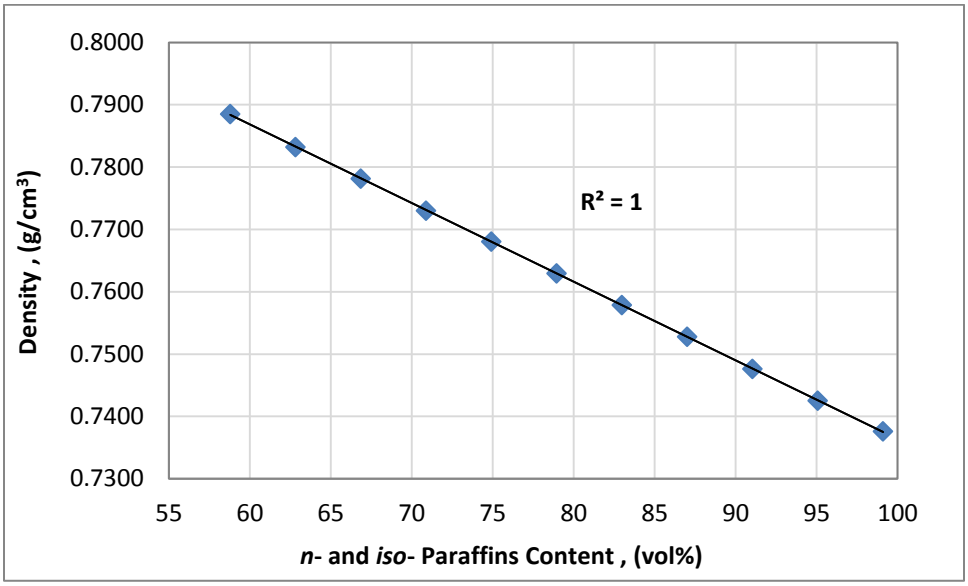

Figure 42. Density with respect to *normal*- and *iso*-paraffins content in jet fuels mixture.

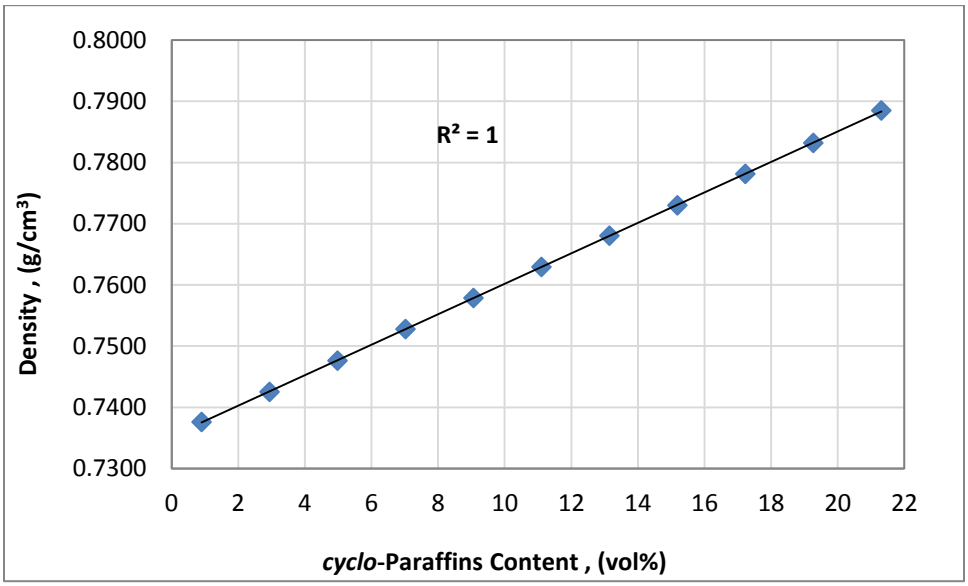

Figure 43. Density with respect to *cyclo*-paraffins content in jet fuels mixture.

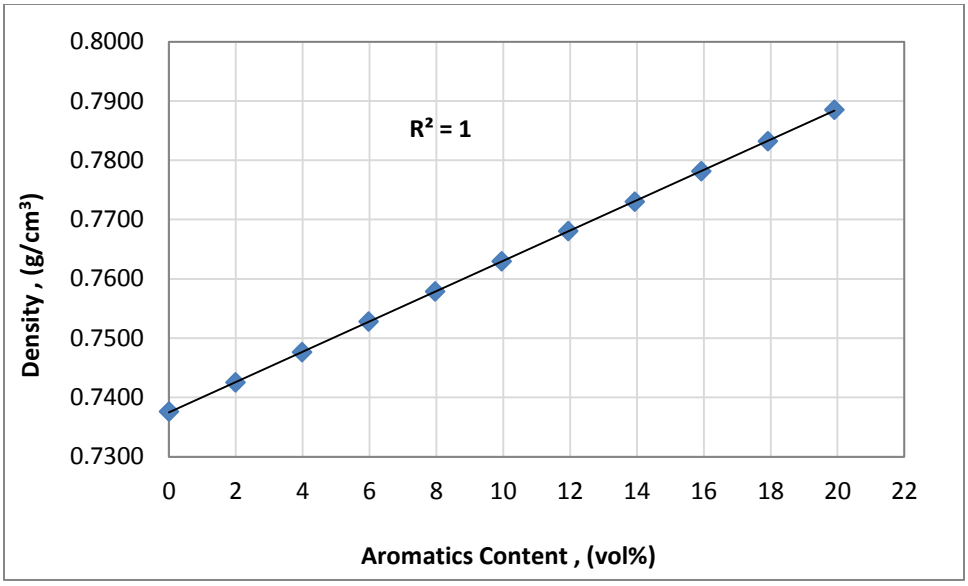

Figure 44: Density with respect to aromatics content in the jet fuels mixture.

The same trend of data was observed previously in the viscosity data with respect to binary mixture combinations, was found through viscosity data with respect to

combined *normal*- and *iso*-paraffins content. The pure components set the limiting boundaries for the rest of the data to rely through. However, identical increasing and decreasing behavior observed in density was observed in this test. The viscosity of the blends decreased almost linearly with increasing *normal*- and *iso*-paraffins content, while it increased nearly linearly with increasing *cyclo*-paraffins or aromatics content as illustrated through Figures 45, 46, and 47.

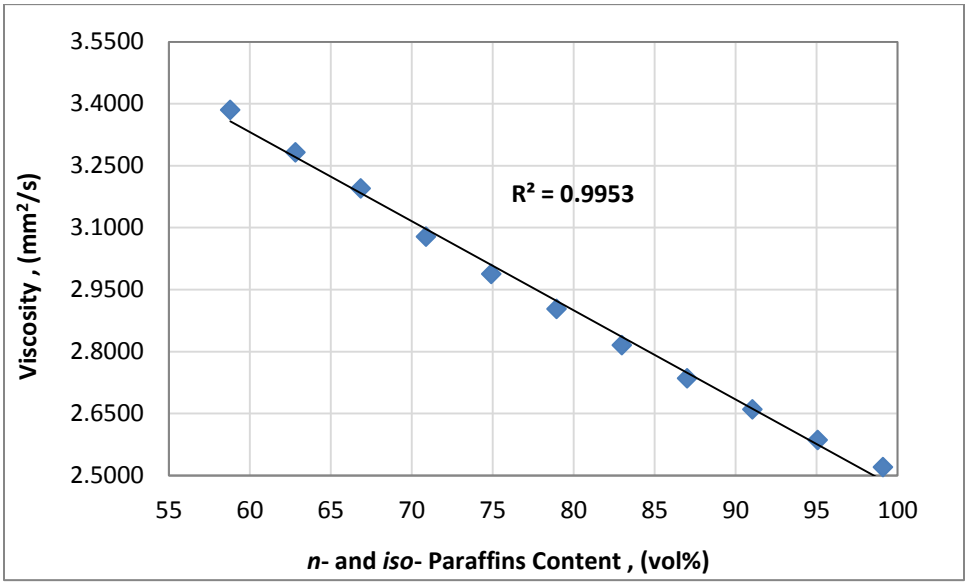

Figure 45. Viscosity with respect to *normal*- and *iso*-paraffins content in jet fuels mixture.

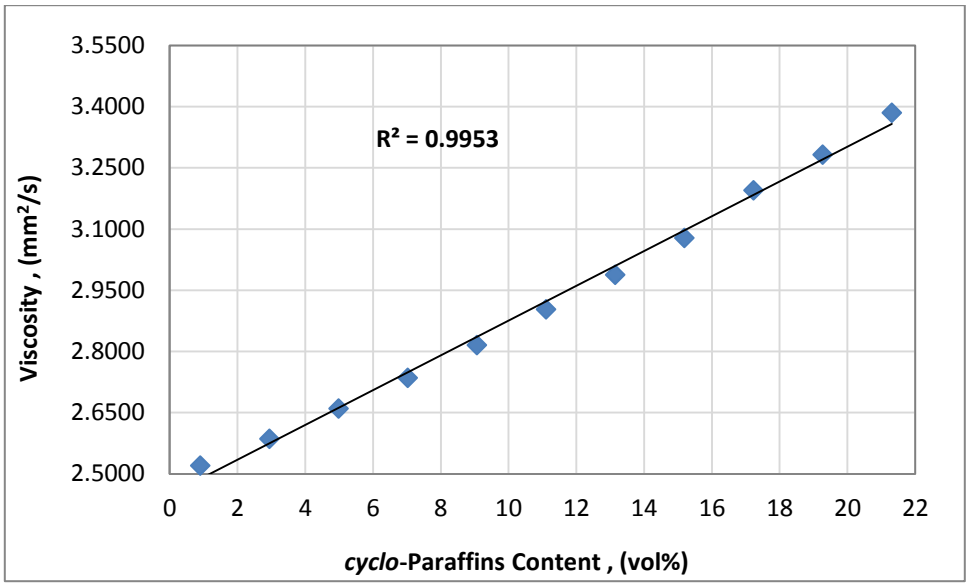

Figure 46. Viscosity with respect to *cyclo*-paraffins content in jet fuels mixture.

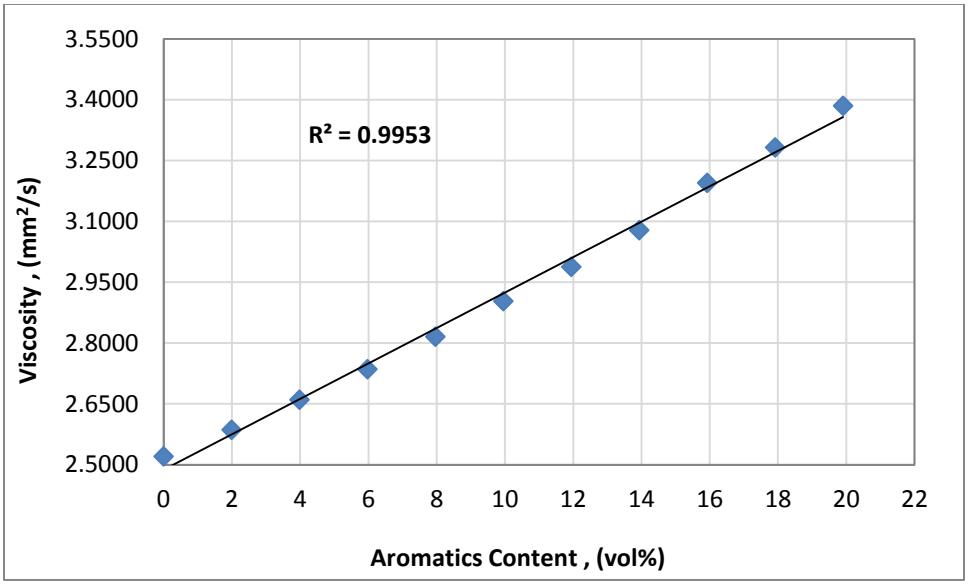

Figure 47: Viscosity with respect to aromatics content in jet fuels mixture.

The same behavior of data was observed before in the net heat of combustion data with respect to binary mixture combinations, was found through current data with

respect to combined *normal*- and *iso*-paraffins content. The pure components again set the limiting boundaries for the rest of the data. Moreover, the overall increasing and decreasing trends were reversed in comparison to density and viscosity tests. The net heat of combustion of the blends increased sharply with increase in *normal*- and *iso*-paraffins content. On the other hand, it decreased sharply with increase in *cyclo*-paraffins or aromatics content as shown through Figures 48, 49, and 50.

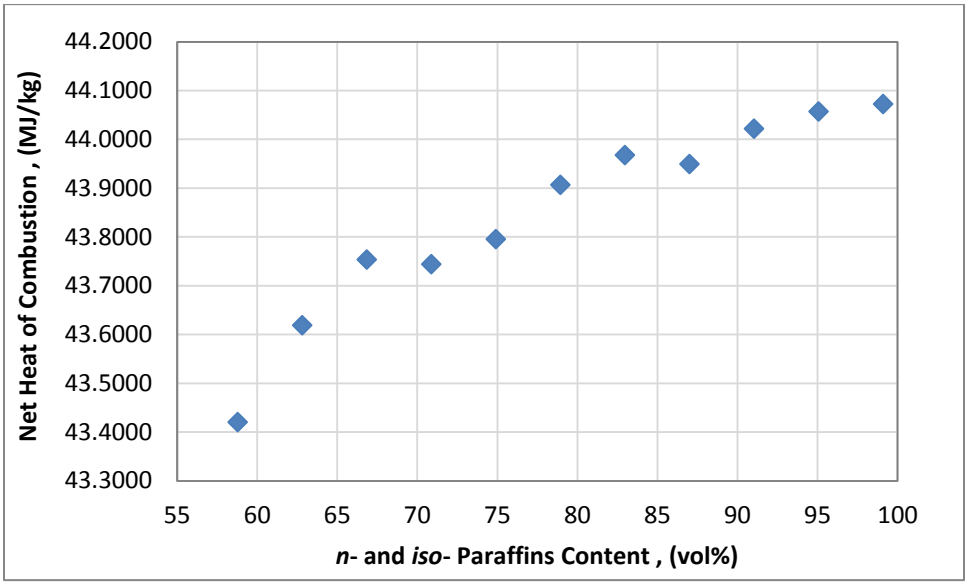

Figure 48. Net heat of combustion with respect to *normal*- and *iso*-paraffins content in jet fuels mixture.

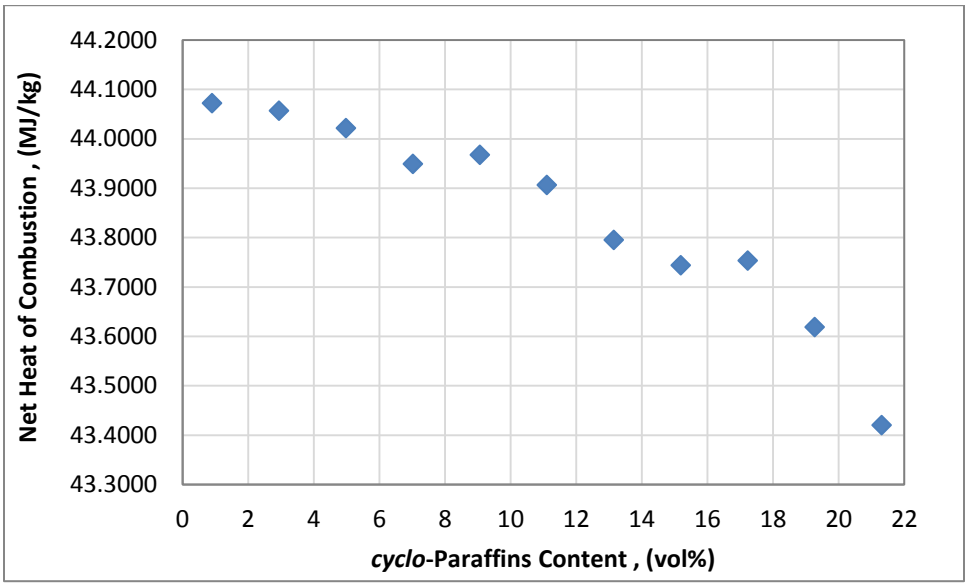

Figure 49. Net heat of combustion with respect to *cyclo*-paraffins content in jet fuels mixture.

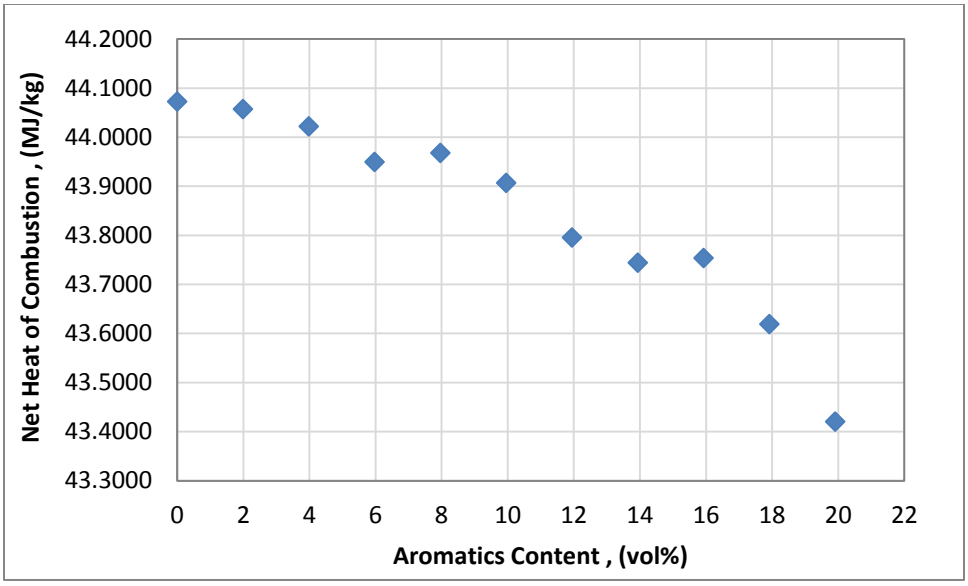

Figure 50: Net heat of combustion with respect to aromatics content in jet fuels mixture.

Identical trend observed for the flash point in regard to jet fuels binary mixture combinations, was observed with respect to analyzed building blocks. The pure

components set the limiting boundaries for five data points, while the rest of the blends exist beyond the limiting region. Both building blocks combined *normal*- and *iso*-paraffins and *cyclo*-paraffins were experiencing the same trend with the only variations in the range of compositions at which the trend pass through and the order, a narrower range of compositions is covered in the *cyclo*-paraffins case since these are the least existing constituents in Jet A-1 sample. Figures 51. 52, and 53 express the flash point of jet fuels mixtures with respect to combined *normal*-/*iso*-paraffins, *cyclo*-paraffins, and aromatics, respectively.

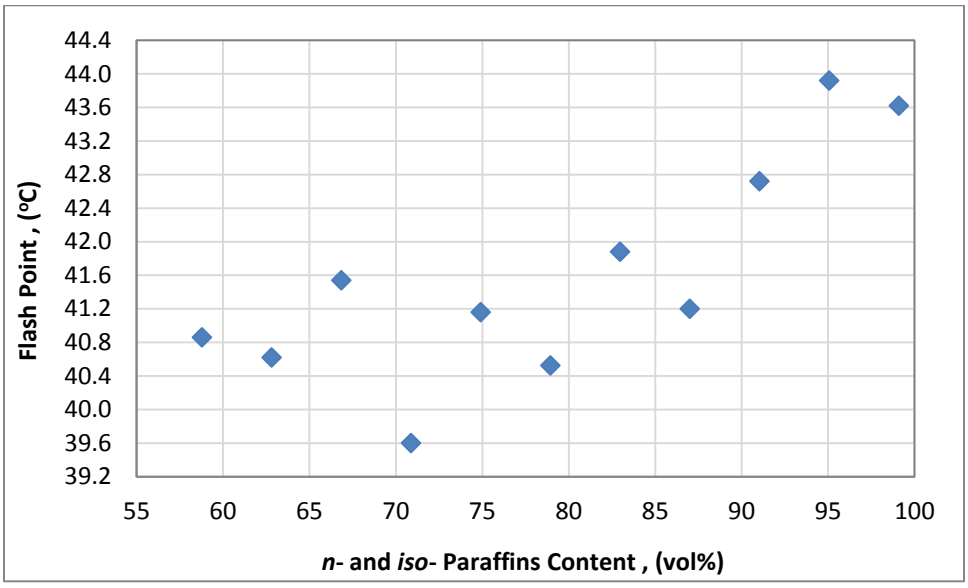

Figure 51. Flash point with respect to *normal*- and *iso*-paraffins content in jet fuels mixture.

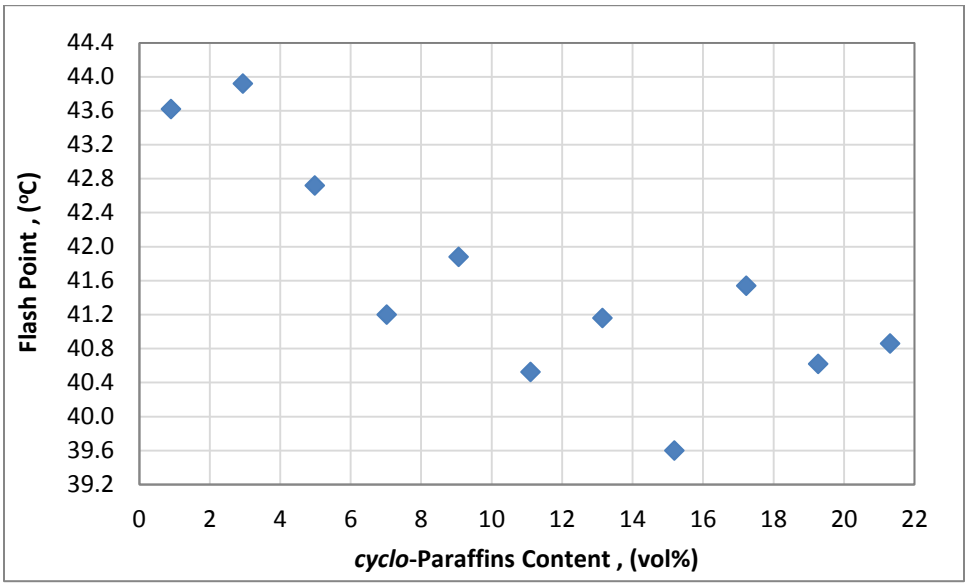

Figure 52. Flash point with respect to *cyclo*-paraffins content in jet fuels mixture.

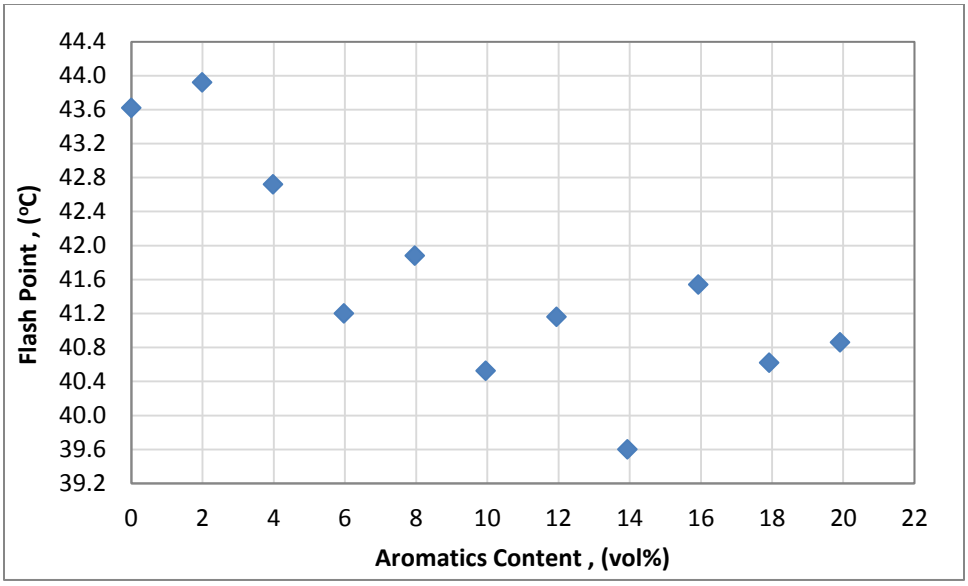

Figure 53: Flash point with respect to aromatics content in jet fuels mixture.

Finally, freezing point was realized to have the same trend been observed earlier against binary mixture combinations, where a depression in the data takes place towards

minimum followed by increase towards the pure Jet A-1. Again both building blocks combined *normal*- and *iso*-paraffins and *cyclo*-paraffins were experiencing the same trend with the only variations in the range of compositions at which the trend pass through and the order, a wider range of compositions is covered in the *normal*- and *iso*-paraffins case since these are the most dominant constituents in Jet A-1 sample. Figures 54, 55, and 56 express the freezing point of jet fuels mixtures with respect to combined *normal*-/*iso*-paraffins, *cyclo*-paraffins, and aromatics respectively.

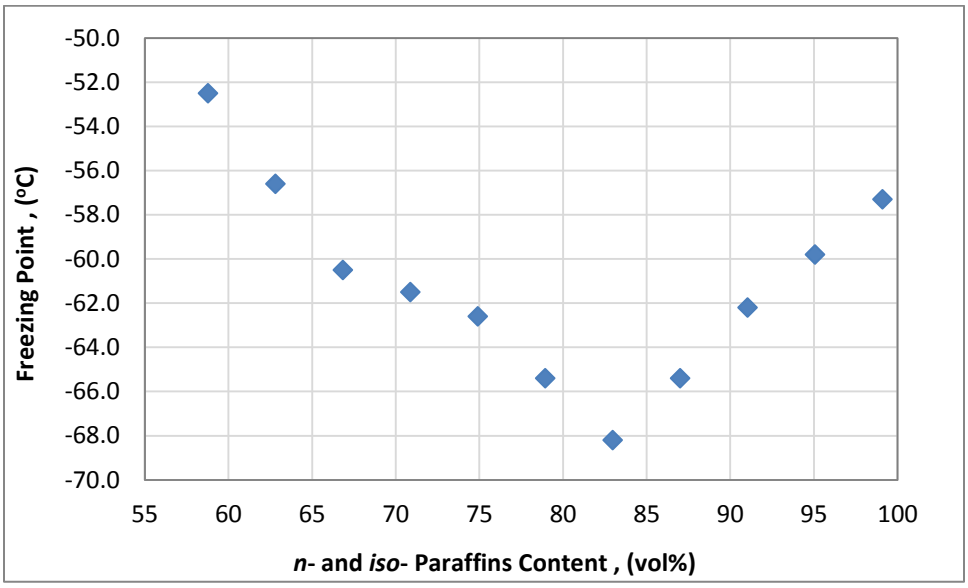

Figure 54. Freezing point with respect to *normal*- and *iso*-paraffins content in jet fuels mixture.

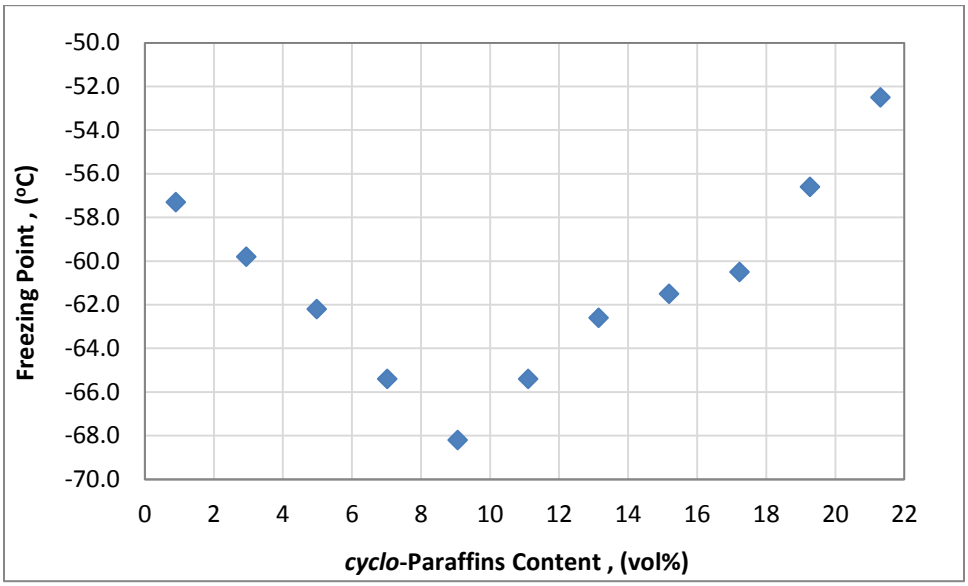

Figure 55. Freezing point with respect to *cyclo*-paraffins content in jet fuels mixture.

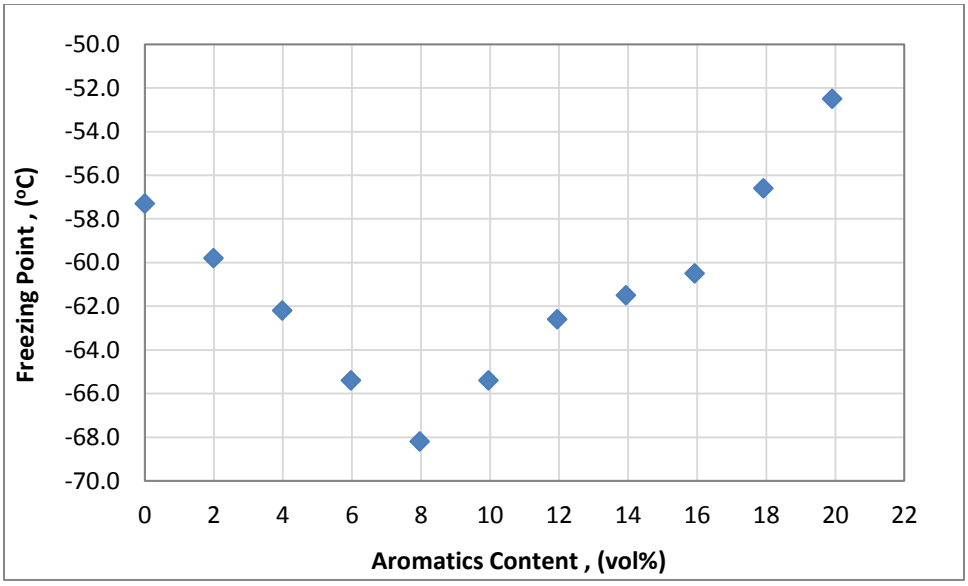

Figure 56: Freezing point with respect to aromatics content in jet fuels mixture.

In summary, this experimental set studying the impact of jet fuels blending on mixture properties showed that Jet A-1 content should exceed 75vol% in order to be

certified as semi-synthetic jet fuel for aviation use. In addition, it was found that the aromatics content in the jet fuel mixture should be within 15.9 to 17.9 vol%, which agrees with the specifications required by aviation market that is limited by maximum boundary of 25 vol%, and the maximum allowable percentage of GTL SPK limited by 50 vol% [13]. It is important to note here that this study relied on five properties only and thus there is huge room for narrowing the range further through other distinctive test to characterize the future synthetic jet fuel.

Statistical Analysis for Jet Fuels Mixtures

Due to the limitation of data points for jet fuels mixtures to exist around the combined *normal*- and *iso*-paraffins apex only as highlighted earlier, non-Artificial neural networks were developed for this experimental set. To avoid modeling the other areas next to the other two apexes (*cyclo*-paraffins and aromatics), which lack of any data points. The role of non-artificial neural network is to identify the profile of the property along the region which of interest, and ignores the rest of the ternary diagram that was kept intact.

Density property again had a very smooth profile along the analyzed region of the ternary diagram where the density of the mixture decreaeses gently and linearly with increasing combined *normal*- and *iso*-paraffins content. Then, Net heat of combustion property had nearly same profile of density with slight reduction as the combined *normal*- and *iso*-paraffins apex is approached. Next, Flash point property had close profile to net heat of combustion. However, the interruption in the profile was

discontinuous and appeared as two distinctive points throughout the profile. After that, Freezing point property showed the expected profile which was observed through experiments, at which the freezing point of mixture reduces to minimum and then increases to maximum as the analyzed apex is approached. Then, viscosity had a similar profile to density with the only variation in the furthest part to the apex, where the viscosity of the mixture remained at intermediate value. It is important to note here that both profiles for flash point and net heat of combustion were skewed due to the heterogeneous nature of the data, where the data are distributed uniformly along a diagonal line, and not spread homogenously among the analyzed region. Thus, the undefined points were associated with higher standard deviation or errors and in turn there was poor data fitting in the region. Accordingly, the generated optimized plot where all the properties meet the requirements for ASTM D7566 or D1655 highlighted an optimum region quite skewed from the one gathered from experiments where the Jet A-1 content relies on a region of low to moderate contribution of Jet A-1. The individual and optimized plots of non-artificial neural networks for this experimental set are placed in Appendix G.

LINGO FORMULATION OUTCOMES

Appendix B displays the outcomes gathered from LINGO software relative to the two cases implemented in current jet fuels optimization problem. The highlighting colors indicate the following results; yellow expresses the minimum cost of the jet fuels mix, green expresses the optimization variables represented by the jet fuels blending ratios

and GTL SPK fractions, and blue expresses the resulted properties for both GTL SPK and final mix.

The first case where the combination of GTL SPK fractions is figured out by the software showed that the ASTM D7566 blending limit for GTL SPK in the jet fuels blend is met with around 46 vol% overall contribution. However, all the properties except for the density of GTL SPK failed to meet the required certification for GTL SPK batch requirements in ASTM D7566 [14]. On the other hand, the second case where the combination of GTL SPK fractions was fed to the software showed that the ASTM D7566 blending limit for GTL SPK in the jet fuels blend is once again met with lower contribution of around 35 vol%. Meanwhile, all the properties of GTL SPK met the required certification for GTL SPK in ASTM D7566 [14]. Another significant point was observed between both cases is that the price of the jet fuels blend increased slightly in second case with respect to first case, that could be referred to the inflexibility added to the software as the GTL SPK fractions are fed in.

CHAPTER VII

CONCLUSIONS

In conclusion, this study has managed to highlight the significance of natural gas based jet fuel to be a promising alternative source of fuel for aircrafts. A promising path for designing future generations of jet fuel was formulated through both, previous studies implemented by the research team and current contribution conducted in the field.

Considering the experimental observations, previous studies revealed through first experimental set that density follows a linear trend and perfectly coheres with theoretical values. Thus, it was used from the beginning as a blend confirmation test. The rest of the properties except for the freezing point were found to decrease with respect to certain paraffinic constituents. The tested combinations of paraffinic building blocks were beyond the acceptance limits at certain cases. However, an optimum region where all the properties meet the aviation standard was located on the artificial neural network. Unfortunately, the elastomers were realized to be affected badly in the absence of aromatics. Therefore, the second experimental set was triggered which showed that density can be raised significantly upon the addition of *mono*-aromatics or *cyclo*-paraffins to GTL SPK mixture. Furthermore, the swelling behavior of elastomers was improved substantially. Nevertheless, both of the net heat of combustion and flash point properties were realized to be impacted negatively with ether additions. Finally, the mixing of jet fuels showed gradual increase in both density and viscosity, while both net

heat of combustion and flash points experienced gradual decrease. However, the freezing point had an interesting trend where it decreases to minimum then increases again. Also, the jet fuels mix was found to meet aviation standards for Jet A-1 content ranging between 75 vol% to nearly pure Jet A-1, at which the aromatics composition approximately between 16-18 vol%. Moreover, the 50:50 blend tested by Qatar Airways was found to be a little below the density limits for ASTM D1655, and that could be refereed to some added additives which raised the density of jet fuels blend during that flight or another heavier conventional cut used in the blend. Nevertheless, the density limits for ASTM D7566 of synthetic FT batch were satisfied.

Summarizing the outcomes for the modeling part. Four correlative models were developed for the properties of interest. Viscosity was realized at advanced stages to be an extra step towards the optimization path. Both density and net heat of combustion were observed to follow linear models presented in thermodynamics book. While, both freezing and flash points were found to follow non-linear models stated in literature or randomly selected from a list of possibilities.

Regarding the optimization track of the study. Two different cases were developed to represent a hypothetical and real mixing cases. The first case resulted with satisfying results in terms of jet fuels blending ratios and certain properties of GTL SPK, while the paraffinic combination of GTL SPK was well deviated from current mix provided by the industry. On the other hand, the second case resulted with even more

satisfying results in regard to analyzed parameters as the desired paraffinic combination is fed to the software.

Still extended research should be attributed to jet fuels characterization, as the feasibility region can be narrowed further by implementing other characterization tests listed in ASTM D1655, and carry further testing using the other divisions of the GTL research consortium. Moreover, other blending scenarios can be still studied since the aircraft will have to be fueled with other local jet fuel supplies at arrival destinations, raising other challenges where ternary mixtures might need to be accounted. In addition, the optimization track can be improved further by setting the boundaries for feasibility region on the ternary diagram, as chemical structure of GTL SPK resulted in case 1 represents a one possibility in cost minimization, and estimating a more thorough subsidy through proper analysis of emitted gas emissions and consideration to relevant carbon tax.

REFERENCES

[1] Chevron. Global Aviation: Aviation Fuels Technical Review. https://www.cgabusinessdesk.com/document/aviation_tech_review.pdf. Published October 2006. Accessed December 28, 2012.

[2] Aviation Jet Fuel Information. CSG Network. http://www.csgnetwork.com/jetfuel.html. Accessed November 16, 2012.

[3] Hileman J, Wong M H, Donohoo P, Weiss M., Waitz L. Alternative Jet fuels. Talk presented at: Partnership for Air Transportation Noise and Emission Reduction; January 12, 2009; Massachusetts Institute of Technology. http://www.trbav030.org/pdf2010/JHileman%20_PARTNER_AltFuels_v02.pdf. Accessed December 28, 2012.

[4] Blakely S, Rye L, Wilson W C. Aviation gas turbine alternative fuels: A review. *Proc. Combust. Inst.* 2011; 33:2863–2885.

[5] The University of Sheffield. E-Futures: How low can you go? Aviation fuel needs to reduce its aromatic content – but by how much?. http://e-futures.group.shef.ac.uk/publications/pdf/134_16%20David%20Anderson.pdf. Published May 2011. Accessed December 28, 2012.

[6] NASA. Alternative Fuels and their Impact on Aviation. http://atlanticgreenfuels.com/ICAS_2006_alt_fuel_rev_Q1.pdf. Published October 2006. Accessed December 28, 2012.

[7] Liu G, Haijie Q, Huiming S, Xiangwen Z, Zhentao M. Theoretical design and preparation of high thermal-stable jet fuel. Science in China Press, *Sci. China Ser* 2008; 51(2):138-144.

[8] Country Analysis Briefs. Energy Information Administration http://www.eia.gov/emeu/cabs/Qatar/Full.html. Accessed September 3, 2012.

[9] Qatar Celebrates Achieving 77 Mta LNG Production Capacity. Ras Laffan Industrial City. http://www.raslaffan.qp.qa/irj/portal/anonymous/rlcnews?xmlFileName=/documents/Qatar%20Petroleum/e-RLC/News/70283eaa-1ffa-2d10-a9b6-c619c444786c.xml. Retrieved on September 14, 2012.

[10] Oryx, Qatar. Hydrocarbons-Technology. http://www.hydrocarbons-technology.com/projects/oryx/. Accessed September 4, 2012.

[11] Pearl GTL – an Overview. Shell Global. http://www.shell.com/home/content/aboutshell/our_strategy/major_projects_2/pearl/overview/. Accessed September 4, 2012.

[12] GTL Jet Fuel approved for use in civil aviation. Shell Global. http://www.shell.com/home/content/media/news_and_media_releases/archive/2009/gtl_jet_fuel_approved_29092009.html. Accessed September 5, 2012.

[13] Bauldreay M J, Bogers F P, & Al-Sharshani A. Use of Surrogate Blends to Explore Combustion-Composition Links for Synthetic Paraffinic Kerosines. Paper presented at: IASH 2011, 12th International Conference on Stability,

Handling and Use of Liquid Fuels; October 16, 2011; Florida, USA. Accessed December 28, 2012.

[14] SAI Global Standards Database. ASTM International. ASTM D1655 “Standard Specification for Aviation Turbine Fuels”. Published October 2011.

[15] SAI Global Standards Database. ASTM International. ASTM D7566 “Standard Specification for Aviation Turbine Fuel Containing Synthesized Hydrocarbons”. Published October 2009.

[16] Cookson D J, Lloyd P, Smith B E. Investigation of the chemical basis of kerosene (jet fuel) specification properties. American Chemical Society. *Energ Fuel* 1987; 1:438-447.

[17] SAI Global Standards Database. ASTM International. ASTM D7042 “Standard Test Method for Dynamic Viscosity and Density of Liquids by Stabinger Viscometer (and the Calculation of Kinematic Viscosity)”. Published October 2012.

[18] SAI Global Standards. ASTM International. ASTM D56 “Standard Test Method for Flash Point by Tag Closed Cup Tester”. Published November 2011.

[19] Cookson D J, Smith B E. Calculation of jet and diesel fuel properties using ^{13}C NMR spectroscopy. *Energ Fuel* 1990; 4:152-156.

[20] Cookson D J, & Smith B E. Composition-property relations for jet and diesel fuels of variable boiling range. *Fuel* 1995; 74(1):70-78.

[21] Liu G, Wang L, Qu H, Shen H, Zhang X, Zhang S, Mi Z. Artificial neural network approaches on composition-property relationships of jet fuels based on GC-MS. *Energ Fuel* 2007; 86:2551-2559.

[22] Coordinating Research Council and Universal Technology Corporation. Comparative Evaluation of Semi-Synthetic Jet Fuels. http://www.crcao.com/reports/recentstudies2008/AV-2-04a/AV-2-04a%20-%20Comparison%20of%20SSJF%20-%20CRC%20Final.pdf. Accessed January 20, 2013.

[23] Joanna M B, Richard J H, Johanne S. Synthetic jet fuels and their role in the future. Paper presented at: IASH 2003, 8th International Conference on Stability and Handling of Liquid Fuels; September 14, 2003; Colorado USA. Accessed April 5, 2013.

[24] World's First Commercial Passenger Flight Powered By Fuel Made From Natural Gas Lands In Qatar. Qatar Airways. http://www1.qatarairways.com/global/en/newsroom/archive/press-release-12Oct09-2.html. Accessed September 5, 2012.

[25] Gas to Liquids Jet Fuels Research. Shell Global. http://www.shell.com.qa/en/products-services/qatartechnology/jet-fuel.html. Accessed January 15, 2013.

[26] Raza, B, Elmalik E, Al-Meer M, Ramahdan H, Al-Mohannadi D, Elbashir N O. Characterization of synthetic Gas-to-Liquid jet fuel blends and properties correlation with hydrocarbon structure. Preprint Paper - American Chemical Society, Division of Fuel Chemistry 2011; 56(2):431-433.

[27] Warrag S, Al-Nuaimi I, Elmalik E, Elbashir O N. Properties Driven Design of Synthetic Jet Fuels Derived from Natural Gas Via Gas-to-Liquid Technology. Preprint Paper - American Chemical Society, Division of Energy & Fuels Chemistry 2012; 57(2):796-797.

[28] Felder M R, Rousseau W R. *Elementary Principles of Chemical Processes*. 3rd ed. Hoboken, NJ: Wiley; 2005.

[29] McAllister A, Chen J, Fernandez-Pello. *Fundamentals of Combustion Processes: Thermodynamics of Combustion*. 1st ed. NY: Springer Publishing Co; 2011.

[30] Keshavarz H M, Motamedoshariatmi H, & Ghanbarzadeh M. A reliable simple method for prediction of the flash points of saturated hydrocarbons in order to improve their safety. *Chemistry* 2011; 20(6):58-75.

[31] SAI Global Standards Database. ASTM International. ASTM D4052 "Standard Test Method for Meter Density, Relative Density, and API Gravity of Liquids by Digital Density Meter". Published November 2011.

[32] Daniel D, Crowl A, Louvar F J. *Chemical Process Safety: Fundamentals with Applications*. 3rd ed. New York, NY: Prentice Hall.

[33] SAI Global Standards Database. ASTM International. ASTM D240 "Standard Test Method for Heat of Combustion of Liquid Hydrocarbon Fuels by Bomb Calorimeter". Published December 2011.

[34] SAI Global Standards Database. ASTM International. ASTM D2786 “Standard Test Method for Freezing Point of Aviation Fuels”. Published November 2011.

[35] Sandler I. S. *Chemical, Biochemical, and Engineering Thermodynamics* . 4th ed. Hoboken, NJ: Wiley; 2006.

[36] Liu Y, Wilson W C, Blakely G S, Theato P. Investigation of Elastomer Compatibility with Alternative Fuels by Mass Change Study, Stress-Relation Test, and FTIR Spectroscopy, Talk presented at: IASH 2011, 12th International Conference on Stability, Handling and Use of Liquid Fuels; October 16, 2011; Florida, USA. Accessed December 25, 2012.

[37] SAI Global Standards Database. ASTM International. ASTM D471 “Standard Test Method for Rubber Property—Effect of Liquids”. Published December 2011.

[38] Fuel Price Analysis. IATA. http://www.iata.org/publications/economics/fuel-monitor/Pages/price-analysis.aspx. Accessed December 25, 2012.

[39] Elbashir N, Elfatih M, Blank J, Al-Nuaimi I, Warag S, et al (2012) “Characterization and Formulation of GTL Derived Synthetic Jet Fuels” QSTP Research Network Program.

[40] Link D D, Gormely J R, Baltrus P J, Anderson R R, Zandhius H P. Potential Additives to Promote Seal Swell in Synthetic Fuels and Their Effect on Thermal Stability. *Energ Fuel* 2008; 22(2):1115-1120.

[41] Witten L M, Zeiger E, Ritchie D G. *Jet Fuel Toxicology*. Danvers, MA: CRC Press; 2011.

APPENDIX A

DATA TRENDING FINAL RESULTS

Table A1. Resulted data for density correlative model.

Blend Name	*n*-P	*iso*-P	*cyclo*-P	Experimental Data (g/cm^3)	Predicted Data (g/cm^3)	Relative Error (%)
***n*-Decane**	1.00	0.00	0.00	0.7346	0.7346	0.00
Shell SolT	0.00	1.00	0.00	0.7613	0.7613	0.00
Decalin	0.00	0.00	1.00	0.8828	0.8828	0.00
IB1	0.00	0.22	0.78	0.8531	0.8525	0.07
IB2	0.00	0.46	0.54	0.8300	0.8222	**0.94**
IB3	0.31	0.32	0.37	0.7936	0.7930	0.08
IB4	0.18	0.18	0.64	0.8281	0.8289	0.10
IB5	0.09	0.27	0.64	0.8301	0.8316	0.18
IB6	0.00	0.72	0.28	0.7949	0.7919	0.38
IB7	0.19	0.58	0.23	0.7763	0.7804	0.53
IB8	0.40	0.41	0.18	0.7700	0.7697	0.04
IB9	0.58	0.30	0.12	0.7577	0.7575	0.03
IB10	0.63	0.17	0.20	0.7650	0.7644	0.08
IB11	0.71	0.00	0.29	0.7724	0.7717	0.10
IB12	0.57	0.15	0.28	0.7765	0.7757	0.11
IB13	0.39	0.15	0.46	0.8020	0.8012	0.10
IB14	0.45	0.00	0.55	0.8091	0.8087	0.05
IB15	0.27	0.09	0.64	0.8273	0.8262	0.13
IB16	0.22	0.00	0.78	0.8461	0.8458	0.04
IB17	0.15	0.40	0.45	0.8079	0.8067	0.15
IB18	0.10	0.62	0.28	0.7897	0.7889	0.09
IB19	0.48	0.51	0.01	0.7495	0.7496	0.01
IB20	0.73	0.26	0.01	0.7427	0.7428	0.02
IB21	0.05	0.89	0.06	0.7670	0.7663	0.09
IB22	0.05	0.84	0.12	0.7730	0.7724	0.08
IB23	0.10	0.84	0.06	0.7654	0.7650	0.06
IB24	0.10	0.79	0.12	0.7715	0.7710	0.06
IB25	0.04	0.04	0.91	0.8703	0.8693	0.11

Table A1. Continued.

Blend Name	*n*-P	*iso*-P	*cyclo*-P	Experimental Data (g/cm^3)	Predicted Data (g/cm^3)	Relative Error (%)
IB26	0.09	0.04	0.87	0.8628	0.8619	0.10
IB27	0.04	0.09	0.87	0.8640	0.8633	0.08
IB28	0.83	0.05	0.12	0.7510	0.7508	0.03
IB29	0.84	0.10	0.06	0.7447	0.7447	0.00
IB30	0.78	0.10	0.12	0.7523	0.7521	0.02
IB31	0.09	0.09	0.83	0.8569	0.8559	0.12
IB32	0.89	0.05	0.06	0.7435	0.7434	0.02

Table A2. Resulted data for net of combustion correlative model.

Blend Name	*n*-P	*iso*-P	*cyclo*-P	Experimental Data (MJ/mol)	Predicted Data (MJ/mol)	Relative Error (%)
***n*-Decane**	1.00	0.00	0.00	0.3109	0.3109	0.00
Shell SolT	0.00	1.00	0.00	0.2547	0.2547	0.00
Decalin	0.00	0.00	1.00	0.3089	0.3089	0.00
IB1	0.00	0.19	0.81	0.2964	0.2988	0.81
IB2	0.00	0.41	0.59	0.2844	0.2868	0.85
IB3	0.32	0.28	0.40	0.2923	0.2946	0.80
IB4	0.18	0.15	0.67	0.2989	0.3010	0.68
IB5	0.09	0.23	0.68	0.2941	0.2964	0.81
IB6	0.00	0.67	0.33	0.2692	0.2724	**1.20**
IB7	0.21	0.53	0.26	0.2779	0.2804	0.89
IB8	0.43	0.37	0.20	0.2873	0.2899	0.90
IB9	0.61	0.26	0.13	0.2933	0.2960	0.90
IB10	0.65	0.14	0.21	0.3006	0.3025	0.61
IB11	0.71	0.00	0.29	0.3084	0.3103	0.64
IB12	0.58	0.12	0.30	0.3017	0.3034	0.57
IB13	0.39	0.13	0.48	0.3011	0.3028	0.57
IB14	0.45	0.00	0.55	0.3090	0.3098	0.25
IB15	0.27	0.08	0.66	0.3040	0.3053	0.44
IB16	0.21	0.00	0.79	0.3084	0.3093	0.29
IB17	0.16	0.35	0.49	0.2879	0.2905	0.89

Table A2. Continued**.**

Blend Name	*n*-P	*iso*-P	*cyclo*-P	Experimental Data (MJ/mol)	Predicted Data (MJ/mol)	Relative Error (%)
IB18	0.11	0.57	0.32	0.2761	0.2785	0.88
IB19	0.53	0.46	0.02	0.2824	0.2851	0.94
IB20	0.77	0.22	0.01	0.2958	0.2985	0.90
IB21	0.06	0.87	0.07	0.2618	0.2618	0.02
IB22	0.06	0.80	0.14	0.2644	0.2654	0.36
IB23	0.11	0.82	0.07	0.2643	0.2649	0.24
IB24	0.11	0.75	0.14	0.2670	0.2684	0.50
IB25	0.04	0.04	0.92	0.3057	0.3071	0.45
IB26	0.08	0.04	0.88	0.3064	0.3071	0.25
IB27	0.04	0.07	0.89	0.3038	0.3051	0.44
IB28	0.09	0.07	0.84	0.3036	0.3051	0.51
IB29	0.90	0.04	0.06	0.3071	0.3084	0.42
IB30	0.84	0.04	0.12	0.3073	0.3083	0.33
IB31	0.85	0.09	0.06	0.3045	0.3060	0.48
IB32	0.79	0.08	0.12	0.3044	0.3059	0.51

Table A3. Resulted model specific parameters for flash point correlative model.

Component	A	C_n	ISP	DSP
Decane	157.6	10.0	0.000	0.000
Shell Sol T	168.6	12.0	0.000	0.000
Decalin	140.3	10.0	0.000	0.000

Table A3. Resulted data for flash point correlative model.

Blend Name	*n*-P	*iso*-P	*cyclo*-P	'A'	C_n	Exp Data (K)	Prd Data (K)	Relative Error (%)
***n*-Decane**	1.00	0.00	0.00	157.65	10.0	319.2	319.1	0.00
Shell SolT	0.00	1.00	0.00	172.65	12.0	334.2	334.1	0.00
Decalin	0.00	0.00	1.00	136.35	10.0	330.2	330.1	0.00
IB1	0.00	0.19	0.81	143.14	10.4	330.2	330.9	0.21
IB2	0.00	0.41	0.59	151.16	10.8	332.6	331.8	0.25
IB3	0.32	0.28	0.40	153.26	10.6	328.7	327.7	0.29
IB4	0.18	0.15	0.67	145.75	10.3	330.3	328.8	0.44
IB5	0.09	0.23	0.68	146.76	10.5	330.5	330.1	0.14
IB6	0.00	0.67	0.33	160.78	11.3	331.8	332.8	0.30
IB7	0.21	0.53	0.26	160.13	11.1	330.8	330.0	0.23
IB8	0.43	0.37	0.20	158.82	10.7	328.8	326.9	0.57
IB9	0.61	0.26	0.13	158.87	10.5	327.7	324.5	0.99
IB10	0.65	0.14	0.21	155.38	10.3	327.5	323.6	1.19
IB11	0.71	0.00	0.29	151.43	10.0	328.5	322.4	1.88
IB12	0.58	0.12	0.30	153.15	10.2	328.2	324.3	1.20
IB13	0.39	0.13	0.48	149.27	10.3	328.5	326.4	0.65
IB14	0.45	0.00	0.55	145.87	10.0	328.2	325.2	0.91
IB15	0.27	0.08	0.66	144.77	10.2	329.2	327.5	0.51
IB16	0.21	0.00	0.79	140.87	10.0	329.6	327.8	0.54
IB17	0.16	0.35	0.49	152.40	10.7	331.6	329.7	0.55
IB18	0.11	0.57	0.32	159.28	11.1	332.6	331.2	0.44
IB19	0.53	0.46	0.02	164.21	10.9	329.8	326.2	1.09
IB20	0.77	0.22	0.01	160.68	10.4	328.2	322.6	1.71
IB21	0.06	0.87	0.07	169.14	11.7	334.0	333.0	0.29
IB22	0.06	0.80	0.14	166.74	11.6	334.5	332.8	0.53
IB23	0.11	0.82	0.07	168.34	11.6	332.4	332.2	0.07
IB24	0.11	0.75	0.14	165.97	11.5	331.9	331.9	0.03
IB25	0.04	0.04	0.92	138.52	10.1	332.2	329.8	0.70
IB26	0.08	0.04	0.88	139.43	10.1	332.6	329.4	0.97
IB27	0.04	0.07	0.89	139.86	10.1	332.9	330.0	0.88
IB28	0.09	0.07	0.84	140.80	10.1	331.4	329.5	0.58
IB29	0.90	0.04	0.06	156.97	10.1	327.5	320.5	**2.14**
IB30	0.84	0.04	0.12	155.69	10.1	327.7	321.1	2.00
IB31	0.85	0.09	0.06	157.61	10.2	327.7	321.1	1.99

Table A3. Continued

Blend Name	*n*-P	*iso*-P	*cyclo*-P	'A'	C_n	Exp Data (K)	Prd Data (K)	Relative Error (%)
IB32	0.79	0.08	0.12	156.30	10.2	328.0	321.8	1.89

Table A4. Resulted data for freezing point correlative model.

Blend Name	*n*-P	*iso*-P	*cyclo*-P	Experimental Data (K)	Predicted Data (K)	Relative Error (%)
***n*-Decane**	1.00	0.00	0.00	243.2	243.2	0.00
Shell SolT	0.00	1.00	0.00	196.2	196.1	0.00
Decalin	0.00	0.00	1.00	230.2	232.2	1.58
IB3	0.32	0.28	0.40	236.0	233.3	5.31
IB4	0.18	0.15	0.67	221.6	221.4	2.51
IB7	0.21	0.53	0.26	227.1	230.7	3.39
IB8	0.43	0.37	0.20	238.8	236.4	3.08
IB9	0.61	0.26	0.13	243.9	239.6	0.90
IB10	0.65	0.14	0.21	241.8	239.4	3.47
IB11	0.71	0.00	0.29	248.0	239.0	0.20
IB12	0.58	0.12	0.30	239.5	236.5	0.07
IB13	0.39	0.13	0.48	236.3	236.0	2.96
IB14	0.45	0.00	0.55	243.2	235.3	1.40
IB15	0.27	0.08	0.66	232.1	232.9	3.63
IB16	0.21	0.00	0.79	224.8	227.9	2.10
IB17	0.16	0.35	0.49	223.3	218.8	1.36
IB18	0.11	0.57	0.32	215.9	228.5	**5.57**
IB23	0.11	0.82	0.07	217.0	207.1	4.54
IB24	0.11	0.75	0.14	218.6	210.2	3.82
IB26	0.08	0.04	0.88	230.5	232.7	0.99
IB28	0.09	0.07	0.84	222.4	233.0	4.77
IB29	0.90	0.04	0.06	246.6	243.4	1.29
IB30	0.84	0.04	0.12	244.1	242.6	0.60
IB31	0.85	0.09	0.06	246.6	242.9	1.49
IB32	0.79	0.08	0.12	245.5	242.1	1.36

APPENDIX B

JET FUELS BLENDING OPTIMIZATION PROBLEM

LINGO FORMULATION

```
! The objective of this formulation is to minimize the overall
  blending cost of GTL SPK and conventional Jet A-1 jet fuels,
  by manipulation of blending ratios with respect to certain
  GTL SPK fractions;

! Objective function;

Min = (GTL_SPK_VolP*GTL_SPK_Cost) + (Jet_A1_VolP*Jet_A1_Cost);

Jet_A1_VolP = 1.00 - GTL_SPK_VolP;

! Prices are in terms of $/bbl;

GTL_SPK_Subsidy = 25;

Jet_A1_Cost = 128.6;
GTL_SPK_Cost = 150.0 - GTL_SPK_Subsidy;

! GTL SPK analysis;

! Case (1);

GTL_SPK_V_NP + GTL_SPK_V_IP + GTL_SPK_V_CP = 1.0000;

! Case (2);

GTL_SPK_V_NP = 0.4340;
GTL_SPK_V_IP = 0.5570;
GTL_SPK_V_CP = 0.0090;

! Jet A-1 relative compositions [Obtained from literature];

Jet_A1_V_NP_IP = 0.5878;
Jet_A1_V_CP = 0.2131;
Jet_A1_V_Aromatics = 0.1991;

! GTL SPK Mixing Correlations;

! Density Correlation [Pure basis of kg/bbl];

Density_GTL_SPK = 1/((GTL_SPK_V_NP/87.59838) + (GTL_SPK_V_IP/90.78226)
+ (GTL_SPK_V_CP/105.27069));
```

```
! Net_Heat_Content Correlation [Pure basis of MJ/bbl];

Net_Heat_of_Combustion_GTL_SPK = (3875.352*GTL_SPK_V_NP) +
(3976.262*GTL_SPK_V_IP) + (4495.623*GTL_SPK_V_CP);

! Flash Point Correlation [Pure basis of K];

Flash_Point_GTL_SPK = A_Bar + Cn_Bar;
A_Bar = (157.6*GTL_SPK_V_NP) + (168.6*GTL_SPK_V_IP) +
(140.3*GTL_SPK_V_CP);
Cn_Bar = 16.15*((10*GTL_SPK_V_NP) + (12*GTL_SPK_V_IP) +
(10*GTL_SPK_V_CP));

! Freezing Point Correlation [Pure basis of K];

Freezing_Point_GTL_SPK = (243.15*GTL_SPK_V_NP) +
(196.15*(GTL_SPK_V_IP^(0.902))) + (230.15*GTL_SPK_V_CP);

! Jet A-1 measured properties;

Jet_A1_Density = 94.02576;
Jet_A1_Net_Heat_of_Combustion = 4082.627;
Jet_A1_Flash_Point = 314.05;
Jet_A1_Freezing_Point = 218.85;

! Properties of final mix;

Mix_Density = (Jet_A1_Density*Jet_A1_VolP) +
(Density_GTL_SPK*GTL_SPK_VolP);
Mix_Net_Heat_of_Combustion =
(Jet_A1_Net_Heat_of_Combustion*Jet_A1_VolP) +
(Net_Heat_of_Combustion_GTL_SPK*GTL_SPK_VolP);
Mix_Flash_Point = (Jet_A1_Flash_Point*Jet_A1_VolP) +
(Flash_Point_GTL_SPK*GTL_SPK_VolP);
Mix_Freezing_Point = (Jet_A1_Freezing_Point*Jet_A1_VolP) +
(Freezing_Point_GTL_SPK*GTL_SPK_VolP);

! Final mix contrains [ASTM D1655];

Mix_Density >= 92.41593;
Mix_Density <= 100.16694;

Mix_Net_Heat_of_Combustion >= (42.8*Mix_Density);

Mix_Flash_Point >= 311.15;

Mix_Freezing_Point <= 226.15;
```

PROPERTIES UNITS CONVERSION

All the properties had to be in volume basis in order to match with volumetric basis calculation proposed for the problem. Therefore, both of the density and net heat of combustion had to be converted into basis of barrel. While, both flash and freezing points were kept intact. Following is a step-by-step procedure for converting the properties of interest from mass basis to volume basis.

$$\rho\left(\frac{kg}{bbl}\right) = \rho\left(\frac{g}{cm^3}\right) x \frac{kg}{10^3\, g} x \frac{10^6\, cm^3}{m^3} x \frac{m^3}{8.386\, bbl}$$

$$\Delta H_{comb}\left(\frac{MJ}{bbl}\right) = \Delta H_{comb}\left(\frac{MJ}{kg}\right) x\, \rho\left(\frac{kg}{bbl}\right)$$

FIRST CASE OUTCOMES

```
Local optimal solution found.
Objective value:                              126.9358
Infeasibilities:                          0.3319137E-06
Total solver iterations:                             72

Model Class:                                        NLP

Total variables:                      15
Nonlinear variables:                   8
Integer variables:                     0

Total constraints:                    18
Nonlinear constraints:                 6

Total nonzeros:                       52
Nonlinear nonzeros:                   12
```

Variable	Value	Reduced Cost
GTL_SPK_VOLP	0.4622822	0.000000
GTL_SPK_COST	125.0000	0.000000
JET_A1_VOLP	0.5377178	0.000000
JET_A1_COST	128.6000	0.000000
GTL_SPK_SUBSIDY	25.00000	0.000000
GTL_SPK_V_NP	0.3454784	0.000000
GTL_SPK_V_IP	0.000000	378.8934
GTL_SPK_V_CP	0.6545216	0.000000
JET_A1_V_NP_IP	0.5878000	0.000000
JET_A1_V_CP	0.2131000	0.000000
JET_A1_V_AROMATICS	0.1991000	0.000000
DENSITY_GTL_SPK	98.41163	0.000000
NET_HEAT_OF_COMBUSTION_GTL_SPK	4281.333	0.000000
FLASH_POINT_GTL_SPK	307.7768	0.000000
A_BAR	146.2768	0.000000
CN_BAR	161.5000	0.000000
FREEZING_POINT_GTL_SPK	234.6412	0.000000
JET_A1_DENSITY	94.02576	0.000000
JET_A1_NET_HEAT_OF_COMBUSTION	4082.627	0.000000
JET_A1_FLASH_POINT	314.0500	0.000000
JET_A1_FREEZING_POINT	218.8500	0.000000
MIX_DENSITY	96.05327	0.000000
MIX_NET_HEAT_OF_COMBUSTION	4174.485	0.000000
MIX_FLASH_POINT	311.1500	0.000000
MIX_FREEZING_POINT	226.1500	0.000000

SECOND CASE OUTCOMES

```
  Global optimal solution found.
  Objective value:                              127.3247
  Infeasibilities:                              0.000000
  Total solver iterations:                             0

  Model Class:                                        LP

  Total variables:                     6
  Nonlinear variables:                 0
  Integer variables:                   0

  Total constraints:                  11
  Nonlinear constraints:               0

  Total nonzeros:                     22
  Nonlinear nonzeros:                  0


                            Variable           Value        Reduced
Cost
                       GTL_SPK_VOLP        0.3542626
0.000000
                       GTL_SPK_COST        125.0000
0.000000
                        JET_A1_VOLP        0.6457374
0.000000
                        JET_A1_COST        128.6000
0.000000
                        GTL_SUBSIDY        25.00000
0.000000
                       GTL_SPK_V_NP        0.4340000
0.000000
                       GTL_SPK_V_IP        0.5570000
0.000000
                       GTL_SPK_V_CP        0.9000000E-02
0.000000
                   JET_A1_V_NP_IP        0.5878000
0.000000
                      JET_A1_V_CP        0.2131000
0.000000
                JET_A1_V_AROMATICS        0.1991000
0.000000
                  DENSITY_GTL_SPK         89.48159
0.000000
        NET_HEAT_OF_COMBUSTION_GTL_SPK         3937.141
0.000000
             FLASH_POINT_GTL_SPK         343.0624
0.000000
                            A_BAR        163.5713
0.000000
```

	CN_BAR	179.4911
0.000000		
	FREEZING_POINT_GTL_SPK	223.3028
0.000000		
	JET_A1_DENSITY	94.02576
0.000000		
	JET_A1_NET_HEAT_OF_COMBUSTION	4082.627
0.000000		
	JET_A1_FLASH_POINT	314.0500
0.000000		
	JET_A1_FREEZING_POINT	218.8500
0.000000		
	MIX_DENSITY	92.41593
0.000000		
	MIX_NET_HEAT_OF_COMBUSTION	4031.087
0.000000		
	MIX_FLASH_POINT	324.3280
0.000000		
	MIX_FREEZING_POINT	220.4275
0.000000		

APPENDIX C

PURE COMPONENTS CHEMICAL & PHYSICAL PROPERTIES

Table C1. Pure components structure.

Pure Component	*n*-Paraffins (vol%)	*iso*-Paraffins (vol%)	*cyclo*-Paraffins (vol%)	Aromatics (vol%)
Shell GTL SPK*	43.40	55.70	0.84	0.00
Shell Sol-T*	0.00	99.74	0.26	0.00
n*-Decane*	100.00	0.00	0.00	0.00
Decalin**	0.00	0.00	100.00	0.00
Toluene**	0.00	0.00	0.00	100.00
Jet A-1 Q-Jet***	58.78		21.31	19.91

* Chemical structure provided from Shell.
** Chemical structure provided by supplier MSDS.
*** Chemical structure gathered from literature [41].

Table C2. Average properties of pure components.

Pure Component	Density (g/cm^3)	Viscosity (mm^2/s)	Net Heat of Combustion (MJ/kg)	Flash Point (^oC)	Freezing Point (^oC)
Shell GTL SPK	0.7376	2.5202	44.0724	43.6	-57.3
Shell Sol-T	0.7613	5.4517	43.8000	61.0	-77.0
***n*-Decane**	0.7346	2.5708	44.2400	46.0	-30.0
Decalin	0.8828	7.5215	42.7054	57.0	-43.0
Toluene*	0.8710	-	40.5900	4.4	-95.0
Jet A-1 Q-Jet	0.7885	3.3850	43.4203	40.9	-52.5

* Properties of pure toluene were not measured due to devices limitations.

APPENDIX D

EXPERIMENTAL SETS DATA

Table D1. Average properties of tested blends in first experimental set.

Tested Blend	*n*-P (vol%)	*iso*-P (vol%)	*cyclo*-P (vol%)	Den. (g/cm^3)	Visc. (mm^2/s)	N. H. of Comb. (MJ/kg)	Fl. Point (^oC)	Fr. Point (^oC)
IB1	0.00	24.94	75.07	0.8531	6.7713	42.8422	57.1	<-75.0
IB2	0.00	49.87	50.13	0.8300	6.2185	43.2271	59.5	<-75.0
IB3	33.33	33.25	33.42	0.7936	4.2892	43.5083	55.5	-37.2
IB4	20.00	19.95	60.05	0.8281	5.2342	43.0877	57.1	-51.6
IB5	10.00	29.92	60.08	0.8301	5.7679	43.0738	57.4	<-75.0
IB6	0.00	74.81	25.20	0.7949	5.7952	43.3257	58.7	<-75.0
IB7	20.00	59.84	20.16	0.7763	4.5266	43.6587	57.6	-46.1
IB8	42.00	41.89	16.11	0.7700	3.8181	43.7732	55.6	-34.4
IB9	60.00	29.92	10.08	0.7577	3.3092	43.8613	54.6	-29.3
IB10	66.00	16.96	17.04	0.7650	3.2411	43.7994	54.3	-31.4
IB11	75.00	0.00	25.00	0.7724	5.2601	43.5120	55.4	-25.2
IB12	60.00	14.96	25.04	0.7765	3.4408	43.6652	55.1	-33.7
IB13	42.00	15.96	42.04	0.8020	4.1080	43.3903	55.4	-36.8
IB14	50.00	0.00	50.00	0.8091	3.9680	43.2795	55.1	-30.0
IB15	30.00	9.97	60.03	0.8273	4.7859	43.1284	56.0	-41.1
IB16	25.00	0.00	75.00	0.8461	3.1323	42.9037	56.4	-48.4
IB17	17.00	41.89	41.11	0.8079	5.0703	43.3548	58.4	-49.9
IB18	11.00	63.83	25.17	0.7897	5.2017	43.5544	59.5	-57.3
IB19	49.00	49.87	1.13	0.7495	3.4936	44.0180	56.6	-31.2
IB20	74.00	24.94	1.07	0.7427	2.9602	44.0145	55.1	-25.3
IB21	5.00	89.77	5.23	0.7670	5.2869	43.9353	60.8	< -75.0
IB22	5.00	84.78	10.22	0.7730	5.2840	43.7922	61.4	< -75.0
IB23	10.00	84.78	5.22	0.7654	4.9534	43.9244	59.3	-56.2
IB24	10.00	79.79	10.21	0.7715	5.0149	43.8065	58.7	-54.6
IB25	5.00	4.99	90.01	0.8703	6.8199	42.6792	59.0	< -75.0
IB26	10.00	4.99	85.01	0.8628	6.2728	42.8285	59.5	-42.7
IB27	5.00	9.97	85.03	0.8640	6.6397	42.7841	59.7	< -75.0
IB28	10.00	9.97	80.03	0.8569	6.1889	42.8210	58.3	-50.8

Table D1. Continued.

Tested Blend	*n*-P (vol%)	*iso*-P (vol%)	*cyclo*-P (vol%)	Den. (g/cm^3)	Visc. (mm^2/s)	N. H. of Comb. (MJ/kg)	Fl. Point (^oC)	Fr. Point (^oC)
IB29	90.00	4.99	5.01	0.7435	2.7317	44.0088	54.3	-26.6
IB30	85.00	4.99	10.01	0.7510	2.8597	43.9582	54.5	-29.1
IB31	85.00	9.97	5.03	0.7447	2.8411	44.0253	54.5	-26.6
IB32	80.00	9.97	10.03	0.7523	2.9360	43.9218	54.8	-27.7

Table D2. Average properties of tested blends in second experimental set.

Tested Blend	*n*-P (vol%)	*iso*-P (vol%)	*cyclo*-P (vol%)	Den. (g/cm^3)	Visc. (mm^2/s)	N. H. of Comb. (MJ/kg)	Fl. Point (^oC)	Fr. Point (^oC)
IB33	42.97	55.14	0.83	1.00	0.7396	44.3211	-53.3	42.0
IB34	42.53	54.59	0.82	2.00	0.7409	44.2541	-51.9	39.7
IB35	41.23	52.92	0.80	5.00	0.7443	44.0910	-56.0	34.4
IB36	39.93	51.24	0.77	8.00	0.748	43.8644	-55.8	30.6
IB37	39.06	50.13	0.76	10.00	0.7506	43.7343	-58.7	30.7
IB38	36.89	47.35	0.71	15.00	0.7569	43.5231	-58.8	25.4
IB39	5.40	6.58	80.02	8.00	0.8658	42.7207	<-75.0	35.3
IB40	20.48	24.96	50.07	4.50	0.8220	43.2886	-47.9	37.9
IB41	35.55	43.34	20.11	0.10	0.7778	43.9852	-34.1	51.9
IB42	13.50	16.46	70.04	0.00	0.8440	43.3104	-44.3	59.7
IB43	18.00	21.94	60.06	0.00	0.8307	43.4299	-48.7	57.4
IB44	20.25	24.69	55.06	0.00	0.8240	43.4432	-46.9	57.4
IB45	22.50	27.43	50.07	0.00	0.8174	43.5492	-45.2	56.9
IB46	24.75	30.17	45.08	0.00	0.8105	43.6635	-43.6	55.8
IB47	27.00	32.91	40.09	0.00	0.8040	43.6929	-38.0	57.8
IB48	31.50	38.40	30.10	0.00	0.7902	43.8536	-37.2	58.3
IB49	36.89	47.35	0.71	25.00	0.7698	42.9661	-56.2	20.8
IB50	17.55	21.39	60.06	1.00	0.8313	43.4039	-46.3	54.2
IB51	12.15	14.81	70.04	3.00	0.8471	43.1429	-43.7	48.2
IB52	21.15	25.78	50.07	3.00	0.8206	43.4141	-41.6	47.1
IB53	30.15	36.75	30.10	3.00	0.7935	43.7418	-36.0	46.4
IB54	15.75	19.20	60.05	5.00	0.8360	43.1615	-45.3	41.0
IB55	24.75	30.17	40.08	5.00	0.8090	43.4555	-40.8	41.5

Table D3. Average properties of tested blends in third experimental set.

Tested Blend	*n*- & *iso*-P (vol%)	*cyclo*-P (vol%)	Aro. (vol%)	Den. (g/cm^3)	Visc. (mm^2/s)	N. H. of Comb. (MJ/kg)	Fl. Point (^oC)	Fr. Point (^oC)
IA.IB1	95.07	2.94	1.99	0.7425	2.5859	44.0571	43.9	-59.8
IA.IB2	91.04	4.98	3.98	0.7476	2.6601	44.0218	42.7	-62.2
IA.IB3	87.00	7.02	5.97	0.7528	2.7353	43.9493	41.2	-65.4
IA.IB4	82.97	9.06	7.96	0.7579	2.8155	43.9677	41.9	-68.2
IA.IB5	78.94	11.11	9.96	0.7629	2.9032	43.9067	40.5	-65.4
IA.IB6	74.91	13.15	11.95	0.7680	2.9879	43.7954	41.2	-62.6
IA.IB7	70.88	15.19	13.94	0.7730	3.0782	43.7440	41.2	-61.5
IA.IB8	66.84	17.23	15.93	0.7781	3.1949	43.7535	41.5	-60.5
IA.IB9	62.81	19.27	17.92	0.7832	3.2823	43.6189	40.6	-56.6

APPENDIX E

INDUSTRIAL CERTIFICATES

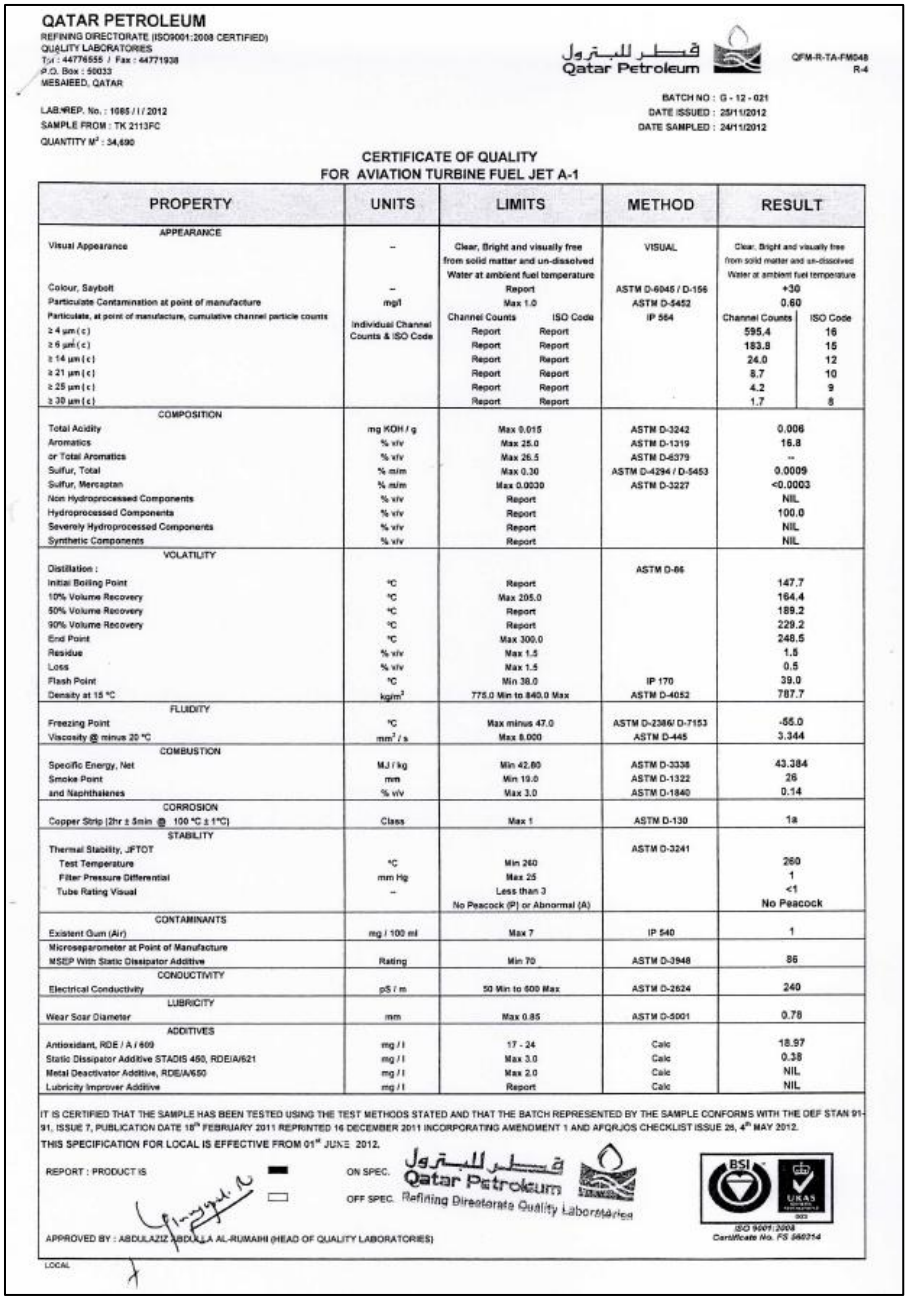

QATAR PETROLEUM
REFINING DIRECTORATE (ISO9001:2008 CERTIFIED)
QUALITY LABORATORIES
Tel : 44776555 / Fax : 44771938
P.O. Box : 50033
MESAIEED, QATAR

قطر للبترول
Qatar Petroleum

QFM-R-TA-FM048
R-4

LAB/REP. No. : 1085 / I / 2012
SAMPLE FROM : TK 2113FC
QUANTITY M³ : 34,690

BATCH NO : G - 12 - 021
DATE ISSUED : 25/11/2012
DATE SAMPLED : 24/11/2012

CERTIFICATE OF QUALITY
FOR AVIATION TURBINE FUEL JET A-1

PROPERTY	UNITS	LIMITS	METHOD	RESULT	
APPEARANCE					
Visual Appearance	–	Clear, Bright and visually free from solid matter and un-dissolved Water at ambient fuel temperature	VISUAL	Clear, Bright and visually free from solid matter and un-dissolved Water at ambient fuel temperature	
Colour, Saybolt	–	Report	ASTM D-6045 / D-156	+30	
Particulate Contamination at point of manufacture	mg/l	Max 1.0	ASTM D-5452	0.60	
Particulate, at point of manufacture, cumulative channel particle counts	Individual Channel Counts & ISO Code	Channel Counts / ISO Code	IP 564	Channel Counts	ISO Code
≥ 4 µm (c)		Report / Report		595.4	16
≥ 6 µm (c)		Report / Report		183.8	15
≥ 14 µm (c)		Report / Report		24.0	12
≥ 21 µm (c)		Report / Report		8.7	10
≥ 25 µm (c)		Report / Report		4.2	9
≥ 30 µm (c)		Report / Report		1.7	8
COMPOSITION					
Total Acidity	mg KOH / g	Max 0.015	ASTM D-3242	0.006	
Aromatics	% v/v	Max 25.0	ASTM D-1319	16.8	
or Total Aromatics	% v/v	Max 26.5	ASTM D-6379	--	
Sulfur, Total	% m/m	Max 0.30	ASTM D-4294 / D-5453	0.0009	
Sulfur, Mercaptan	% m/m	Max 0.0030	ASTM D-3227	<0.0003	
Non Hydroprocessed Components	% v/v	Report		NIL	
Hydroprocessed Components	% v/v	Report		100.0	
Severely Hydroprocessed Components	% v/v	Report		NIL	
Synthetic Components	% v/v	Report		NIL	
VOLATILITY					
Distillation :			ASTM D-86		
Initial Boiling Point	°C	Report		147.7	
10% Volume Recovery	°C	Max 205.0		164.4	
50% Volume Recovery	°C	Report		189.2	
90% Volume Recovery	°C	Report		229.2	
End Point	°C	Max 300.0		248.5	
Residue	% v/v	Max 1.5		1.5	
Loss	% v/v	Max 1.5		0.5	
Flash Point	°C	Min 38.0	IP 170	39.0	
Density at 15 °C	kg/m³	775.0 Min to 840.0 Max	ASTM D-4052	787.7	
FLUIDITY					
Freezing Point	°C	Max minus 47.0	ASTM D-2386/ D-7153	-55.0	
Viscosity @ minus 20 °C	mm² / s	Max 8.000	ASTM D-445	3.344	
COMBUSTION					
Specific Energy, Net	MJ / kg	Min 42.80	ASTM D-3338	43.384	
Smoke Point	mm	Min 19.0	ASTM D-1322	26	
and Naphthalenes	% v/v	Max 3.0	ASTM D-1840	0.14	
CORROSION					
Copper Strip (2hr ± 5min @ 100 °C ± 1°C)	Class	Max 1	ASTM D-130	1a	
STABILITY					
Thermal Stability, JFTOT			ASTM D-3241		
Test Temperature	°C	Min 260		260	
Filter Pressure Differential	mm Hg	Max 25		1	
Tube Rating Visual	–	Less than 3 No Peacock (P) or Abnormal (A)		<1 No Peacock	
CONTAMINANTS					
Existent Gum (Air)	mg / 100 ml	Max 7	IP 540	1	
Microseparometer at Point of Manufacture					
MSEP With Static Dissipator Additive	Rating	Min 70	ASTM D-3948	86	
CONDUCTIVITY					
Electrical Conductivity	pS / m	50 Min to 600 Max	ASTM D-2624	240	
LUBRICITY					
Wear Scar Diameter	mm	Max 0.85	ASTM D-5001	0.78	
ADDITIVES					
Antioxidant, RDE / A / 609	mg / l	17 - 24	Calc	18.97	
Static Dissipator Additive STADIS 450, RDE/A/621	mg / l	Max 3.0	Calc	0.38	
Metal Deactivator Additive, RDE/A/650	mg / l	Max 2.0	Calc	NIL	
Lubricity Improver Additive	mg / l	Report	Calc	NIL	

IT IS CERTIFIED THAT THE SAMPLE HAS BEEN TESTED USING THE TEST METHODS STATED AND THAT THE BATCH REPRESENTED BY THE SAMPLE CONFORMS WITH THE DEF STAN 91-91, ISSUE 7, PUBLICATION DATE 18TH FEBRUARY 2011 REPRINTED 16 DECEMBER 2011 INCORPORATING AMENDMENT 1 AND AFQRJOS CHECKLIST ISSUE 26, 4TH MAY 2012.
THIS SPECIFICATION FOR LOCAL IS EFFECTIVE FROM 01ST JUNE 2012.

REPORT : PRODUCT IS ■ ON SPEC. ☐ OFF SPEC.

قطر للبترول Qatar Petroleum
Refining Directorate Quality Laboratories

APPROVED BY : ABDULAZIZ ABDULLA AL-RUMAIHI (HEAD OF QUALITY LABORATORIES)

BSI ISO 9001:2008 Certificate No. FS 560314

LOCAL

Figure E1. Jet A-1 sample certificate provided by Q-Jet.

LABORATORY INVESTIGATION REPORT

QSGTL Production Technical Laboratory

Request ID 293

Subject: TAMUQ FCL – Blends Characterization
From: Laboratory
To:
Department:
Copy:
Request Leader: Signature
Worked Hours:
Date Finished: 21 February 2013
Date Printed:
Filed at:

1. INTRODUCTIONS / PURPOSE

FW Request!.msg

Refer attach email.

2. SAMPLES

5 x 200 ml various sample

3. RESULTS

Sample	Results			
	Density, g/cm3 (ASTM D4052)	Viscosity@-20 mm2/s (ASTM D445)	Flash point, °C (IP 170)	Freezing Point , °C (ASTM D5972)
Jet A-1	0.7883	3.381	37.0	-53.4
IA.IB2	0.7478	2.673	35.5	-68.3
IA.IB6	0.7682	2.992	36.5	-58.6
IA.IB9	0.7833	3.273	38.0	-54.4
SHELL SOL-T	0.7607	5.245	53.0	-

Figure E2. Results provided by Shell labs for sent samples.

APPENDIX F

STATISTICAL ANALYSES OUTCOMES

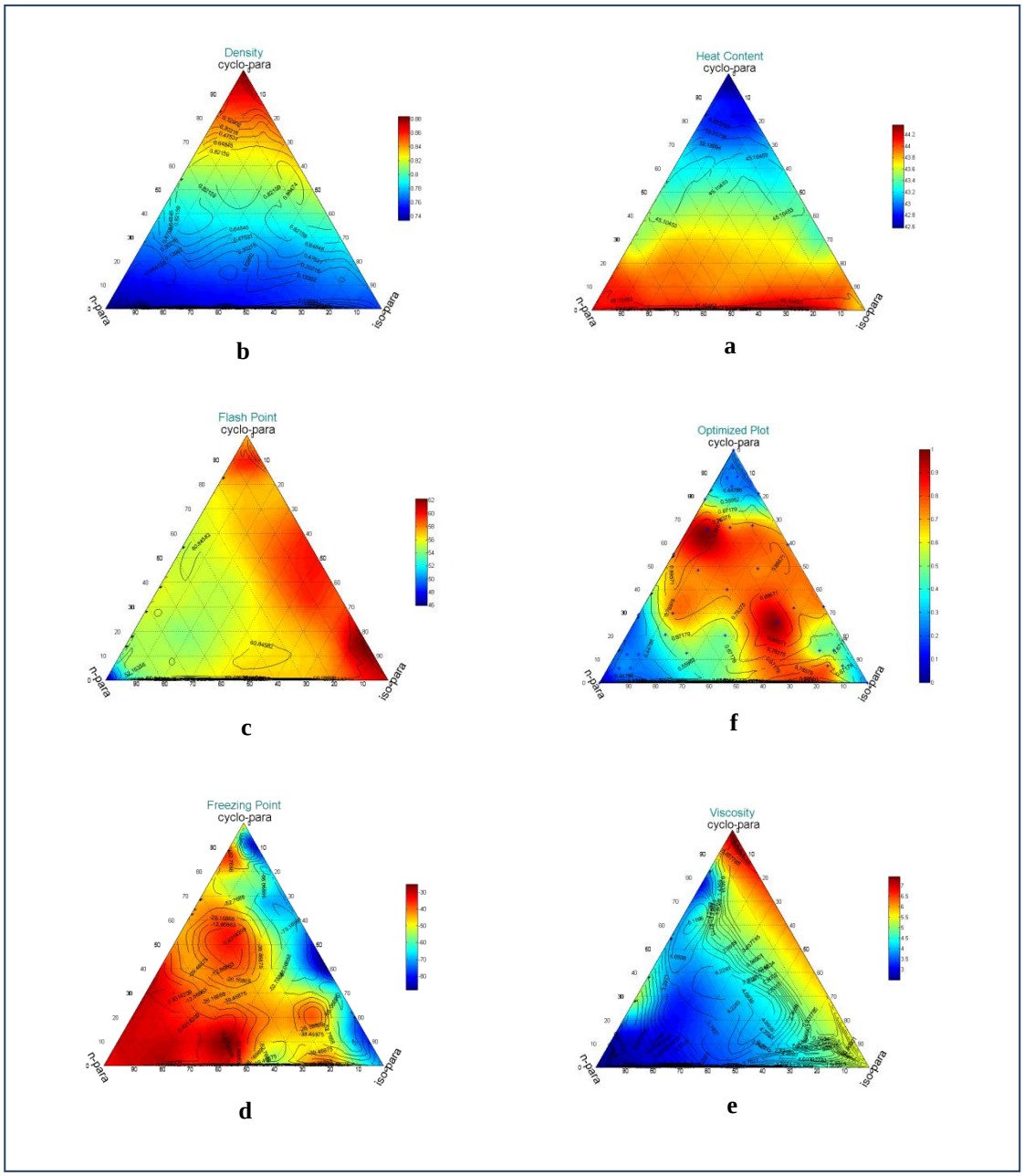

Figure F1. Generated artificial neural networks for first experimental set: a) density, b) net heat of combustion., c) flash point, d) freezing point, e) viscosity, and f) all together.

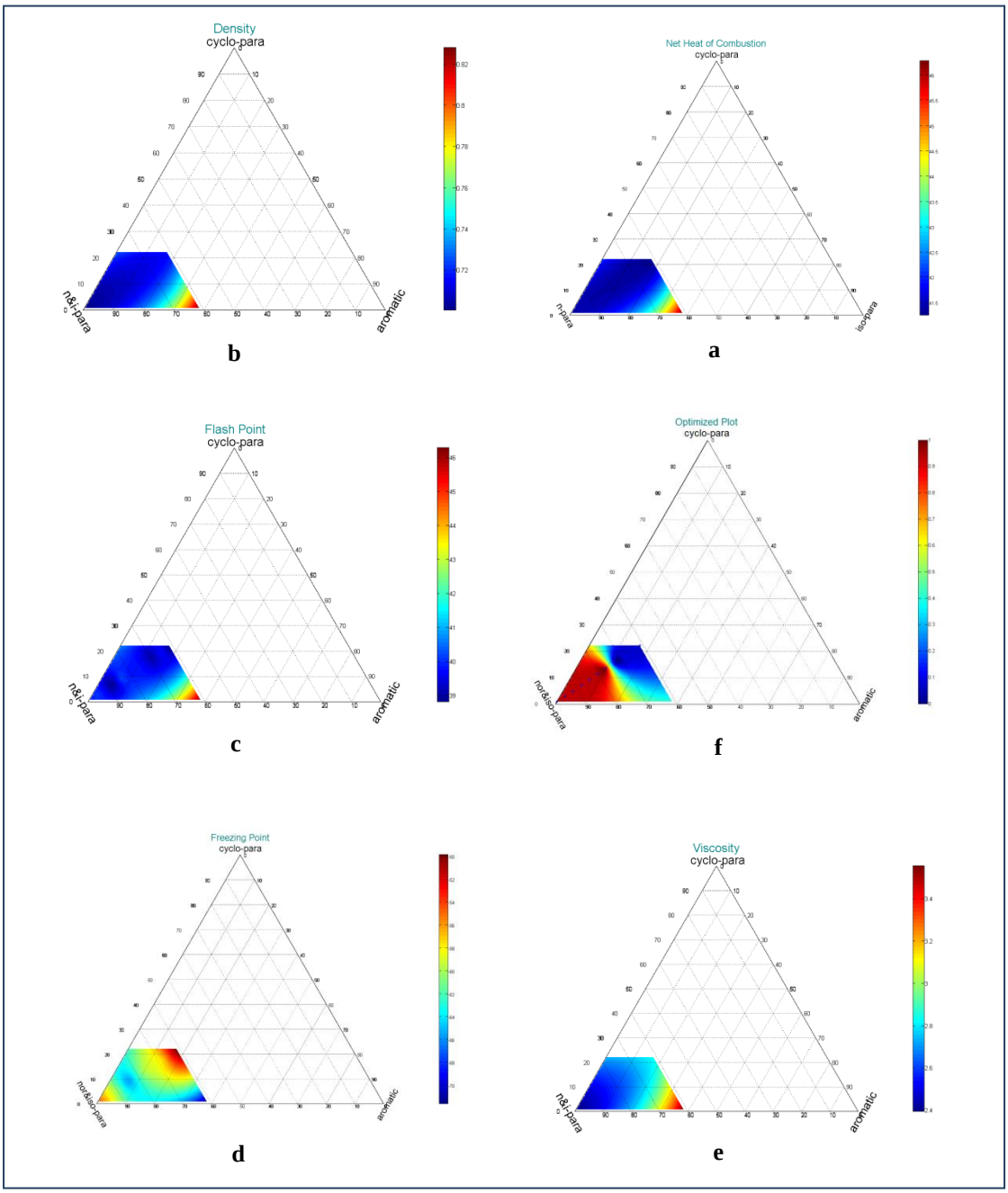

Figure F2. Generated non-artificial neural networks for third experimental set: a) density, b) net heat of combustion., c) flash point, d) freezing point, e) viscosity, and f) all together.

APPENDIX G

REPRODUCIBILITY DATA

Table G1. Density data produced by first operator.

Blend	IB.IA4	IB.IA9
Reading 1	0.7587	0.7835
Reading 2	0.7587	0.7836
Reading 3	0.7588	0.7536
Reading 4	0.7588	0.7536
Reading 5	0.7588	0.7536
Average	**0.7588**	**0.7536**

Table G2. Density data produced by second operator.

Blend	IB.IA4	IB.IA9
Reading 1	0.7578	0.7831
Reading 2	0.7578	0.7832
Reading 3	0.7577	0.7532
Reading 4	0.7577	0.7532
Reading 5	0.7577	0.7532
Average	**0.7577**	**0.7532**

Table G3. Comparison of Jet A-1 data.

Testing Center		**FCL**		**QP**	
Property	Unit	Testing Method	Resulted Data	Testing Method	Resulted Data
Density	g/cm^3	ASTM D4052	0.7885	ASTM D4052	0.7884
Viscosity	mm^2/s	ASTM D7042	3.3850	ASTM D445	3.3970
Neat Heat of Combustion	MJ/kg	ASTM D240	43.4203	ASTM D3308	43.3870

Table G3. Continued.

Testing Center	FCL	QP	Testing Center	FCL	QP
Flash Point	°C	ASTM D56	40.9	IP 170	38.0
Freezing Point	°C	ASTM D2386	-52.5	ASTM D2386	-53.7

Table G4. Comparison of tested samples results with respect to Shell labs.

Testing Facility			FCL		Shell	
Property	Unit	Tested Sample	Testing Method	Resulted Data	Testing Method	Resulted Data
Density	g/cm^3	IA.IB2	ASTM D4052	0.7476	ASTM D4052	0.7478
		IA.IB6		0.7680		0.7682
		IA.IB9		0.7832		0.7833
		Jet A-1		0.7885		0.7883
Viscosity	mm^2/s	IA.IB2	ASTM D7042	2.6601	ASTM D445	2.6730
		IA.IB6		2.9879		2.9920
		IA.IB9		3.2823		3.2730
		Jet A-1		3.3850		3.3810
Flash Point	°C	IA.IB2	ASTM D56	42.7	IP 170	35.5
		IA.IB6		41.2		36.5
		IA.IB9		40.6		38.0
		Jet A-1		40.9		37.0
Freezing Point	°C	IA.IB2	ASTM D2386	-62.2	ASTM D5972	-68.3
		IA.IB6		-62.6		-58.6
		IA.IB9		-56.6		-54.4
		Jet A-1		-52.5		-53.4

APPENDIX H

GC-FID ANALYSIS

All the blends among the third experimental set including the pure jet fuels were injected into GC-FID, in order to verify the chemical structure of prepared blends with regard to desired combinations. Figures H1-H3 display the peak profiles for pure jet fuels individually including the overlays between blends and pure fuels together.

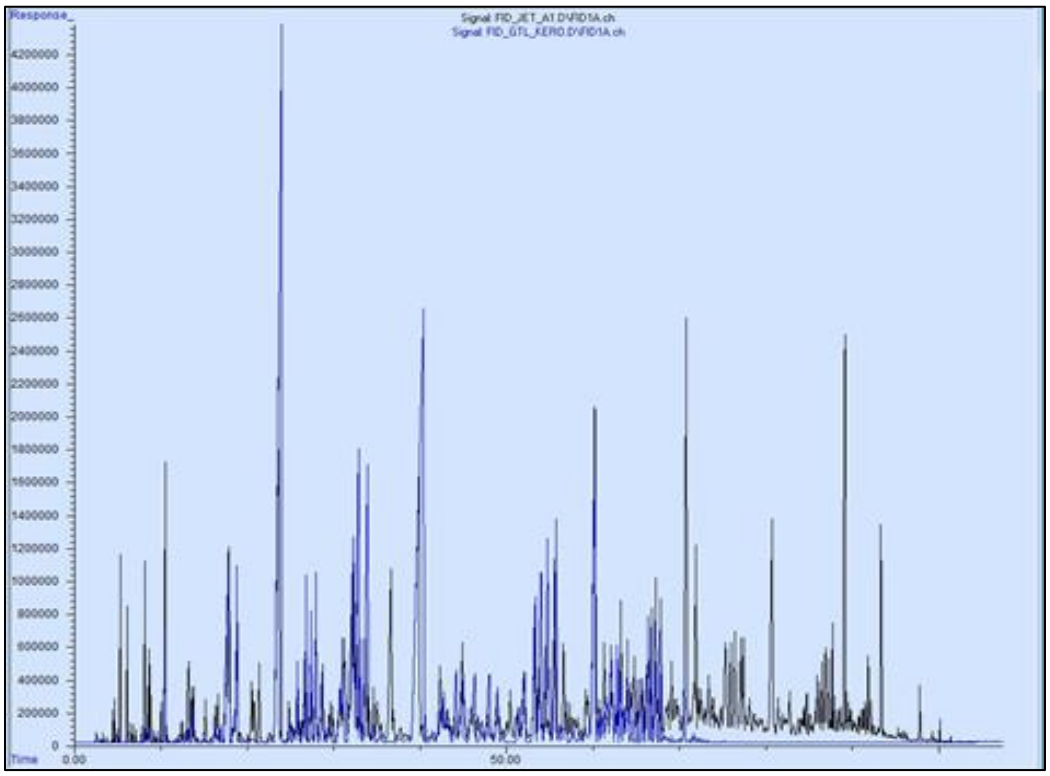

Figure H1. Snapshot from GC-FID data analysis for overlay of pure jet fuels chromatographs in third experimental set.

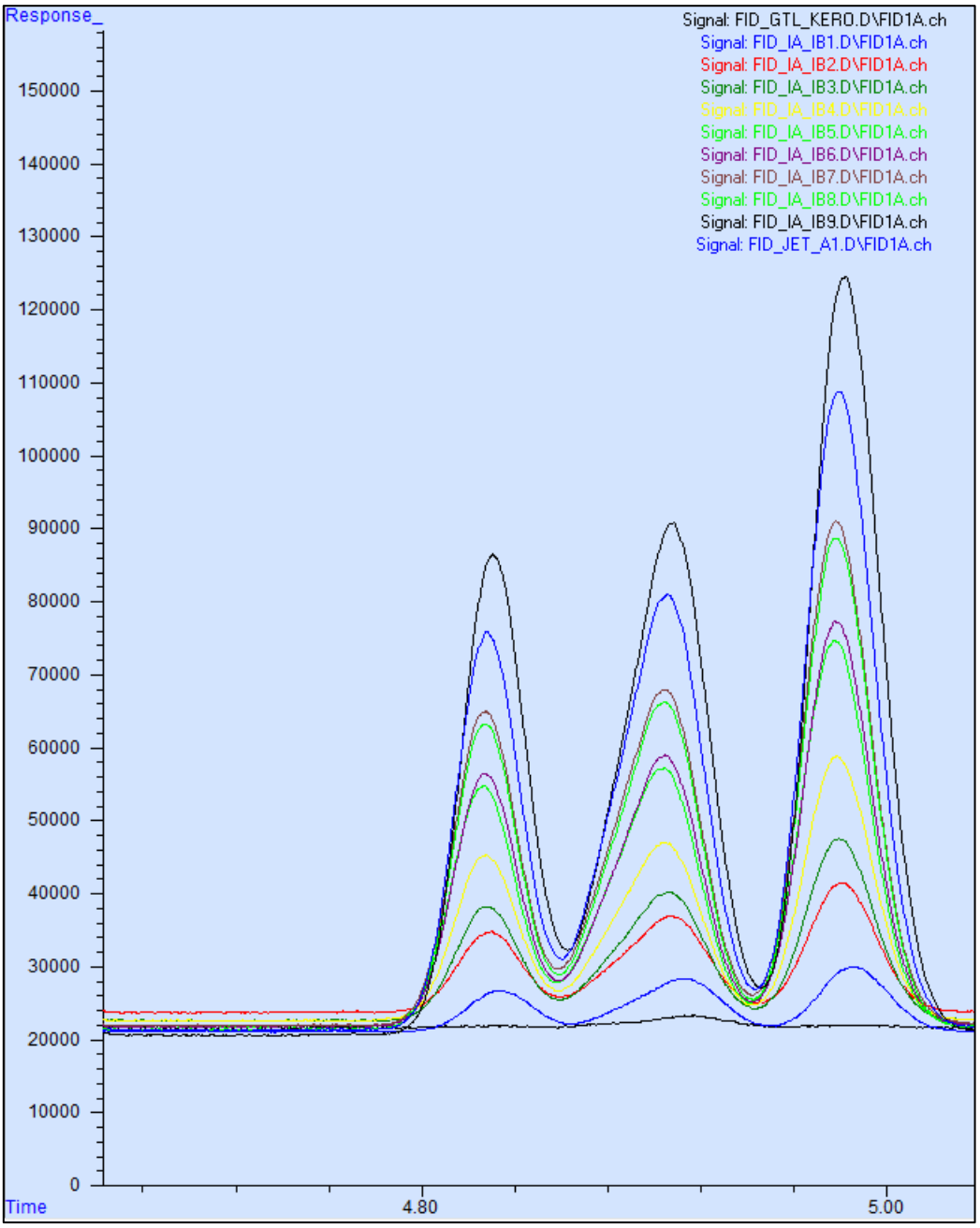

Figure H2. Snapshot from GC-FID data analysis for overlay of all chromatographs through specific peaks in third experimental set.

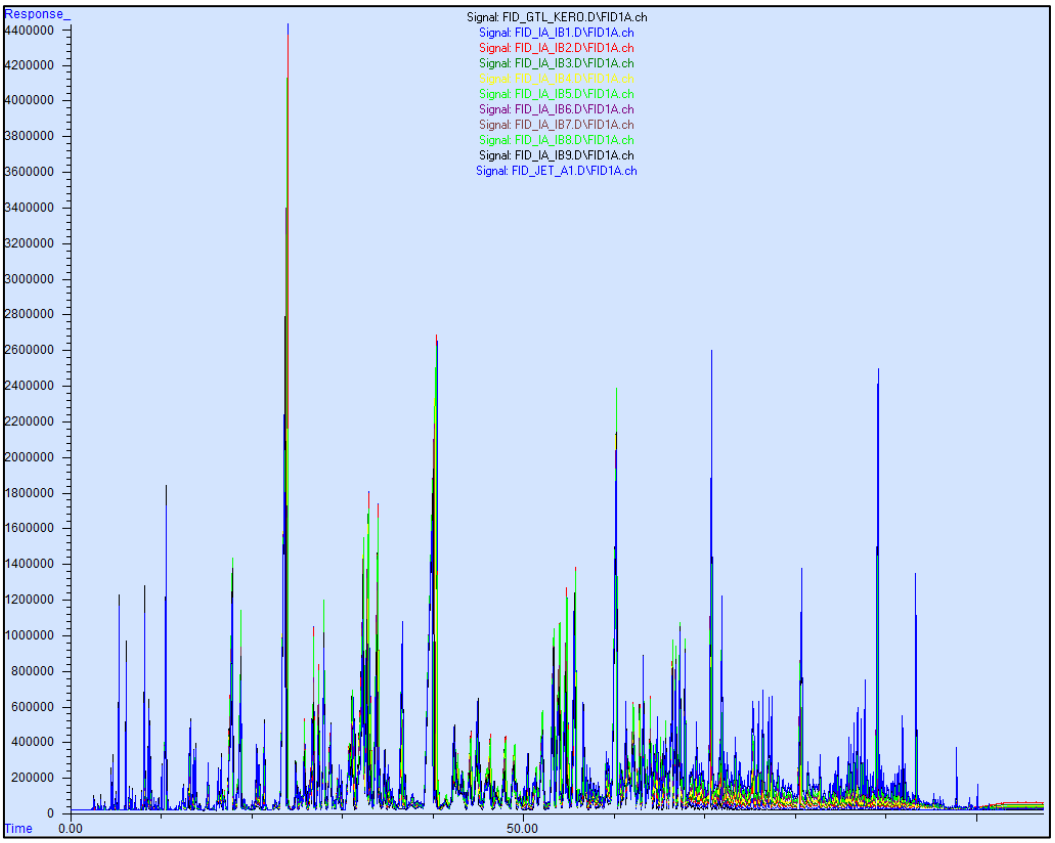

Figure H3. Snapshot from GC-FID data analysis for overlay of all chromatographs in third experimental set.

It was observed that GTL SPK has components set that are essentially a subset of Jet A-1 sample, in which Jet A-1 showed unique peaks that were not contained or minimally existed in GTL SPK. The Jet A-1 fractions were determined by comparing the relative peak sizes of specific peaks in these pure components. A total of 3 peaks were selected from the peaks profile which were characterized by unique characteristics:

1. Isolated.

2. Associated with sufficient intensity.

In order to correct for varying injection volumes, a certain peak was located that showed very similar peak areas for both GTL SPK and Jet A-1. Regardless of the composition of the blends, this peak should remain of similar size, depending on the injection volume. To determine the normalized fraction of Jet A-1, the relative intensity of the Jet A-1 unique peak was divided by the correction factor. Figures H4-H6 show excellent linear and consistent tends followed by the three selected peaks.

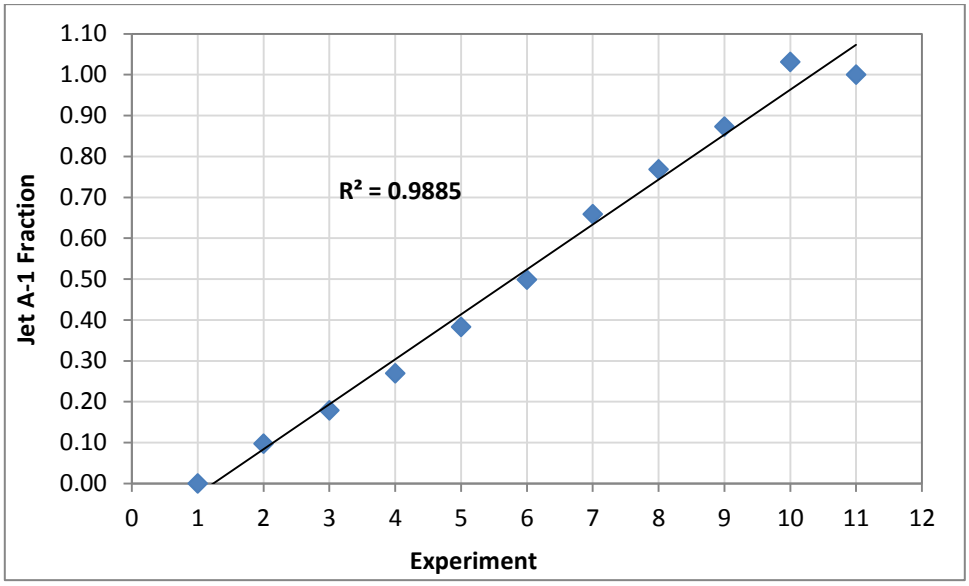

Figure H4. Jet A-1 fractions based on GC-FID analysis for first selected peak.

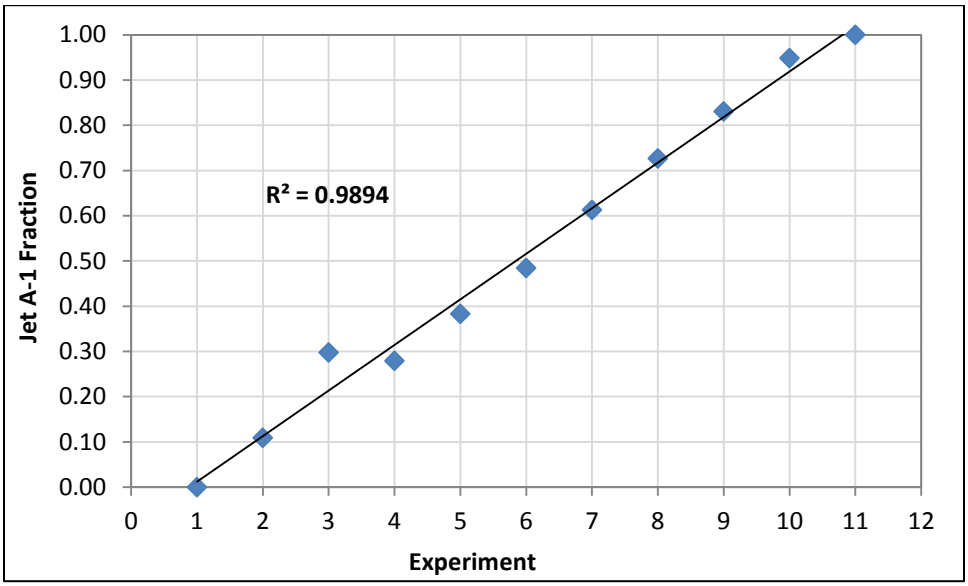

Figure H5. Jet A-1 fractions based on GC-FID analysis for second selected peak.

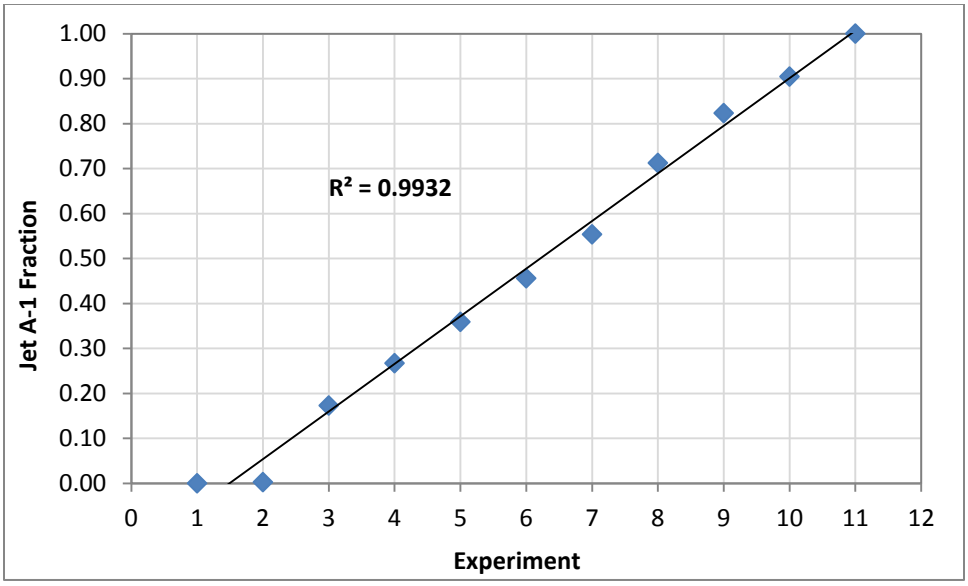

Figure H6. Jet A-1 fractions based on GC-FID analysis for third selected peak.

Since both GTL SPK and Jet A-1 consist of large number of components, it was really difficult to locate an efficient separation technique to obtain the pure components.

The quality and statistical distribution of the complete dataset was assessed by combining all the numbers together. Luckily, the total scatter was very low with least square error R^2 of 0.9850 as illustrated through Figures H7 and H8.

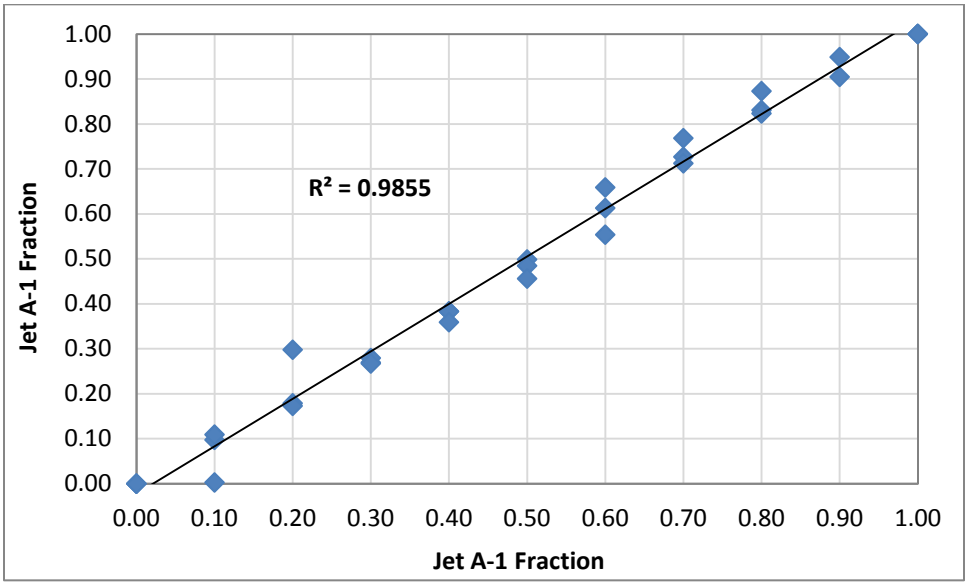

Figure H7. The relative spread in the complete dataset.

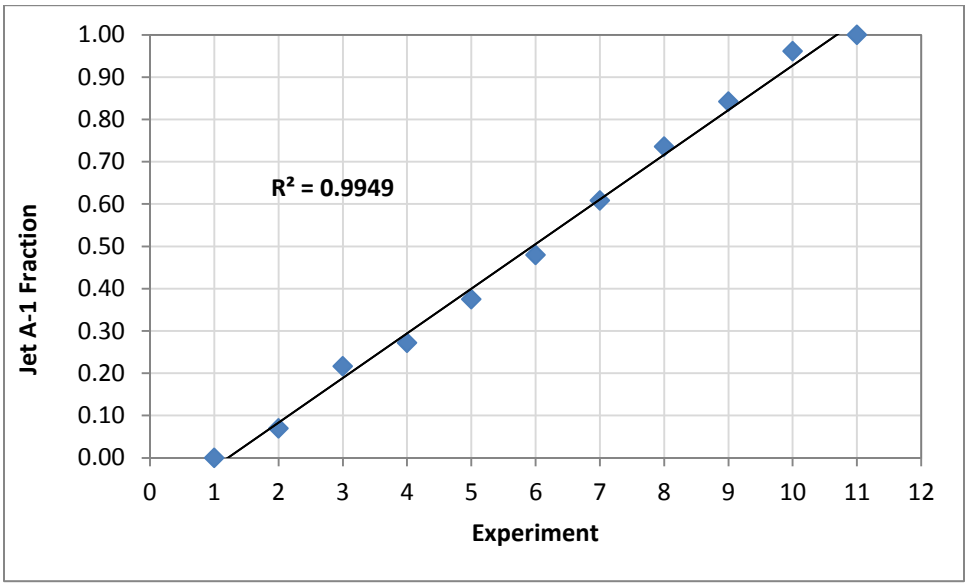

Figure H8. The resulted average fractions of Jet A-1.

In summary, a nearly consistent increase was detected throughout the analyzed data based on the previously explained GC-FID analysis. In addition, the estimated fractions were found in good agreement with desired Jet A-1 fractions as emphasized through Table H1.

Table H1. Estimated average fractions of Jet A-1 in third experimental set blends.

Sample	Jet A-1 Fraction	Sigma
FID_IA_IB1	0.0697	0.0584
FID_IA_IB2	0.2165	0.0705
FID_IA_IB3	0.2720	0.0065
FID_IA_IB4	0.3750	0.0139
FID_IA_IB5	0.4796	0.0217
FID_IA_IB6	0.6084	0.0527
FID_IA_IB7	0.7358	0.0290
FID_IA_IB8	0.8422	0.0268
FID_IA_IB9	0.9614	0.0643